

Lieb-Robinson Bounds on Entanglement Gaps from Symmetry-Protected Topology

Zongping Gong,¹ Naoto Kura,¹ Masatoshi Sato,² and Masahito Ueda^{1,3,4}

¹*Department of Physics, University of Tokyo, 7-3-1 Hongo, Bunkyo-ku, Tokyo 113-0033, Japan*

²*Yukawa Institute for Theoretical Physics, Kyoto University, Kyoto 606-8502, Japan*

³*Institute for Physics of Intelligence, University of Tokyo, 7-3-1 Hongo, Bunkyo-ku, Tokyo 113-0033, Japan*

⁴*RIKEN Center for Emergent Matter Science (CEMS), Wako, Saitama 351-0198, Japan*

(Dated: July 23, 2019)

A quantum quench is the simplest protocol to investigate nonequilibrium many-body quantum dynamics. Previous studies on the entanglement properties of quenched quantum many-body systems mainly focus on the growth of entanglement entropy. Several rigorous results and phenomenological guiding principles have been established, such as the no-faster-than-linear entanglement growth generated by generic local Hamiltonians and the peculiar logarithmic growth for many-body localized systems. However, little is known about the dynamical behavior of the full entanglement spectrum, which is a refined character closely related to the topological nature of the wave function. Here, we establish a *rigorous* and universal result for the entanglement spectra of one-dimensional symmetry-protected topological (SPT) systems evolving out of equilibrium. Our result is derived both for free-fermion SPT systems and interacting ones. For free-fermion systems with Altland-Zirnbauer symmetries, we prove that the single-particle entanglement gap after quenches obeys essentially the same Lieb-Robinson bound as that on the equal-time correlation, provided that there is no dynamical symmetry breaking. As a notable byproduct, we obtain a new type of Lieb-Robinson velocity which is related to the band dispersion with a complex wave number and reaches the minimum as the maximal (relative) group velocity. Within the framework of tensor networks, i.e., for SPT matrix-product states evolved by symmetric and trivial matrix-product unitaries, we also identify a Lieb-Robinson bound on the many-body entanglement gap for general quenched interacting SPT systems. This result suggests high potential of tensor-network approaches for exploring rigorous results on long-time quantum dynamics. Influence of partial symmetry breaking, effects of disorder, and the relaxation property in the long-time limit are also discussed. Our work establishes a paradigm for exploring rigorous results of SPT systems out of equilibrium.

I. INTRODUCTION

Recent years have witnessed remarkable experimental developments in atomic, molecular and optical physics, which have enabled us to engineer and control artificial quantum many-body systems at the level of individual atoms, ions and photons [1–3]. Particular attention is focused on nonequilibrium quantum dynamics [4–7], of which the arguably simplest situation is *quantum quenches* [8–10] — the system is initialized as a wave function $|\Psi_0\rangle$ which then evolves unitarily by a Hamiltonian H , with respect to which $|\Psi_0\rangle$ is typically a highly excited superposition state. The wave function at time t is then formally given by $|\Psi_t\rangle = e^{-iHt}|\Psi_0\rangle$. To model realistic quantum simulators, especially ultracold atoms and superconducting circuits with short-range interactions, we usually assume H to be *local*, in the sense that it can be written as a sum of short-range operators. In light of the rapid development of topological material science [11–14], there is growing interest in topological aspects of quench dynamics [15–36]. A fundamental question in this context is: given $|\Psi_0\rangle$ as the ground state of a gapped Hamiltonian H_0 , which may be trivial or topological, whether the topology of $|\Psi_t\rangle$ will change during time evolution, and, if yes, in what way. To make the topology well-defined, we may have to impose certain symmetries. For the sake of concreteness, we assume that H_0 and H share the same symmetries, if any. The answer to the above question has recently been given and is somewhat negative: for unitary symmetries or/and anti-unitary anti-symmetries [37], $|\Psi_t\rangle$ stays in the same *symmetry-protected topological* (SPT) phase [16, 17, 33, 34]. For anti-unitary symme-

tries or/and unitary anti-symmetries, the topological number of $|\Psi_t\rangle$ generally becomes ill-defined (or reduces) due to *dynamical symmetry breaking* [33, 34]. To understand this, we only have to note that $|\Psi_t\rangle$ is the ground state of [32, 33]

$$H(t) \equiv e^{-iHt} H_0 e^{iHt}, \quad (1)$$

which shares the same spectrum as H_0 . The conservation of topological number follows from the fact that $H(t)$ is gapped and continuously deformed from H_0 in a symmetry-preserving manner.

Since topological numbers are rather abstract quantities and take very different forms depending on the specific systems, we need a universal topological indicator to formalize the above qualitative analysis into a general, rigorous and, in principle, experimentally verifiable statement. Entanglement turns out to be an ideal candidate to demonstrate the persistence of topology. We can trace the time evolution of the *entanglement spectrum* (ES) for a proper bipartition, which contains crucial information of the entanglement pattern and is arguably the most widely used universal topological indicator that is applicable to both noninteracting [38–41] and interacting systems [42–47]. The ES is expected to be accessible in near-future ultracold-atom and trapped-ion experiments [48–50]. The persistence of SPT order thus manifests itself in that the ES stays gapless or degenerate [33, 34].

However, a vital point is missing in the above argument of topology conservation — defining SPT phases requires *locality* in the Hamiltonian [51], while $H(t)$ in Eq. (1) may become highly nonlocal after a long time. That is to say, the dynamically generated non-locality could obscure the SPT order in

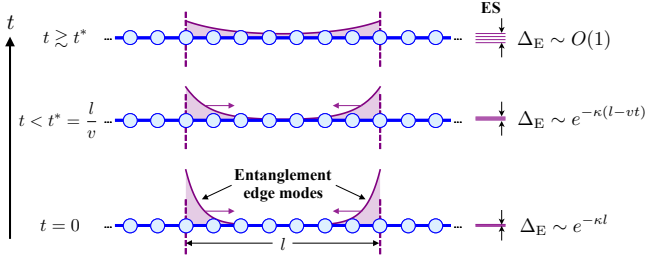


FIG. 1. Schematic illustration of the main result. (Bottom) Initially, the entanglement gap Δ_E of a length- l segment embedded in a 1D topological system is of the order of $e^{-\kappa l}$ due to an exponentially small overlap between the tails of the two entanglement edge modes. (Middle) After quench, these edge modes diffuse no faster than linearly, leading to an exponential increase in Δ_E . (Top) After a time proportional to l , these modes significantly diffuse into the bulk and the quasi-degeneracy in the ES is clearly lifted.

experimentally relevant length scales, which are often limited. It is thus practically, and of course theoretically important to understand at which length scale SPT order survives. Intuitively, we expect from the *bulk-edge correspondence* [52] that the SPT order should persist up to a time scale t^* when topological edge modes at different boundaries start to interfere and diffuse into the bulk, though a more refined analysis is needed to reach a definite conclusion.

A key concept to make the intuitive argument rigorous is the *Lieb-Robinson bound*. A natural assumption on locality has a striking consequence known as the *light-cone effect* — a local operator evolved by H spreads no faster than an emergent “light velocity” v_{LR} . Precisely speaking, there can be a nonzero leakage outside the light cone, which nevertheless decays exponentially with respect to the distance from the light cone. This rigorous result was derived by Lieb and Robinson nearly half a century ago [53], and is known as the Lieb-Robinson bound. An important implication of this bound is that, for two remote local operators separated by l , the equal-time correlation should stay exponentially small up to a time scale $t^* = \frac{l}{2v_{\text{LR}}}$, provided that the initial correlation decays exponentially [54]. Such a light-cone spreading of correlation as well as its breakdown for long-range interactions has recently been examined in ultracold-atom and trapped-ion experiments [55–57].

The Lieb-Robinson bound has been employed to reveal universal behaviors of quantum many-body systems. In addition to correlations between observables, *entanglement entropy* [58–60], which quantifies genuinely quantum correlation between a subsystem and its complement, has also been widely studied in quench dynamics [61–65]. Again, locality of H sets very fundamental limitations on the growth of entanglement entropy. From a quasi-particle viewpoint [66], we can infer from the Lieb-Robinson bound that the entanglement growth cannot be faster than linearly in time [54]. In particular, with the Lieb-Robinson bound applied to quasiadiabatic continuation [67], it has been proved that given $|\Psi_1\rangle$ and $|\Psi_2\rangle$ as the ground states of two gapped local Hamiltonians H_1 and H_2 that can be adiabatically connected to each other, $|\Psi_1\rangle$

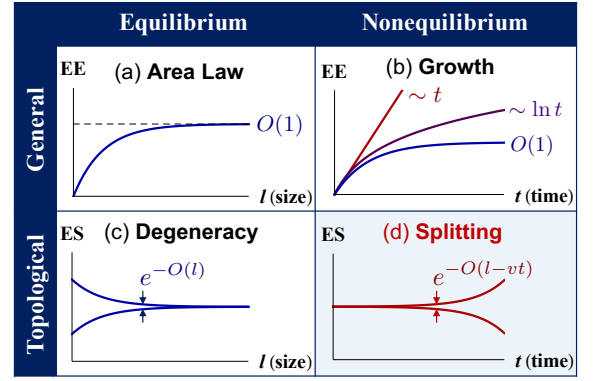


FIG. 2. Schematic illustrations of the most fundamental results on entanglement in 1D quantum many-body systems in and out of equilibrium, where the shaded part is rigorously established in this work. (a) The ground state of an arbitrary gapped local Hamiltonian obeys an entanglement-entropy (EE) area law. (b) After a quench, the entanglement-entropy growth exhibits universal features such as linear (red), logarithmic growth (purple) or saturation (blue), depending on whether the postquench Hamiltonian is thermal, many-body localized or Anderson localized, respectively. (c) If the system is in an SPT phase, the ES is degenerate up to an exponentially small correction. (d) Rigorous Lieb-Robinson bound on the lifting of ES degeneracy for SPT systems after quenches, which constitutes the primary result of this paper.

obeys an entanglement *area law* [68] if and only if $|\Psi_2\rangle$ also does [69]. In one dimension (1D), where all the gapped local Hamiltonians are adiabatically connected [70–72], we always obtain an area law by choosing $|\Psi_1\rangle$ to be a product state. It is worth mentioning that, without referring to any Hamiltonian, all the 1D wave functions with exponentially decaying correlations have recently been proved to obey the area law [73–75]. Moreover, the measurement of the entanglement (Rényi) entropy has been achieved in ultracold-atom and trapped-ion experiments [76–79].

According to the light-cone picture, we can anticipate that the time scale of the Lieb-Robinson bound roughly estimates how long it takes for a topological edge mode to completely diffuse into the bulk, after which the SPT order becomes invisible. This argument may remain applicable if the physical edge is replaced by an artificial entanglement cut, which can always be done even if there are no physical boundaries. In this case, reinterpreting l as a subsystem size, we expect that the ES should stay nearly gapless or degenerate with precision $e^{-O(l)}$ until t^* [80]. Such an expectation has been numerically verified in several free-fermion models [81–83]. It is thus natural to conjecture the existence of a Lieb-Robinson bound on the *entanglement gap* (to be exactly defined in a moment):

$$\Delta_E \leq C e^{-\kappa(l-vt)}. \quad (2)$$

Here $v = 2v_{\text{LR}}$, κ estimates an inverse correlation length and C is a prefactor that is at most polynomial in terms of l and t . See Fig. 1 for a schematic illustration for 1D systems.

In this paper, we *prove* Eq. (2) for general 1D SPT systems undergoing nonequilibrium unitary evolution. In fact, a rig-

orous result has been obtained for intrinsic topological order from the perspective of local indistinguishability between degenerate ground states [54]. However, unlike the derivation in Ref. [54] which is a rather straightforward application of the Lieb-Robinson bound on operator spreading [53] and is irrelevant to symmetries, the ES is not a conventional observable and symmetries play a crucial role in protecting 1D topological phases. Nevertheless, we find that the entanglement gap can be rigorously bounded by some correlation-related quantities, which obey the Lieb-Robinson bound. The central idea is based on the powerful *Weyl's perturbation theorem* [84], which guarantees the spectral shift between two Hermitian operators to be rigorously bounded by the operator norm of their difference. In addition to the several well-known results such as the entanglement area law [85–89], the bounds on entanglement growth [69, 90] and the entanglement detection of topological phases [38–47, 91, 92], our work brings about yet another rigorous and fundamental result on the entanglement in quantum many-body systems [93–95]. As shown Fig. 2, our work lays a corner stone for exploring *exact results* on the entanglement properties of SPT systems out of equilibrium. Also, we hope that the ideas and methods developed in this work could stimulate further exploration of rigorous results on various spectra, which appear ubiquitously in physics.

This paper is structured as follows. In Sec. II, we review the basic properties of the ES and the notion of dynamical symmetry breaking. In Sec. III, we define the entanglement gap and present the main results, i.e., the explicit forms of Lieb-Robinson bounds. In Sec. IV, we focus on the single-particle entanglement gap in quenched free-fermion systems and derive the first main result (Theorem 1). In particular, we derive an almost optimal Lieb-Robinson bound for free-fermion systems and justify the quasi-particle picture. In Sec. V, we focus on the many-body entanglement gap in the tensor-network setting and derive the second main result (Theorem 2). We discuss the impact of partial symmetry breaking, the effects of disorder and long-time dynamics in Sec. VI. Finally, we summarize the main results of this paper and provide some outlook in Sec. VII. We relegate some technical details to appendices to avoid digressing from the main subject.

II. PRELIMINARIES

We begin by clarifying the definitions of single-particle and many-body ES for free-fermion and general systems. We also briefly review why 1D SPT order renders the many-body ES to be degenerate. Finally, we review the notion of dynamical symmetry breaking and point out the relevant symmetries that can protect SPT order in quench dynamics.

A. Definition of the ES

We consider a 1D lattice with the total number of unit cells denoted as L . Each unit cell contains d internal degrees of freedoms, including spins, orbitals, sublattices and so on. For spin systems, d gives the Hilbert-space dimension of a single

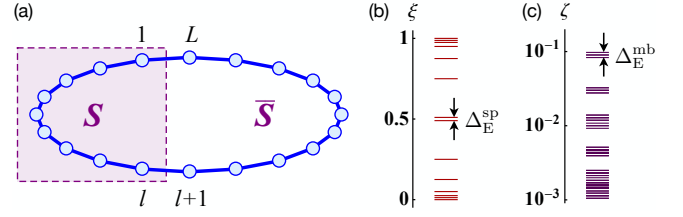


FIG. 3. (a) Entanglement bipartition in a 1D lattice subject to the periodic boundary condition. The reduced density operator ρ_S is obtained by tracing out the degrees of freedom in \bar{S} . The total length and the length of subsystem S are denoted as L and l , respectively. (b) Typical single-particle ES of a topological particle-hole symmetric system. The single-particle entanglement gap Δ_E^{sp} (16) is defined as the splitting between the two modes closest to one half in the ES. (c) Typical many-body ES of an SPT system. The many-body entanglement gap Δ_E^{mb} (25) is defined to be the width of those modes in the ground-state manifold of the many-body entanglement Hamiltonian that become generate in the thermodynamic limit.

unit cell. Given a local basis $\{|j\rangle\}_{j=1}^d$, an arbitrary many-body wave function can be expressed as a superposition of Fock states $|j_1 j_2 \dots j_L\rangle \equiv |j_1\rangle \otimes |j_2\rangle \otimes \dots \otimes |j_L\rangle$ with $j_s = 1, 2, \dots, d$ for $\forall s = 1, 2, \dots, L$. For fermionic systems, the local Hilbert-space dimension is 2^d since each mode can be either occupied or unoccupied. A complete fermionic Fock basis is given by $\prod_{\{n_{ja}\}} (c_{ja}^\dagger)^{n_{ja}} |\text{vac}\rangle$ with $n_{ja} = 0, 1$ for $\forall j = 1, 2, \dots, L$ and $a = 1, 2, \dots, d$, where $|\text{vac}\rangle$ is the Fock vacuum and c_{ja}^\dagger creates a fermion with internal state a in the j th unit cell and satisfies $\{c_{j'a'}, c_{ja}\} = \delta_{j'j} \delta_{a'a}$ and $\{c_{j'a'}, c_{ja}\} = 0$.

To study the bipartite entanglement properties, we divide the entire system into two subsystems S and \bar{S} (see Fig. 3), which consists of l and $L-l$ adjacent unit cells, respectively. For convenience, we label the unit cells in S as $1, 2, \dots, l$. Given a many-body wave function $|\Psi\rangle$, we can always define the *many-body ES* as the eigenvalues of the reduced density operator

$$\rho_S = \text{Tr}_{\bar{S}} |\Psi\rangle\langle\Psi|. \quad (3)$$

For simplicity, we require the ES to be positive since we can always truncate the Hilbert space of S into a subspace, within which ρ_S is positive definite. In particular, for free-fermion systems, ρ_S is a *Gaussian state* [96] in the sense that there exists a quadratic entanglement Hamiltonian $H_S = \sum_{j,j'=1}^l \sum_{a,a'=1}^d [H_S]_{j'a',ja} c_{j'a'}^\dagger c_{ja}$ [97] such that

$$\rho_S = \frac{e^{-H_S}}{\text{Tr} e^{-H_S}}. \quad (4)$$

Diagonalizing the entanglement Hamiltonian as $H_S = \sum_{n=1}^{ld} \epsilon_n f_n^\dagger f_n$, where f_n 's are related to c_{ja} 's via a unitary transformation, we can identify the *single-particle ES* as [98]

$$\xi_n = \frac{1}{e^{\epsilon_n} + 1}, \quad n = 1, 2, \dots, ld, \quad (5)$$

in terms of which the many-body ES reads

$$\zeta_{\{s_n\}} = \prod_{\{n: 0 < \xi_n < 1\}} \left[\frac{1}{2} + \frac{1}{2} s_n (1 - 2\xi_n) \right], \quad (6)$$

where $s_n = \pm 1$.

B. SPT-enforced ES degeneracy

For free-fermion systems, it is known that $\{1 - 2\xi_n\}_n$ is *exactly* the energy spectrum subject to the open boundary condition after band flattening [39]. To see this, we consider a gapped quadratic Hamiltonian in the diagonalized form $H = \sum_n E_n \psi_n^\dagger \psi_n$, which may not correspond to a translation-invariant system. Assuming the Fermi energy to be zero without loss of generality, we can define the single-particle projector onto the Fermi sea as

$$P_{<} \equiv \sum_{\{n: E_n < 0\}} |\psi_n\rangle \langle \psi_n|, \quad (7)$$

where $|\psi_n\rangle \equiv \psi_n^\dagger |\text{vac}\rangle$ is a single-particle eigenstate. With P_S denoted as the projector onto the single-particle Hilbert space of S , the single-particle ES $\{\xi_n\}_n$ coincides with the spectrum of $P_S P_{<} P_S$ [98]. The statement made in the beginning of this subsection follows from the fact that the involutory (i.e., being its own inverse) flattened Hamiltonian is given by

$$H^{\text{flat}} = \mathbb{I}^{\text{sp}} - 2P_{<}, \quad (8)$$

where \mathbb{I}^{sp} is the identity operator in the single-particle sector. From this exact correspondence, we know that there should be $\xi_n = \frac{1}{2}$ modes in the single particle ES for a topological insulator with boundary zero modes. According to Eq. (6), the corresponding many-body ES is necessarily degenerate.

To analyze noncritical interacting systems in 1D, we employ the *matrix-product-state* (MPS) formalism [99–102]. The validity of this formalism is rooted in the entanglement area law [68]. For simplicity, we focus on translation-invariant MPSs, which take the form of

$$|\Psi\rangle = \sum_{\{j_s\}_{s=1}^L} \text{Tr}[A_{j_1} A_{j_2} \dots A_{j_L}] |j_1 j_2 \dots j_L\rangle, \quad (9)$$

where $j_s = 1, 2, \dots, d$ and A_j 's are $D \times D$ matrices with D being the bond dimension. Each MPS is associated with a linear map on $\mathbb{C}^{D \times D}$:

$$\mathcal{E}(\cdot) \equiv \sum_{j=1}^d A_j(\cdot) A_j^\dagger. \quad (10)$$

Assuming the MPS to be *normal* [103], which rules out the possibility of spontaneous symmetry breaking, we can always perform gauge transformations of A_j 's, i.e., $A_j \rightarrow X A_j X^{-1}$ that leaves $|\Psi\rangle$ in Eq. (9) invariant, such that \mathcal{E} is a *unital channel*:

$$\mathcal{E}(\mathbb{1}_v) = \sum_{j=1}^d A_j A_j^\dagger = \mathbb{1}_v \quad (11)$$

TABLE I. Dynamical stability of unitary symmetries ($a = b = +$), anti-unitary symmetries ($a = -b = +$), unitary anti-symmetries ($a = -b = -$), and anti-unitary anti-symmetries ($a = b = -$), where a and b are given in Eq. (14).

a	b	Dynamical stability	Example
+	+	✓	Parity symmetry
+	−	×	Time-reversal symmetry
−	+	×	Chiral symmetry
−	−	✓	Particle-hole symmetry

where $\mathbb{1}_v$ is the identity in $\mathbb{C}^{D \times D}$ acting on the *virtual* Hilbert space. If we further impose an on-site unitary symmetry, i.e., $\rho_g^{\otimes L} |\Psi\rangle = |\Psi\rangle$ for $\forall g \in G$ with G being a group and $\rho_g \in \text{U}(d)$ being a unitary representation of G , we can find a *projective representation* V_g with $V_g V_h = \omega_{g,h} V_{gh}$, $\omega_{g,h} \in \text{U}(1)$ for $\forall g, h \in G$ such that [104]

$$\sum_{j'=1}^d [\rho_g]_{jj'} A_{j'} = V_g^\dagger A_j V_g, \quad \forall j = 1, 2, \dots, d. \quad (12)$$

In the thermodynamic limit of subsystem S with length l , i.e., $\lim_{l \rightarrow \infty} \lim_{L \rightarrow \infty}$, the many-body ES is exactly given by $\{\lambda_\alpha \lambda_\beta\}_{\alpha, \beta=1}^D$, where $\{\lambda_\alpha\}_{\alpha=1}^D$ is the spectrum of Λ (> 0), that is uniquely determined from [100]

$$\mathcal{E}^\dagger(\Lambda) \equiv \sum_{j=1}^d A_j^\dagger \Lambda A_j = \Lambda, \quad \text{Tr } \Lambda = 1. \quad (13)$$

If $|\Psi\rangle$ is in an SPT phase, $\omega_{g,h}$ must correspond to a nontrivial element in the second cohomology group $H^2(G, \text{U}(1))$ [70–72], leading to degeneracy in λ_α 's [43]. This is because a nondegenerate λ_α implies that $\omega_{g,h}$ must be trivial, as will be proved in Sec. V B.

C. Dynamical symmetry breaking

While there is a huge variety of symmetries, we can classify them into four groups depending on whether the symmetry operator S commutes or anti-commutes with the Hamiltonian, and whether it is unitary or anti-unitary:

$$S H S^{-1} = a H, \quad S i S^{-1} = b i, \quad (14)$$

where $a, b = \pm$. Concretely, S is said to be symmetric (an anti-symmetric) if $a = +$ ($a = -$), and S is said to be unitary (anti-unitary) if $b = +$ ($b = -$). Note that H in Eq. (14) can be either on the single-particle level (for free-fermion systems) or on the many-body level (for interacting systems).

Now let us impose Eq. (14) to both H_0 and H , i.e., the Hamiltonians before and after a quench. Regarding the symmetry action on the parent Hamiltonian (1), we have

$$\begin{aligned} S H(t) S^{-1} &= S e^{-i H t} H_0 e^{i H t} S^{-1} \\ &= e^{-i a b H t} a H_0 e^{i a b H t} = a H(a b t). \end{aligned} \quad (15)$$

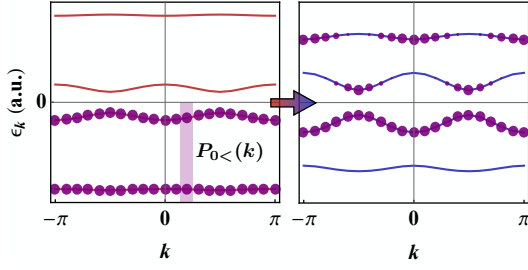


FIG. 4. Setting of Theorem 1 — quench in a free-fermion system with particle-hole symmetry. Initially, only the particle bands ($\epsilon_k < 0$) are occupied and the Bloch projector is denoted as $P_{0<}(k)$ (see Eq. (17)). The initial state is, in general, a highly excited state of the postquench Hamiltonian, whose hole bands ($\epsilon_k > 0$) can be significantly occupied.

Accordingly, when $ab = 1$, which means that S is either unitary and symmetric or anti-unitary and anti-symmetric, we have $[S, H(t)] = 0$ for $\forall t$. Otherwise, $H(t)$ no longer respects S in general due to the fact that $H(t)$ generally differs from $H(-t)$. This phenomenon is dubbed *dynamical symmetry breaking*, which reduces the number of symmetries relevant to SPT orders in quench dynamics [33]. See Table I for a brief summary.

III. MAIN RESULTS

We are now in a position to present the exact statement of our main results — Lieb-Robinson bounds on entanglement gaps.

For free-fermion systems, we examine all the Altland-Zirnbauer classes [105]. In 1D, it is known that there are five nontrivial classes, including one complex class AIII and four real classes BDI, D, DIII and CII [106, 107]. According to the previous analysis on dynamical symmetry breaking (especially Table I), we know that both classes BDI and DIII reduce to class D, class CII reduces to class C and class AIII reduces to class A. Since classes C and A are both trivial, it suffices to consider *class D*, which has an involutory particle-hole symmetry and is characterized by a \mathbb{Z}_2 topological number in 1D [108]. This is the only Altland-Zirnbauer class in 1D that does not suffer from dynamical symmetry breaking so that the SPT order persists in the thermodynamic limit [33].

Since the energy spectrum of a free-fermion system in class D is paired as $(\epsilon, -\epsilon)$, the ES should be divided as $(\xi, 1 - \xi)$. Hence, we can define the single-particle entanglement gap as

$$\Delta_E^{\text{sp}} \equiv 2 \min_n \left| \xi_n - \frac{1}{2} \right|. \quad (16)$$

In the presence of translation invariance, we can simply deal with the Bloch Hamiltonians and prove the following theorem.

Theorem 1 (Free fermions) *Consider two 1D translation-invariant lattice systems in class D, whose Bloch Hamiltonians are given by $H_0(k)$ and $H(k)$ and the former is gapped*

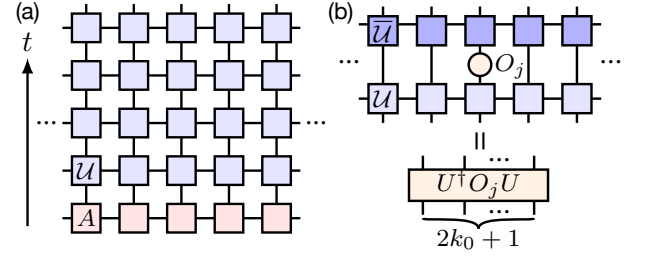


FIG. 5. (a) Setting of Theorem 2 — stroboscopic time evolution governed by an MPU (22) generated by $\mathcal{U}_{jj'}$, starting from an MPS (9) generated by A_j . (b) After evolution by an MPU, an on-site operator O_j stays local but acts nontrivially on (at most) $2k_0 + 1$ sites. Here k_0 is the smallest integer k such that the blocked tensor \mathcal{U}_k in Eq. (23) is simple.

and topologically nontrivial. We start from the ground state of $H_0(k)$ and make the following two assumptions: (i) the initial Bloch projector

$$P_{0<}(k) \equiv \oint_{\gamma_{<}} \frac{dz}{2\pi i} \frac{1}{z - H_0(k)} \quad (17)$$

is analytic on $\{k : |\text{Im}k| \leq \kappa, |\text{Re}k| \leq \pi\}$, where $\kappa > 0$ and $\gamma_{<}$ is a loop that encircles all the particle bands; (ii) $H(k + i\kappa)$ is well-defined and diagonalizable for $\forall k \in [-\pi, \pi]$, i.e.,

$$H(k + i\kappa) = \sum_{\alpha=1}^d \epsilon_{k+i\kappa, \alpha} |u_{k+i\kappa, \alpha}^{\text{R}}\rangle \langle u_{k+i\kappa, \alpha}^{\text{L}}|, \quad (18)$$

where $|u_{k+i\kappa, \alpha}^{\text{R}}\rangle$ ($\langle u_{k+i\kappa, \alpha}^{\text{L}}|$) is the right (left) Bloch eigenstate of the α -th band. Then the single-particle entanglement gap (16) of a length- l segment is upper bounded by

$$\Delta_E^{\text{sp}} \leq C e^{-\kappa(l-vt)} \quad (19)$$

during the time evolution governed by $H(k)$. Here

$$C = \int_{-\pi}^{\pi} \frac{dk}{2\pi} \left(\sum_{\alpha=1}^d \| |u_{k+i\kappa, \alpha}^{\text{R}}\rangle \| \| |u_{k+i\kappa, \alpha}^{\text{L}}\rangle \| \right)^2 \| P_{0<}(k+i\kappa) \| \quad (20)$$

with $\| \cdot \|$ being the operator norm and

$$v = \kappa^{-1} \max_{k \in [-\pi, \pi], \alpha, \beta} \text{Im}(\epsilon_{k+i\kappa, \alpha} - \epsilon_{k+i\kappa, \beta}) \quad (21)$$

depends on neither l nor t .

As illustrated in Fig. 4, this theorem depends crucially on the band picture of translation-invariant free-fermion systems. We can show that a positive κ satisfying (i) and (ii) exists under quite general assumptions (see Appendix A).

For interacting SPT systems, we restrict ourselves to the tensor networks formalisms. That is, as illustrated in Fig. 5(a), we start from an MPS and consider the *stroboscopic* dynamics governed by a *matrix-product unitary* (MPU) [109–112]

$$U = \sum_{\{j_s, j'_s\}_{s=1}^L} \text{Tr}[\mathcal{U}_{j_1 j'_1} \mathcal{U}_{j_2 j'_2} \dots \mathcal{U}_{j_L j'_L}] |j_1 j_2 \dots j_L\rangle \langle j'_1 j'_2 \dots j'_L|, \quad (22)$$

which is a special class of matrix-product operators [113] satisfying $U^\dagger U = \mathbb{1}^{\otimes L}$. We assume that the MPU respects the same symmetries of the initial MPS, i.e., $[\rho_g^{\otimes L}, U] = 0$ for $\forall g \in G$, and that it belongs to the trivial cohomology class so that the time-evolved MPS stays in the same SPT phase [111]. It is known that by putting together k sites into one such that the building block \mathcal{U} becomes \mathcal{U}_k :

$$\mathcal{U}_k \equiv \underbrace{\mathcal{U} \mathcal{U} \cdots \mathcal{U}}_k, \quad (23)$$

the MPU can for sufficiently large k be represented as a bilayer unitary circuit with each unitary operator acting on two adjacent blocked sites [114]:

$$\mathcal{U}_k \mathcal{U}_k \mathcal{U}_k \mathcal{U}_k \mathcal{U}_k = \begin{array}{c} \text{---} \text{---} \text{---} \text{---} \text{---} \\ \text{---} \text{---} \text{---} \text{---} \text{---} \\ \text{---} \text{---} \text{---} \text{---} \text{---} \end{array} \quad (24)$$

Whenever such a representation is possible, we call the building-block tensor *simple* [110]. In fact, given \mathcal{U} and k such that \mathcal{U}_k is simple, $\mathcal{U}_{k'}$ is also simple for $\forall k' \geq k$. The smallest k that makes \mathcal{U}_k simple, which we denote as k_0 , has a clear physical interpretation as the *Lieb-Robinson length* — as shown in Fig. 5(b), any on-site operator evolved by the MPU generated by \mathcal{U} acts nontrivially on at most $2k_0 + 1$ sites. Further details on MPUs can be found in Appendix E.

Unlike free-fermion systems in class D, which are characterized by a \mathbb{Z}_2 number so that there is at most one pair of stable topological entanglement modes near $\xi = \frac{1}{2}$ (leading to $2^2 = 4$ -fold degeneracy in the many-body ES), the many-body ES of an SPT MPS can be r^2 -fold degenerate for $\forall r = 2, 3, 4, \dots$ in the thermodynamic limit. Here the square r^2 arises from the fact that a subsystem has two edges. Minimal symmetries that realize these SPT MPSs are $\mathbb{Z}_r \times \mathbb{Z}_r$, whose second-order cohomology groups read $H^2(\mathbb{Z}_r \times \mathbb{Z}_r, \text{U}(1)) = \mathbb{Z}_r$. Given r and a many-body ES $\{\zeta_n\}_n$ with $\zeta_n \geq \zeta_{n+1}$ (note that larger ζ corresponds to lower eigenvalue of the entanglement Hamiltonian), we define the many-body entanglement gap to be

$$\Delta_E^{\text{mb}} \equiv |\zeta_1 - \zeta_{r^2}|. \quad (25)$$

Our main theorem is the following.

Theorem 2 (Interacting systems) *Starting from an infinite SPT MPS with bond dimension D , the many-body entanglement gap (25) of a length- l subsystem after t steps of time evolution by a trivial symmetric MPU generated by \mathcal{U} with bond dimension D_U is bounded from above by*

$$\Delta_E^{\text{mb}} \leq C(l - 2k_0 t)^{D^2-1} e^{-\kappa(l-vt)} \quad (26)$$

for any $l - 2k_0 t \geq \frac{1+\mu}{1-\mu}$. Here k_0 is the smallest integer blocking number that makes \mathcal{U}_{k_0} simple and μ is the spectrum radius of $\mathcal{E} - \mathcal{E}^\infty$, where \mathcal{E} is defined in Eq. (10) for the initial

MPS and $\mathcal{E}^\infty \equiv \lim_{n \rightarrow \infty} \mathcal{E}^n$, $\kappa = -\ln \mu$, $v = 2k_0 - \frac{\ln D_U}{\ln \mu}$, and the coefficient

$$C = 4e^2 D^2 (D^2 + 1) \mu^{1-D^2} (1 + \mu)^{D^2 + \frac{1}{2}} (1 - \mu)^{D^2 - \frac{5}{2}} \quad (27)$$

depends only on the initial MPS.

Let us explain why we focus on the stroboscopic dynamics generated by an MPU rather than a continuous dynamics generated by a local Hamiltonian. First, we expect this setting to be good enough because we can efficiently approximate a finite-time evolution generated by a local Hamiltonian as a bilayer unitary circuit [115], which is equivalent to an MPU or a quantum cellular automaton [110]. The efficiency is ensured by the conventional Lieb-Robinson bound. By showing that the spectral shift is rigorously bounded by the approximation error, we expect a similar Lieb-Robinson bound on the many-body entanglement gap for continuous quench dynamics (see Appendix F). Second, this formalism is of intrinsic interest for its own sake — it gives exact descriptions for some Floquet systems [116–118] and quantum circuits [119–127], which have intensively been studied in the context of nonequilibrium phases of matter and information scrambling. Moreover, this theorem exemplifies the power of tensor networks as *analytical* methods for predicting long-time dynamical behaviors of interacting quantum many-body systems far from equilibrium, which are hardly accessible in numerics.

IV. FREE FERMIONS

As mentioned above, for quench dynamics within the same Altland-Zirnbauer class [105–107], the only nontrivial class in 1D that does not suffer from (partial) “dynamical symmetry breaking” is class D [33]. In fact, previous numerical studies on the Su-Schrieffer-Heeger (SSH) model [81] and the Kitaev chain [82] have revealed that the $\xi = \frac{1}{2}$ modes split after a characteristic time scale $t^* \sim \frac{l}{2v_{\text{max}}}$, where l is the length of the subsystem and v_{max} is the maximal group velocity of band dispersions. In Fig. 6(b), we reproduce the splitting dynamics in the SSH model (Fig. 6(a)), which shows that not only the topological entanglement mode but also the *full* ES splits. In the following, we rigorously establish the underlying Lieb-Robinson bound on the ES splitting stated in Theorem 1.

A. Zero entanglement gap for symmetric bipartition

We first point out a crucial proposition — for half-chain entanglement cut, i.e., $l = \frac{L}{2}$, the topological entanglement modes will be pinned *exactly* at $\frac{1}{2}$ at any time (see Fig. 6(b)). Note that we can always choose the anti-unitary and involutory particle-hole-symmetry operator \mathcal{C} to be the complex conjugation \mathcal{K} [128]. Under this basis, we have $H = iR$ with R being a skew-symmetric real matrix. Suppose that H is flat-topped so that $R^2 = -\mathbb{I}^{\text{sp}}$. If $\text{Pf } R = -1$, where Pf denotes the Pfaffian, there will be a pair of topological entanglement modes exponentially close to $\xi = \frac{1}{2}$. With the translation

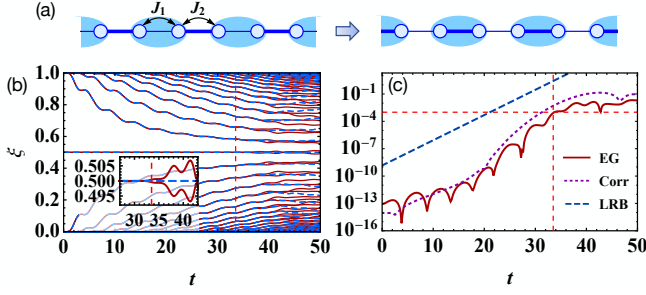


FIG. 6. (a) Quench protocol in the SSH model. (b) Single-particle ES dynamics after the quench. The parameters are quenched as $(J_1, J_2) = (0.5, 1) \rightarrow (1, 0.5)$ and $l = 40$. The red solid and blue dashed curves correspond to $L = \infty$ and $L = 2l$, respectively. In the former case, the single-particle ES splits after $t^* \sim 33$ (indicated by the red dashed line and determined by threshold $\Delta_E^{\text{sp}} = 10^{-3}$ as shown in (c)). Inset: Zoom in on the splitting of the topological entanglement modes. (c) Dynamics of the single-particle entanglement gap for $L = \infty$ (solid curve). The equal-time correlation $\|\langle j | P_{\infty}^{\infty}(t) | j + l \rangle\|$ (purple dotted curve) and the Lieb-Robinson bound (blue dashed curve) given by Theorem 1 with $\kappa = 0.6$ are superimposed for the sake of comparison.

invariance assumed, the system at least exhibits a *half-chain translation symmetry*, leading to

$$R = \begin{bmatrix} R_d & R_o \\ R_o & R_d \end{bmatrix} = \sigma^0 \otimes R_d + \sigma^x \otimes R_o, \quad (28)$$

where R_d and R_o are both real and skew-symmetric and $\sigma^0 = \begin{bmatrix} 1 & 0 \\ 0 & 1 \end{bmatrix}$, $\sigma^x = \begin{bmatrix} 0 & 1 \\ 1 & 0 \end{bmatrix}$. Moreover, the half-chain ES is given by the spectrum of $\frac{1}{2}(1 - iR_d)$. From $R^2 = -\mathbb{I}^{\text{sp}}$ we obtain

$$R_d^2 + R_o^2 = -\mathbb{I}^{\text{half}}, \quad \{R_d, R_o\} = \mathbb{O}^{\text{half}}, \quad (29)$$

where \mathbb{I}^{half} and \mathbb{O}^{half} are the half-chain identity and zero operators within the single-particle sector. Provided that $R_o^2 < 0$, we can find an anti-unitary operator

$$\mathcal{A} \equiv i(-R_o^2)^{-\frac{1}{2}} R_o \mathcal{K}, \quad (30)$$

such that

$$\mathcal{A}^2 = -\mathbb{I}^{\text{half}}, \quad [\mathcal{A}, iR_d] = 0. \quad (31)$$

Due to the interplay between the *Kramers degeneracy* enforced by \mathcal{A} and the nontrivial \mathbb{Z}_2 topology, two quasi-zero modes of iR_d must be pinned exactly at zero. Since the \mathbb{Z}_2 index stays unchanged in quench dynamics, the topological entanglement mode should always be pinned at $\frac{1}{2}$, leading to a persistent zero single-particle entanglement gap.

Even if R_o is not invertible so that \mathcal{A} in Eq. (30) becomes ill-defined, we can still show that all the eigenvalues of iR_d falling in the range $(-1, 1)$ are degenerate. For an arbitrary normalized eigenvector ϕ with $iR_d \phi = \epsilon \phi$, $\epsilon \in (-1, 1)$, we can construct

$$\tilde{\phi} \equiv \frac{1}{\sqrt{1 - \epsilon^2}} R_o \bar{\phi}, \quad (32)$$

such that $\tilde{\phi}^\dagger \tilde{\phi} = 1$ and $iR_d \tilde{\phi} = \epsilon \tilde{\phi}$. Moreover, we have

$$\begin{aligned} \phi^\dagger \tilde{\phi} &= \frac{1}{\sqrt{1 - \epsilon^2}} \phi^\dagger R_o \bar{\phi} = \frac{1}{\sqrt{1 - \epsilon^2}} (\phi^\dagger R_o \bar{\phi})^T \\ &= -\frac{1}{\sqrt{1 - \epsilon^2}} \phi^\dagger R_o \bar{\phi} = -\phi^\dagger \tilde{\phi}, \end{aligned} \quad (33)$$

which means $\tilde{\phi}$ is orthogonal to ϕ .

It is worth mentioning that such an emergent symmetry in ES has systematically been studied in Ref. [41]. In addition to the above physical analysis, we also provide a rigorous proof in Appendix B.

B. General idea

To highlight the finite size of a periodic lattice, we will hereafter use $P_{<}^{(L)}$ instead of $P_{<}$ in Eq. (7) as the single-particle projector onto the Fermi sea, where L denotes the number of unit cells. As mentioned in Sec. II B, with the single-particle projector onto a subsystem S denoted as P_S , the single-particle ES coincides with the spectrum of $P_S P_{<}^{(L)} P_S$ [98]. We have shown in the previous subsection that for $L = 2l$ with l being the length of S , whenever H^{flat} in Eq. (8) is characterized by a nontrivial \mathbb{Z}_2 number protected by the particle-hole symmetry, the spectrum of $P_S P_{<}^{(L)} P_S$ contains two degenerate eigenstates with eigenvalue $\frac{1}{2}$ and the entanglement gap exactly vanishes. To prove Theorem 1, it suffices to prove that the spectral shift from $P_S P_{<}^{(2l)} P_S$ to $P_S P_{<}^{(\infty)} P_S$ is exponentially small until a time scale proportional to l . To this end, a natural idea is to utilize the following Weyl's perturbation theorem.

Theorem 3 (Weyl's perturbation theorem) *Consider two Hermitian operators O and O' on a finite Hilbert space. Denoting the j th largest eigenvalue of O and O' as λ_j and λ'_j , respectively, we have*

$$|\lambda_j - \lambda'_j| \leq \|O - O'\|. \quad (34)$$

For self-containedness, we provide a brief proof in Appendix C. According to this theorem, denoting the n th largest eigenvalue of $P_S P_{<}^{(L)} P_S$ as $\xi_n^{(L)}$, we have

$$|\xi_n^{(L)} - \xi_n^{(\infty)}| \leq \|P_S P_{<}^{(L)} P_S - P_S P_{<}^{(\infty)} P_S\|. \quad (35)$$

According to Eq. (16), we have the following corollary: for a topological class D system, the single-particle entanglement gap is bounded from above as

$$\Delta_E^{\text{sp}} \leq 2\|P_S P_{<}^{(2l)} P_S - P_S P_{<}^{(\infty)} P_S\|. \quad (36)$$

It is thus sufficient to find a Lieb-Robinson bound on the right-hand side (rhs) of Eq. (36), which measures the finite-size correction to the correlation in a finite subsystem S .

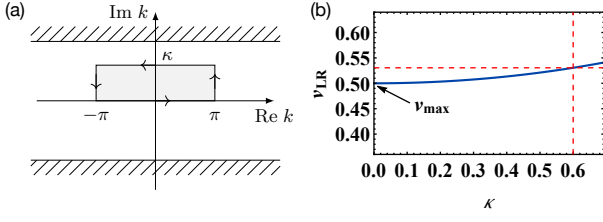


FIG. 7. (a) Contour deformation used in Eq. (42). For sufficiently small κ , the shaded area inside the contour $\partial\{k : |\text{Re } k| \leq \pi, 0 \leq \text{Im } k \leq \kappa\}$ contains no poles and thus $\int_{-\pi}^{\pi} = \int_{-\pi+i\kappa}^{\pi+i\kappa}$. Note that the two integrals along the vertical edges cancel out due to the 2π -periodicity in $\text{Re } k$. (b) κ dependence of the Lieb-Robinson velocity $v_{\text{LR}} = \frac{1}{2}v$ predicted by Lemma 1 for the SSH model with $(J_1, J_2) = (1, 0.5)$. The maximal group velocity $v_{\text{max}} = \min\{J_1, J_2\}$ naturally appears in the limit of $\kappa \rightarrow 0$. The red dashed lines correspond to the specific choice $\kappa = 0.6$ used in Fig. 6(c). The monotonicity of v_{LR} with respect to κ holds for general analytic Bloch Hamiltonians (see Appendix A 3).

Before going into rigorous proofs, let us first give an intuitive argument based on the *Wannier-function* picture [129]. Note that the projector onto the Fermi sea can be expressed as

$$P_{<}^{(L)} = \sum_{j \in \mathbb{Z}_L, \alpha \in \mathcal{O}} |W_{j\alpha}^{(L)}\rangle \langle W_{j\alpha}^{(L)}|, \quad (37)$$

where $|W_{j\alpha}^{(L)}\rangle$ is a Wannier function of the α th band centered at the j th site, $\mathbb{Z}_L \equiv \{1, 2, \dots, L\}$ consists of all the sites and \mathcal{O} consists of all the occupied bands. Since $|W_{j\alpha}^{(L)}\rangle$ is exponentially localized in real space [130–132], we expect an exponentially small difference between $|W_{j\alpha}^{(L)}\rangle$ and $|W_{j\alpha}^{(\infty)}\rangle$. By the same token, although $P_{<}^{(\infty)}$ contains infinitely more Wannier-function projectors than $P_{<}^{(L)}$, such a difference should again become exponentially small after being projected by P_S , provided that both l and $L - l$ are sufficiently large compared with the localization length of a Wannier function. When the system is driven out of equilibrium, we expect the Wannier function to spread no faster than linearly, leading to a light-cone behavior of $\|P_S P_{<}^{(L)} P_S - P_S P_{<}^{(\infty)} P_S\|$. We will later make this argument rigorous for translation-invariant systems. Note that the above argument seems to be equally applicable to disordered systems with exponentially localized Wannier functions [133].

C. Lieb-Robinson bound on correlations in free-fermion systems

An important ingredient in our proof is the conventional Lieb-Robinson bound on correlation functions. While the Lieb-Robinson bound for general interacting systems is certainly applicable to free-fermion systems, such a bound is usually very loose since it only involves a very limited amount of information about the system such as the hopping range and the maximal hopping amplitude. Here, we derive a greatly

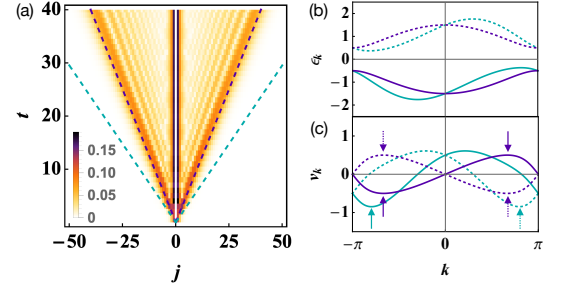


FIG. 8. (a) Dynamics of spatial correlations $\| \langle j | P_{<}(t) | 0 \rangle \|$ ($j \neq 0$) in an SSH chain involving $L = 101$ unit cells. The parameters are the same as those in Fig. 6. An additional particle-hole symmetric term $H_{\text{PHS}} = \sum_{j,a=A,B} iJ(c_{j+1,a}^\dagger c_{ja} - \text{H.c.})$ does not change the dynamics of correlations. The dashed lines are given by $j = \pm v_{\text{max}} t$, where v_{max} is the largest group velocity of the SSH model with (green) or without (purple) the additional term H_{PHS} . (b) Band dispersions and (c) the corresponding group velocities of the SSH model (purple curves) and that with the additional term (green curves) with $J = 0.5$. The arrows indicate where $v_{k\alpha}$ reaches its maximal absolute value. The solid and dotted curves correspond to the particle and hole bands, respectively.

improved Lieb-Robinson bound on the correlation functions in translation-invariant free-fermion systems. Our result is almost optimal in the sense that the Lieb-Robinson velocity reaches the maximal (relative) group velocity of band dispersions in the semiclassical limit.

A nice property of free-fermion systems is that, according to Wick's theorem, all the correlation functions can be decomposed into two-point correlation functions. Moreover, if the wave function is a particle-number eigenstate, only the correlators like $\langle c^\dagger c \rangle$ are relevant. To compute such a correlator in the quench dynamics, we can use the formula

$$\langle \Psi_t | c_{j'a'}^\dagger c_{ja} | \Psi_t \rangle = \langle j'a' | P_{<}(t) | ja \rangle, \quad (38)$$

where $|ja\rangle = c_{ja}^\dagger |\text{vac}\rangle$ and $P_{<}(t) \equiv e^{-iHt} P_{0<} e^{iHt}$ is the time-evolved single-particle projector onto the Fermi sea. To measure the strength of correlation at the length scale $|j - j'|$, we can consider the norm of $\langle j | P_{<}(t) | j' \rangle$, which can be shown to obey a Lieb-Robinson bound given by the following lemma.

Lemma 1 Consider a time-evolved projector $P_{<}^{(L)}(t) \equiv e^{-iHt} P_{0<}^{(L)} e^{iHt}$, where $P_{0<}^{(L)}$ is the projector onto the Fermi sea of H_0 , which is gapped, and denote the Bloch Hamiltonians of H_0 and H as $H_0(k)$ and $H(k)$, respectively. Then for $\forall \kappa > 0$ such that (i) $P_{0<}(k) \equiv \sum_{\alpha \in \mathcal{O}} |u_{k\alpha}\rangle \langle u_{k\alpha}|$ (see also Eq. (17)) is analytic over $\{k : |\text{Re } k| \leq \pi, |\text{Im } k| \leq \kappa\}$, where $|u_{k\alpha}\rangle, \alpha \in \mathcal{O}$ is the normalized Bloch eigenstate of the α th occupied band, and (ii) $H(k + i\kappa)$ is well-defined and diagonalizable for $\forall k \in [-\pi, \pi]$, we have

$$\| \langle j | P_{<}^{(\infty)}(t) | j' \rangle \| \leq C e^{-\kappa(|j-j'| - vt)}, \quad \forall j, j' \in \mathbb{Z}, \quad (39)$$

where $|j\rangle$ is the state localized at the j th site, and C and v are given in Eqs. (20) and (21).

Proof.— After analytic continuation, the Hermiticity constraints on the Bloch Hamiltonians are generalized to $H_0(k)^\dagger = H_0(\bar{k})$ and $H(k)^\dagger = H(\bar{k})$ (see Appendix A 1). Accordingly, the Bloch projector $P_{0<}(k)$ satisfies

$$\begin{aligned} P_{0<}(k)^\dagger &\equiv - \oint_{\gamma_{<}} \frac{d\bar{z}}{2\pi i} \frac{1}{\bar{z} - H_0(k)^\dagger} \\ &= \oint_{\gamma_{<}} \frac{d\bar{z}}{2\pi i} \frac{1}{\bar{z} - H_0(\bar{k})} = P_{0<}(\bar{k}), \end{aligned} \quad (40)$$

where $\gamma_{<}$ is a loop that encircles the energies of all the occu-

pied bands. Note that

$$\begin{aligned} \langle j | P_{<}^{(\infty)}(t) | j' \rangle &= \int_{-\pi}^{\pi} \frac{dk}{2\pi} e^{ik(j-j')} P_{<}(k, t) \\ &= (\langle j' | P_{<}^{(\infty)}(t) | j \rangle)^\dagger, \end{aligned} \quad (41)$$

where $P_{<}(k, t) \equiv e^{-iH(k)t} P_{0<}(k) e^{iH(k)t}$. This implies $\|\langle j | P_{<}^{(\infty)}(t) | j' \rangle\| = \|\langle j' | P_{<}^{(\infty)}(t) | j \rangle\|$, and therefore we can assume $j \geq j'$ without loss of generality. By deforming the contour of integration (see Fig. 7(a)) and applying spectral decomposition to $H(k + i\kappa)$, which is generally non-Hermitian, we can bound the norm of Eq. (41) from above by

$$\begin{aligned} \|\langle j | P_{<}^{(\infty)}(t) | j' \rangle\| &= e^{-\kappa|j-j'|} \left\| \int_{-\pi}^{\pi} \frac{dk}{2\pi} e^{ik(j-j')} e^{-iH(k+i\kappa)t} P_{0<}(k+i\kappa) e^{iH(k+i\kappa)t} \right\| \\ &= e^{-\kappa|j-j'|} \left\| \sum_{\alpha, \beta} \int_{-\pi}^{\pi} \frac{dk}{2\pi} e^{ik(j-j')} e^{-i(\epsilon_{k+i\kappa, \alpha} - \epsilon_{k+i\kappa, \beta})t} |u_{k+i\kappa, \alpha}^R\rangle \langle u_{k+i\kappa, \alpha}^L| P_{0<}(k+i\kappa) |u_{k+i\kappa, \beta}^R\rangle \langle u_{k+i\kappa, \beta}^L| \right\| \\ &\leq \sum_{\alpha, \beta} e^{-\kappa|j-j'|} \int_{-\pi}^{\pi} \frac{dk}{2\pi} e^{\text{Im}(\epsilon_{k+i\kappa, \alpha} - \epsilon_{k+i\kappa, \beta})t} \| |u_{k+i\kappa, \alpha}^R\rangle \langle u_{k+i\kappa, \alpha}^L| P_{0<}(k+i\kappa) |u_{k+i\kappa, \beta}^R\rangle \langle u_{k+i\kappa, \beta}^L| \| \\ &\leq e^{-\kappa|j-j'| + \max_{k \in [-\pi, \pi], \alpha, \beta} \text{Im}(\epsilon_{k+i\kappa, \alpha} - \epsilon_{k+i\kappa, \beta})t} \sum_{\alpha, \beta} \int_{-\pi}^{\pi} \frac{dk}{2\pi} \| |u_{k+i\kappa, \alpha}^R\rangle \langle u_{k+i\kappa, \alpha}^L| \| \| P_{0<}(k+i\kappa) \| \| |u_{k+i\kappa, \beta}^R\rangle \langle u_{k+i\kappa, \beta}^L| \|, \end{aligned} \quad (42)$$

which completes the proof of Lemma 1. \square

Let us discuss how our result is related to the conventional group velocity [134]

$$v_{k\alpha} = \frac{d\epsilon_{k\alpha}}{dk}. \quad (43)$$

In the presence of the sublattice symmetry, as is the case of the SSH model, the eigenenergies are paired as $\pm\epsilon_k$ for $\forall k \in [-\pi, \pi]$ (see purple curves in Fig. 8(b)), and v in Eq. (21) becomes

$$v = 2\kappa^{-1} \max_{k \in [-\pi, \pi], \alpha} |\text{Im} \epsilon_{k+i\kappa, \alpha}|. \quad (44)$$

The maximal group velocity

$$v_{\max} \equiv \max_{k \in [-\pi, \pi], \alpha} \left| \frac{d\epsilon_{k\alpha}}{dk} \right| \quad (45)$$

thus naturally emerges when $\kappa \rightarrow 0$ (see Fig. 7(b)) due to the relation $\epsilon_{k+i\kappa, \alpha} = \epsilon_{k\alpha} + i \frac{d\epsilon_{k\alpha}}{dk} \kappa + O(\kappa^2)$. Since the bound in Eq. (39) can be made rather small by a sufficiently large l for a given small κ , we expect that the Lieb-Robinson velocity $v_{\text{LR}} = \frac{1}{2}v$ [54] is essentially given by v_{\max} at large length scales. More precisely, suppose that we scale up l and t simultaneously while keeping $\frac{l}{t}$ fixed; then, as long as $\frac{l}{t} < 2v_{\max}$, we can always choose $\kappa > 0$ such that the bound in Eq. (39) scales like $e^{-O(l)}$ and thus vanishes in the thermodynamic limit. This is quite reasonable since the group velocity in Eq. (43) is derived in the semiclassical regime, where the length scale is much larger than the lattice constant [134].

In general, however, the energy dispersions are not paired at each k . This can be the case even if there is a particle-hole symmetry, which only requires $\epsilon_{k\alpha} = -\epsilon_{-k\bar{\alpha}}$ with $\bar{\alpha}$ being the particle-hole conjugation of α (see, for example, green curves in Fig. 8(b)). In the limit of $\kappa \rightarrow 0$, v in Eq. (21) generally reaches the maximal *relative group velocity*

$$v_{\text{mr}} \equiv \max_{k \in [-\pi, \pi], \alpha, \beta} \left(\frac{d\epsilon_{k\alpha}}{dk} - \frac{d\epsilon_{k\beta}}{dk} \right), \quad (46)$$

which is smaller than twice of the maximal group velocity (45) and thus gives a tighter bound on the propagation of correlation. For example, as shown in Fig. 8(a), the dynamics of correlation in the SSH model does not change in the presence of an additional particle-hole symmetric term, which enhances the maximal group velocity (see Fig. 8(c)) but leaves the relative group velocity invariant over the entire Brillouin zone.

One may ask whether v in Eq. (21) can be made smaller than Eq. (46) for some $\kappa > 0$ so that the Lieb-Robinson velocity can be even tighter. However, by employing a continuous version of the *majorization* technique [135], we can prove that Eq. (21) *increases monotonically* with respect to κ (see Fig. 7(b) for example and Appendix A 3 for the general proof). Therefore, our rigorous bound does *not* lead to any tighter bound than the maximal relative group velocity. This is physically reasonable since a completely destructive interference between the modes with maximal relative group velocities seems impossible due to the difference in wave numbers. Our result thus quantitatively justifies and refines the widely used quasiparticle picture on the propagation of correlation in

the quench dynamics [9], which, to our knowledge, has analytically been confirmed only in specific situations [136–138].

D. Proof of Theorem 1

We are now in a position to prove the first main result. To bound the single-particle entanglement gap (19) from the exponential decay in the correlation function, we need the following lemma.

Lemma 2 Denoting $P_{<}^{(L)}$ as the projector onto the Fermi sea of a length- L lattice system, we have

$$\langle j|P_{<}^{(L)}|j'\rangle - \langle j|P_{<}^{(\infty)}|j'\rangle = \sum_{n \in \mathbb{Z} \setminus \{0\}} \langle j|P_{<}^{(\infty)}|j' + nL\rangle \quad (47)$$

for $\forall j, j' \in \mathbb{Z}_L$.

This result arises from the combination of Eq. (37) and the relation between the Wannier functions on finite and infinite lattices (see Appendix D). Lemma 2 can be used to derive a bound on the finite-size correction to the correlation matrix, which determines the ES.

Lemma 3 Consider a length- l segment embedded in a gapped translation invariant 1D lattice system with length L ($1 \leq l < L \leq \infty$) under the periodic boundary condition. We denote the projector onto the Fermi sea as $P_{<}^{(L)}$. In the thermodynamic limit ($L \rightarrow \infty$), we assume that (justified in Lemma 1)

$$\|\langle j|P_{<}^{(\infty)}|j'\rangle\| \leq Ce^{-\kappa|j-j'|}, \quad \forall j, j' \in \mathbb{Z}, \quad (48)$$

where C and $\kappa > 0$ do not depend on j and j' . Then, we have

$$\|P_S P_{<}^{(L)} P_S - P_S P_{<}^{(\infty)} P_S\| \leq \frac{2C \sinh \kappa l}{(e^{\kappa L} - 1) \sinh \kappa}, \quad (49)$$

where $P_S \equiv \sum_{j=1}^l |j\rangle\langle j| \otimes \mathbb{1}_I$ is the projector onto the segment.

Proof.— According to Eq. (47), the norm of $\langle j|P_{<}^{(L)}|j'\rangle - \langle j|P_{<}^{(\infty)}|j'\rangle$ is bounded from above by

$$\begin{aligned} & \|\langle j|P_{<}^{(L)}|j'\rangle - \langle j|P_{<}^{(\infty)}|j'\rangle\| \\ & \leq \sum_{n \in \mathbb{Z} \setminus \{0\}} \|\langle j|P_{<}^{(\infty)}|j' + nL\rangle\| \\ & \leq C \sum_{n \in \mathbb{Z} \setminus \{0\}} e^{-\kappa|j-j'-nL|} \\ & = C \sum_{n=1}^{\infty} [e^{-\kappa(nL+j'-j)} + e^{-\kappa(nL+j-j')}] \\ & = \frac{2C \cosh \kappa(j-j')}{e^{\kappa L} - 1}, \end{aligned} \quad (50)$$

where Eq. (48) has been used. Using Eq. (50) and the norm inequality [139]

$$\|O\|^2 \leq \sum_{j,j'} \|O_{jj'}\|^2, \quad (51)$$

with $O_{jj'} \equiv P_j O P_{j'}$, $P_j P_{j'} = \delta_{jj'} P_j$ and $\sum_j P_j = \mathbb{1}$ for an arbitrary bounded partitioned operator $O = \sum_{j,j'} O_{jj'}$, we obtain

$$\begin{aligned} & \|P_S P_{<}^{(L)} P_S - P_S P_{<}^{(\infty)} P_S\|^2 \\ & \leq \sum_{j,j'=0}^{l-1} \|\langle j|P_{<}^{(L)}|j'\rangle - \langle j|P_{<}^{(\infty)}|j'\rangle\|^2 \\ & \leq 4C^2 \sum_{j,j'=1}^l \frac{\cosh^2 \kappa(j-j')}{(e^{\kappa L} - 1)^2} \\ & = \frac{2C^2 [(\sum_{j=1}^l e^{2\kappa j})(\sum_{j'=1}^l e^{-2\kappa j'}) + l^2]}{(e^{\kappa L} - 1)^2} \\ & \leq \left[\frac{2C \sinh \kappa l}{(e^{\kappa L} - 1) \sinh \kappa} \right]^2, \end{aligned} \quad (52)$$

where we have used $\sinh \kappa l \geq l \sinh \kappa$ for $l \geq 1$. \square

The remaining step to prove Theorem 1 is simply to combine Lemmas 3 and 1 with Eq. 36. By identifying C in Eq. (48) with $Ce^{\kappa vt}$ in Eq. (39), we find that Eq. (36) leads to Theorem 1.

Finally, let us discuss how to generalize Theorem 1 to a finite lattice with length $L > l$. The existence of such a Lieb-Robinson bound is already clear from the triangle inequality $|\xi_n^{(L)} - \xi_n^{(2l)}| \leq |\xi_n^{(2l)} - \xi_n^{(\infty)}| + |\xi_n^{(L)} - \xi_n^{(\infty)}|$, the rhs of which can be further bounded by Lemma 3. However, this bound is too loose since the exact degeneracy is not reproduced when $L = 2l$. To obtain a tighter bound, we use the following generalization of Lemma 2:

$$\begin{aligned} & \langle j|P_{<}^{(L_1)}|j'\rangle - \langle j|P_{<}^{(L_2)}|j'\rangle \\ & = \sum_{n_1 \in \mathbb{Z} \setminus \frac{\text{LCM}(L_1, L_2)}{L_1} \mathbb{Z}} \langle j|P_{<}^{(\infty)}|j' + n_1 L_1\rangle \\ & - \sum_{n_2 \in \mathbb{Z} \setminus \frac{\text{LCM}(L_1, L_2)}{L_2} \mathbb{Z}} \langle j|P_{<}^{(\infty)}|j' + n_2 L_2\rangle, \end{aligned} \quad (53)$$

where LCM denotes the least common multiple. Following the calculations in Lemma 3, we can use Eq. (53) to derive

$$\begin{aligned} \Delta_E^{\text{sp}} & \leq \frac{4C \sinh \kappa l}{\sinh \kappa} e^{\kappa vt} \\ & \times \left(\frac{1}{e^{\kappa L} - 1} + \frac{1}{e^{2\kappa l} - 1} - \frac{2}{e^{\kappa \text{LCM}(L, 2l)} - 1} \right), \end{aligned} \quad (54)$$

which reproduces Eq. (19) for $L = \infty$ and $\Delta_E^{\text{sp}} = 0$ for $L = 2l$. Moreover, the bound is $O(1)$ when L is close to l . This is reasonable because the many-body ES of a length- l segment should be the same as its complement with length $L-l$. If $L-l$ is comparable to or even smaller than the localization length of the entanglement edge modes, both many-body and single-particle entanglement gaps will be significantly nonzero.

V. INTERACTING SYSTEMS

Let us move on to interacting systems. It suffices to consider spin (bosonic) systems since interacting fermions can

be mapped onto spin systems via the Jordan-Wigner transformation, which preserves the locality in the presence of the fermion-parity superselection rule [140]. The only thing we should be cautious about is that fermionic SPT states with Majorana modes will be transformed into spontaneous symmetry broken states, as will be discussed in details in Sec. VE. Although the very notion of the band is no longer applicable, we can employ MPSs to efficiently describe the ground state of a gapped local Hamiltonian [141]. While the formalism is different, we can again upper bound the entanglement gap by a quantity closely related to the correlation of two local observables at the boundaries of the subsystem, as detailed in the following.

A. ES of an MPS

We consider a translation-invariant normal MPS in the canonical form [142], as given in Eq. (9). For an arbitrary orthonormal basis $\{|\alpha\rangle\}_{\alpha=1}^D$ on the virtual level, we can decompose Eq. (9) into

$$|\Psi\rangle = \sum_{\alpha,\beta} |\psi_{\alpha\beta}\rangle |\Phi_{\beta\alpha}\rangle, \quad (55)$$

where

$$\begin{aligned} |\psi_{\alpha\beta}\rangle &= \sum_{\{j_s\}_{s=1}^l} \langle\alpha|A_{j_1}A_{j_2}\dots A_{j_l}|\beta\rangle |j_1j_2\dots j_l\rangle, \\ |\Phi_{\beta\alpha}\rangle &= \sum_{\{j_s\}_{s=l+1}^L} \langle\beta|A_{j_{l+1}}A_{j_{l+2}}\dots A_{j_L}|\alpha\rangle |j_{l+1}j_{l+2}\dots j_L\rangle. \end{aligned} \quad (56)$$

In particular, if $|\alpha\rangle$'s are chosen to be the eigenstates of Λ in Eq. (13) with eigenvalues λ_α 's ($\sum_{\alpha=1}^D \lambda_\alpha = 1$), we have in the thermodynamic limit $L \rightarrow \infty$ [100]

$$\begin{aligned} \langle\Phi_{\beta\alpha}|\Phi_{\beta'\alpha'}\rangle &= \lim_{L\rightarrow\infty} \langle\beta'|\mathcal{E}^{L-l}(|\alpha'\rangle\langle\alpha|)|\beta\rangle \\ &= \langle\beta'|\mathcal{E}^\infty(|\alpha'\rangle\langle\alpha|)|\beta\rangle \\ &= \langle\beta'|\text{Tr}[\Lambda|\alpha'\rangle\langle\alpha|]\mathbb{1}_V|\beta\rangle \\ &= \lambda_\alpha \delta_{\beta,\beta'} \delta_{\alpha,\alpha'}. \end{aligned} \quad (57)$$

where $\mathcal{E}^\infty(\cdot) \equiv \lim_{L\rightarrow\infty} \mathcal{E}^L(\cdot) = \text{Tr}[\Lambda \cdot] \mathbb{1}_V$. Therefore, the reduced density matrix of subsystem $[1, l] \subset \mathbb{Z}$ (i.e., the segment consisting of sites $1, 2, \dots, l$) can be written as

$$\rho_{[1,l]} = \sum_{\alpha,\beta} \lambda_\alpha |\psi_{\alpha\beta}\rangle \langle\psi_{\alpha\beta}|. \quad (58)$$

Unlike $|\Phi_{\beta\alpha}\rangle$'s, $|\psi_{\alpha\beta}\rangle$'s are not strictly orthogonal to each other:

$$\begin{aligned} \langle\psi_{\alpha\beta}|\psi_{\alpha'\beta'}\rangle &= \lambda_\beta \delta_{\alpha,\alpha'} \delta_{\beta,\beta'} + \epsilon_{\alpha\beta,\alpha'\beta'}, \\ \epsilon_{\alpha\beta,\alpha'\beta'} &= \langle\alpha'|(\mathcal{E}^l - \mathcal{E}^\infty)(|\beta'\rangle\langle\beta|)|\alpha\rangle. \end{aligned} \quad (59)$$

Defining $|\phi_{\alpha\beta}\rangle \equiv \sqrt{\lambda_\alpha} |\psi_{\alpha\beta}\rangle$, we can simplify Eq. (58) as

$$\rho_{[1,l]} = \sum_{\alpha,\beta} |\phi_{\alpha\beta}\rangle \langle\phi_{\alpha\beta}| \quad (60)$$

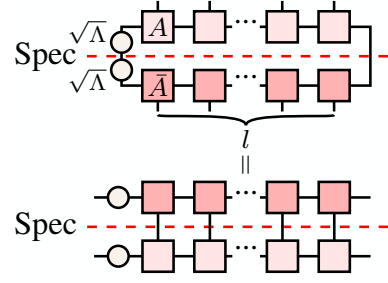


FIG. 9. The spectrum of Eq. (60) (top), which is nothing but the many-body ES of a length- l segment embedded in an infinite MPS, coincides with that of Eq. (68) (bottom) according to Lemma 4.

with

$$\langle\phi_{\alpha\beta}|\phi_{\alpha'\beta'}\rangle = \lambda_\alpha \lambda_\beta \delta_{\alpha,\alpha'} \delta_{\beta,\beta'} + \sqrt{\lambda_\alpha \lambda_{\alpha'}} \epsilon_{\alpha\beta,\alpha'\beta'}. \quad (61)$$

To estimate the spectrum of $\rho_{[1,l]}$, we need the following lemma.

Lemma 4 *Given a Hermitian operator $\rho = \sum_{j=1}^J |\phi_j\rangle\langle\phi_j| > 0$, where $|\phi_j\rangle$'s are generally neither normalized nor orthogonal to each other, the spectrum of ρ coincides with the nonzero part of the spectrum of $M \in \mathbb{C}^{J \times J}$ with $M_{jj'} = \langle\phi_j|\phi_{j'}\rangle$.*

Proof.— Denoting $\mathcal{V} = \text{span}\{|\phi_j\rangle\}_{j=1}^J$ on which ρ acts, we can expand any $|\psi\rangle \in \mathcal{V}$ as $|\psi\rangle = |\phi\rangle \mathbf{c} = \sum_{j=1}^J c_j |\phi_j\rangle$, where $|\phi\rangle \equiv [|\phi_1\rangle, |\phi_2\rangle, \dots, |\phi_J\rangle]$ and $\mathbf{c} = [c_1, c_2, \dots, c_J]^T$. Defining $\langle\phi| = [\langle\phi_1|, \langle\phi_2|, \dots, \langle\phi_J|]^T$, we have $\rho = |\phi\rangle\langle\phi|$ and $M = \langle\phi|\phi\rangle$. Now we prove the following equivalence.

*There are r linearly independent eigenstates $\{|\psi_j\rangle\}_{j=1}^r$ of ρ with the same eigenvalue $\lambda \neq 0$.
 \Leftrightarrow There are r linearly independent eigenvectors $\{\mathbf{v}_j\}_{j=1}^r$ of M with eigenvalue $\lambda \neq 0$.*

This statement implies Lemma 4.

\Rightarrow : Expanding $|\psi_j\rangle$ as $|\phi\rangle \mathbf{v}_j$, by assumption we have

$$\rho |\psi_j\rangle = |\phi\rangle \langle\phi|\phi\rangle \mathbf{v}_j = |\phi\rangle M \mathbf{v}_j = \lambda |\psi_j\rangle = \lambda |\phi\rangle \mathbf{v}_j. \quad (62)$$

Multiplying $\langle\phi|$ from the left of Eq. (62), we obtain $M^2 \mathbf{v}_j = \lambda M \mathbf{v}_j$, implying that $M \mathbf{v}_j \neq \mathbf{0}$ (otherwise $\rho |\psi_j\rangle = 0$) is an eigenvector of M with eigenvalue λ . Suppose that $M \mathbf{v}_j$'s are not linearly independent, which means

$$\sum_{j=1}^r k_j M \mathbf{v}_j = \mathbf{0} \quad (63)$$

for some k_j 's with $\sum_{j=1}^r |k_j|^2 \neq 0$. Operating Eq. (63) on $|\phi\rangle$ gives $\sum_{j=1}^r k_j \rho |\psi_j\rangle = \lambda \sum_{j=1}^r k_j |\psi_j\rangle = 0$, which contradicts the linear independence of $\{|\psi_j\rangle\}_{j=1}^r$.

\Leftarrow : By assumption, we have $M \mathbf{v}_j = \lambda \mathbf{v}_j$ for $j = 1, 2, \dots, r$. Defining $|\psi_j\rangle = |\phi\rangle \mathbf{v}_j$, we again obtain Eq. (62),

implying that $|\psi_j\rangle$ is an eigenstate of ρ with eigenvalue λ . Suppose that $|\psi_j\rangle$'s are not linearly independent, which means

$$\sum_{j=1}^r k_j |\psi_j\rangle = \sum_{j=1}^r k_j |\phi\rangle v_j = 0 \quad (64)$$

for some k_j 's with $\sum_{j=1}^r |k_j|^2 \neq 0$. Operating Eq. (64) on $\langle\phi|$ gives $\sum_{j=1}^r k_j M v_j = \lambda \sum_{j=1}^r k_j v_j = 0$, which contradicts the linear independence of $\{v_j\}_{j=1}^r$. \square

According to Lemma 4, with the unimportant zero part neglected, the ES is nothing but the spectrum of $M_{\alpha\beta, \alpha'\beta'} = \langle\phi_{\alpha\beta}|\phi_{\alpha'\beta'}\rangle$, whose entries are given in Eq. (61).

B. Exact ES degeneracy in the thermodynamic limit

In the limit of $l \rightarrow \infty$, $\epsilon_{\alpha\beta, \alpha'\beta'}$ in Eq. (59) vanishes. Hence, $M_{\alpha\beta, \alpha'\beta'} = \langle\phi_{\alpha\beta}|\phi_{\alpha'\beta'}\rangle$ becomes diagonalized and the ES is simply given by $\{\lambda_\alpha \lambda_{\beta'}\}_{\alpha, \beta'=1}^D$, which is the spectrum of $\Lambda^{\otimes 2}$. In this case, SPT order enforces the ES to be exactly degenerate, as a result of symmetry fractionalization on the virtual level.

Lemma 5 *The ES of any topologically nontrivial MPS protected by unitary symmetries is at least four-fold degenerate in the thermodynamic limit of a subsystem.*

Proof.— Denoting the symmetry group as G and its projective representation on the virtual level as V_g , we have [104]

$$[V_g, \Lambda] = 0, \quad \forall g \in G, \quad (65)$$

where Λ is the unique left fixed point of the unital channel associated with the MPS. Suppose that there is a non-degenerate eigenvalue λ associated with eigenstate $|\lambda\rangle$. From Eq. (65) we have

$$V_g |\lambda\rangle = \nu_g |\lambda\rangle, \quad \nu_g \in U(1), \quad \forall g \in G. \quad (66)$$

Since $V_g V_h = \omega_{g,h} V_{gh}$ for $\forall g, h \in G$, Eq. (66) implies

$$\nu_g \nu_h = \omega_{g,h} \nu_{gh} \Leftrightarrow \omega_{g,h} = \frac{\nu_g \nu_h}{\nu_{gh}}, \quad \forall g, h \in G. \quad (67)$$

Hence, $\omega_{g,h}$ belongs to the trivial cohomology class, contradicting the assumption that $|\Psi\rangle$ is topological. Therefore, the ES in the thermodynamic limit of a subsystem, which is nothing but the spectrum of $\Lambda^{\otimes 2}$, must be at least four-fold degenerate. \square

We mention that anti-unitary symmetries can also support nontrivial interacting SPT phases with the exactly degenerate ES in the thermodynamic limit. A prototypical example is the involutory ($\mathcal{T}^2 = 1$) time-reversal symmetry, which may be fractionalized into an anti-involutory ($\mathcal{T}_v^2 = -1$) anti-unitary symmetry on the virtual level, leading to the Kramers degeneracy in Λ [43]. However, since anti-unitary symmetries suffer dynamical symmetry breaking [33], the corresponding SPT order cannot be dynamically stable.

C. Bound on the many-body entanglement gap

In general, $M_{\alpha\beta, \alpha'\beta'}$ for a finite l can be decomposed into $[\Lambda^{\otimes 2}]_{\alpha\beta, \alpha'\beta'}$ and a perturbative term:

$$M_{\alpha\beta, \alpha'\beta'} = [\Lambda^{\otimes 2}]_{\alpha\beta, \alpha'\beta'} + P_{\alpha\beta, \alpha'\beta'}, \quad (68)$$

where

$$P_{\alpha\beta, \alpha'\beta'} = \sqrt{\lambda_\alpha \lambda_{\alpha'}} \langle\alpha' | (\mathcal{E}^l - \mathcal{E}^\infty) (|\beta'\rangle \langle\beta|) |\alpha\rangle. \quad (69)$$

It is clear from Eq. (68) that the exact eigenvalue degeneracy in $\Lambda^{\otimes 2}$ is generally lifted by P . However, according to Weyl's perturbation theorem, the many-body entanglement gap should be upper bounded by twice the norm of P :

$$\Delta_E^{\text{mb}} \leq 2\|P\|. \quad (70)$$

To proceed further, we upper bound $\|P\|$ by $\|P\|_2 \equiv \sqrt{\text{Tr}[P^\dagger P]}$, which is the Schatten 2-norm and its square takes a rather simple form:

$$\begin{aligned} \|P\|_2^2 &= \sum_{\alpha, \alpha', \beta, \beta'=1}^D \lambda_\alpha \lambda_{\alpha'} \langle\alpha' | (\mathcal{E}^l - \mathcal{E}^\infty) (|\beta'\rangle \langle\beta|) |\alpha\rangle \langle\alpha| (\mathcal{E}^l - \mathcal{E}^\infty) (|\beta\rangle \langle\beta'|) |\alpha'\rangle \\ &= \sum_{\alpha, \alpha', \beta, \beta'=1}^D \lambda_\alpha \lambda_{\alpha'} \langle\alpha' \alpha | (\mathcal{E}^l - \mathcal{E}^\infty)^{\otimes 2} (|\beta'\beta\rangle \langle\beta\beta'|) | \alpha\alpha'\rangle \\ &= \sum_{\alpha, \alpha', \beta, \beta'=1}^D \text{Tr}[\Lambda^{\otimes 2} |\alpha\alpha'\rangle \langle\alpha'\alpha| (\mathcal{E}^l - \mathcal{E}^\infty)^{\otimes 2} (|\beta'\beta\rangle \langle\beta\beta'|)] \\ &= \text{Tr}[\Lambda^{\otimes 2} \mathbb{S} (\mathcal{E}^l - \mathcal{E}^\infty)^{\otimes 2} (\mathbb{S})], \end{aligned} \quad (71)$$

where we have used $[\mathcal{E}(O)]^\dagger = \mathcal{E}(O^\dagger)$ and $\mathbb{S} \equiv \sum_{\alpha, \beta=1}^D |\alpha\beta\rangle \langle\beta\alpha|$ is the swap operator acting on two copies

of virtual Hilbert spaces. By defining the norm of a superop-

erator as $\|\mathcal{L}\| \equiv \max_{\|O_1\|_2=\|O_2\|_2=1} |\text{Tr}[O_2^\dagger \mathcal{L}(O_1)]|$, we can bound $\|P\|_2^2$ by

$$\begin{aligned} \|P\|_2^2 &\leq \|\Lambda^{\otimes 2} \mathbb{S}\|_2 \|\mathbb{S}\|_2 \|(\mathcal{E}^l - \mathcal{E}^\infty)^{\otimes 2}\| \\ &\leq \frac{D}{2} \|\mathcal{E}^l - \mathcal{E}^\infty\|^2, \end{aligned} \quad (72)$$

where D arises from $\|\mathbb{S}\|_2$, and $\frac{1}{2}$ upper bounds $\|\Lambda^{\otimes 2} \mathbb{S}\|_2 = \text{Tr}[\Lambda^2]$ since the spectrum of Λ is at least two-fold degenerate. Combining Eq. (72) with Eq. (70), we obtain

$$\Delta_{\mathbb{E}}^{\text{mb}} \leq \sqrt{2D} \|\mathcal{E}^l - \mathcal{E}^\infty\|. \quad (73)$$

Note that $\mathcal{E}^l - \mathcal{E}^\infty$ appears routinely in the correlation functions of MPSs and leads to an exponential decay [99–101]. Quantitatively, $\|\mathcal{E}^l - \mathcal{E}^\infty\|$ can be upper bounded by $c_\epsilon(\mu + \epsilon)^l$ for $\forall \epsilon > 0$, where μ is the spectral radius of $\mathcal{E} - \mathcal{E}^\infty$ and c_ϵ does not depend on l [99], implying that $\Delta_{\mathbb{E}}^{\text{mb}}$ is also exponentially small just like the correlation functions mentioned above. We emphasize that $\|\mathcal{E}^l - \mathcal{E}^\infty\|$ may scale like $\text{poly}(l)\mu^l$ [143], in which case a nonzero ϵ is *necessary* for giving a rigorous bound like $c_\epsilon(\mu + \epsilon)^l$.

D. Proof of Theorem 2

Let us analyze how the bound given in Eq. (73) changes when an MPS evolves according to a symmetric and trivial MPU. Denoting the bond dimension of the MPU as D_U , that of the MPS after t steps of evolutions is no more than DD_U^t . Moreover, the spectrum of the associated unital channel *stays invariant* during the time evolution as a result of unitarity [111] (see also Lemma 10 in Appendix E), and so does μ . Having in mind that $\|\mathcal{E}^l - \mathcal{E}^\infty\|$ is bounded by $c_\epsilon(\mu + \epsilon)^l$, it is natural to expect a Lieb-Robinson bound from Eq. (73). However, this expectation may fail — given ϵ , c_ϵ may grow faster than exponentially in time. To rule out this possibility, we utilize the *function-algebra*-based techniques developed in Ref. [144] to carefully estimate the growth of $\|\mathcal{E}^l - \mathcal{E}^\infty\|$.

The main idea of Ref. [144] is represented by the following lemma.

Lemma 6 *Given an operator \mathcal{M} on a finite linear space generating a bounded semigroup $\{\mathcal{M}^n\}_{n \in \mathbb{N}}$, i.e., $\|\mathcal{M}^n\| \leq C_{\mathcal{M}}$ for $\forall n \in \mathbb{N}$, and an element f in the Wiener algebra $W \equiv \{f \in \text{Hol}(\mathbb{D}) : f(z) = \sum_{p \in \mathbb{N}} f_p z^p, \|f\|_W \equiv \sum_{p \in \mathbb{N}} |f_p| < \infty\}$ ($\text{Hol}(\mathbb{D})$: set of holomorphic functions within the unit disk $\mathbb{D} \equiv \{z \in \mathbb{C} : |z| < 1\}$), we have*

$$\|f(\mathcal{M})\| \leq C_{\mathcal{M}} \|f\|_{W/m_{\mathcal{M}}W}, \quad (74)$$

where $\|f\|_{W/m_{\mathcal{M}}W} \equiv \inf\{\|g\|_W : g = f + m_{\mathcal{M}}h, h \in W\}$ and $m_{\mathcal{M}} \in W$ is the minimal polynomial of \mathcal{M} , i.e., the nonzero polynomial with the lowest degree such that

$m_{\mathcal{M}}(\mathcal{M}) = 0$ and the leading coefficient (that of the highest degree) is equal to 1.

Proof.— Due to $\|\mathcal{M}^n\| \leq C_{\mathcal{M}}$ for $\forall n \in \mathbb{N}$, for $\forall f \in W$, the norm of $f(\mathcal{M})$ can be upper bounded by

$$\|f(\mathcal{M})\| \leq \sum_{p \in \mathbb{N}} |f_p| \|\mathcal{M}^p\| \leq C_{\mathcal{M}} \sum_{p \in \mathbb{N}} |f_p| = \|f\|_W. \quad (75)$$

Since $m_{\mathcal{M}}$ is the minimal polynomial of \mathcal{M} , for $\forall h \in W$, we have

$$f(\mathcal{M}) = (f + m_{\mathcal{M}}h)(\mathcal{M}). \quad (76)$$

Applying Eq. (75) to the rhs of Eq. (76) gives

$$\|f(\mathcal{M})\| \leq C_{\mathcal{M}} \|f + m_{\mathcal{M}}h\|_W, \quad \forall h \in W. \quad (77)$$

Equation (74) then follows from minimization of the rhs of Eq. (77). \square

An arbitrary unital channel \mathcal{E} satisfies the condition in Lemma 6 due to the fact that \mathcal{E}^n is again a unital channel and $\|\mathcal{E}^n\| \leq \sqrt{\frac{D}{2}}$, where D is the Hilbert-space dimension [145]. Accordingly, $\mathcal{E} - \mathcal{E}^\infty$ also satisfies the condition.

Regarding the minimal polynomial of $\mathcal{E} - \mathcal{E}^\infty$ during time evolution, we have the following lemma.

Lemma 7 *Suppose that a single step of evolution by an MPU generated by \mathcal{U} changes the associated unital channel of an MPS from \mathcal{E} into \mathcal{E}' . Denoting the minimal polynomials of $\mathcal{E} - \mathcal{E}^\infty$ and $\mathcal{E}' - \mathcal{E}'^\infty$ as m and m' , respectively, we have*

$$m'(z) | z^{2k_0} m(z), \quad (78)$$

namely, $m'(z)$ is a divisor of $z^{2k_0} m(z)$, where k_0 is the smallest integer such that \mathcal{U}_{k_0} is simple.

Proof.— By assumption, for $\forall k \geq 2k_0$, the open boundary tensor $\bar{\mathcal{U}}_k \mathcal{U}_k$ can be decomposed into

$$\underbrace{\bar{\mathcal{U}} \mathcal{U} \bar{\mathcal{U}} \mathcal{U} \dots \bar{\mathcal{U}} \mathcal{U}}_k \equiv \bar{\mathcal{U}}_k \mathcal{U}_k = \bar{\mathcal{U}}_{k_0} \mathcal{U}_{k_0} \left(\mathbb{1}^{\otimes k-2k_0} \right) \bar{\mathcal{U}}_{k_0} \mathcal{U}_{k_0}. \quad (79)$$

We express m explicitly as $\sum_k c_k z^k$, which satisfies $c_0 = 0$ (due to that the spectrum of $\mathcal{E} - \mathcal{E}^\infty$ contains zero) and

$$\begin{aligned} m(\mathcal{E} - \mathcal{E}^\infty) &= \sum_k c_k (\mathcal{E}^k - \mathcal{E}^\infty) = 0 \\ \Leftrightarrow \sum_k c_k \mathcal{E}^k &= \sum_k c_k \mathcal{E}^\infty. \end{aligned} \quad (80)$$

Then, using Eq. (79), we can evaluate $z^{2k_0} m(z)|_{z=\mathcal{E}'}$ as

$$\begin{aligned}
& \sum_k c_k \left[\begin{array}{c} \bar{A} \\ \bar{U} \\ U \\ A \end{array} \right]_{k+2k_0} \dots = \left[\sum_k c_k \right] \left[\begin{array}{c} \bar{A}_{k_0} \\ \bar{U}_{k_0} \\ U_{k_0} \\ A_{k_0} \end{array} \right] \rho \left[\begin{array}{c} \bar{A}_k \\ \bar{U}_k \\ U_k \\ A_k \end{array} \right] = \left[\lim_{l \rightarrow \infty} \sum_k c_k \right] \left[\begin{array}{c} \bar{A}_{k_0} \\ \bar{U}_{k_0} \\ U_{k_0} \\ A_{k_0} \end{array} \right] \rho \left[\begin{array}{c} \bar{A}_l \\ \bar{U}_l \\ U_l \\ A_l \end{array} \right] \\
& = \left(\sum_k c_k \right) \lim_{l \rightarrow \infty} \left[\begin{array}{c} \bar{A}_{k_0} \\ \bar{U}_{k_0} \\ U_{k_0} \\ A_{k_0} \end{array} \right] \rho \left[\begin{array}{c} \bar{A}_l \\ \bar{U}_l \\ U_l \\ A_l \end{array} \right] = \left(\sum_k c_k \right) \lim_{l \rightarrow \infty} \left[\begin{array}{c} \bar{A}_l \\ \bar{U}_l \\ U_l \\ A_l \end{array} \right],
\end{aligned} \tag{81}$$

where we have used Eq. (80) (enclosed in dashed rectangles) and Eq. (79). Lemma 7 follows immediately from Eq. (81), which is the tensor-network representation of $\mathcal{E}^{2k_0} m(\mathcal{E}') = \sum_k c_k \mathcal{E}'^\infty \Leftrightarrow z^{2k_0} m(z)|_{z=\mathcal{E}'-\mathcal{E}'^\infty} = 0$. \square

A direct corollary of Lemma 7 (applying t times) is $m_t(z)|z^{2k_0 t} m(z)$, where $m_t(z)$ ($m(z) \equiv m_0(z)$) is the minimal polynomial of $\mathcal{E}_t - \mathcal{E}_t^\infty$, with \mathcal{E}_t determined from the MPS at time t . Using this fact, as long as $l > 2k_0 t$, we have

$$\begin{aligned}
& \|z^l\|_{W/m_t W} \\
& \leq \inf\{\|g\|_W : g = z^l + z^{2k_0 t} m h, h \in W\} \tag{82} \\
& = \|z^{l-2k_0 t}\|_{W/mW},
\end{aligned}$$

where we have used $\|g\|_W = \|z^n g\|_W$ for $\forall n \in \mathbb{N}$. According to the main result of Ref. [144], which is summarized as Theorem 6 in Appendix G, when $l - 2k_0 t > \frac{\mu}{1-\mu}$, we can bound $\|\mathcal{E}_t^l - \mathcal{E}_t^\infty\|$ from above by

$$\begin{aligned}
& \mu^{l-2k_0 t+1} \frac{4C_t e^2 \sqrt{|m_\mathcal{E}|} (|m_\mathcal{E}| + 1)}{(l - 2k_0 t) [1 - (1 + \frac{1}{l-2k_0 t}) \mu]^{\frac{3}{2}}} \\
& \times \sup_{|z|=\mu(1+\frac{1}{l-2k_0 t})} \frac{1}{|B(z)|}, \tag{83}
\end{aligned}$$

where $C_t \equiv \sup_{n \in \mathbb{N}} \|\mathcal{E}_t^n\|$ and $B(z)$ is the Blaschke product (G1) with respect to the spectrum of $\mathcal{E} \equiv \mathcal{E}_0$. If we further require $l - 2k_0 t \geq \frac{1+\mu}{1-\mu}$, even in the worst case, $\|\mathcal{E}_t^l - \mathcal{E}_t^\infty\|$ is bounded by an exponentially small quantity up to polynomial corrections (see Eq. (20) in Ref. [144]):

$$\begin{aligned}
& \|\mathcal{E}_t^l - \mathcal{E}_t^\infty\| \leq 4e^2 C_t \sqrt{|m|} (|m| + 1) \left(\frac{1+\mu}{1-\mu} \right)^{\frac{3}{2}} \\
& \times \left[\frac{1-\mu^2}{\mu} (l - 2k_0 t) \right]^{|m|-1} \mu^{l-2k_0 t}. \tag{84}
\end{aligned}$$

Denoting the bond dimension of the initial MPS $|\Psi_0\rangle$ and that of $|\Psi_t\rangle = U^t |\Psi_0\rangle$ after t steps of time evolutions as D and

D_t , respectively, we have

$$D_t \leq D D_t^t = D e^{t \ln D_t}, \tag{85}$$

and hence [145]

$$C_t \leq \sqrt{\frac{D_t}{2}} \leq \sqrt{\frac{D}{2}} e^{\frac{\ln D_t}{2} t}. \tag{86}$$

Combining Eq. (73) and Eqs. (84)-(86) with $|m| \leq D^2$ ($D \geq 2$, otherwise $|\Psi\rangle$ is a product state), we obtain Theorem 2.

Our theorem rigorously establishes the dynamical stability for general SPT systems in 1D. Yet another important implication of Theorem 2 is that the *topological discrete time-crystalline oscillation*, which is a toggle between different SPT phases [146] generated by an MPU with nontrivial cohomology [111], persists up to a time scale which increases at least linearly with respect to the system size. To see this, we have only to apply the theorem to U^p with trivial cohomology, where p is the order of the cohomology group.

E. Applicability to interacting fermions

As mentioned in the beginning of this section, a fermionic system in 1D can always be mapped into a spin chain through the Jordan-Wigner transformation:

$$c_{ja}^\dagger = \sigma_{(j-1)d+a}^+ \prod_{l < (j-1)d+a} \sigma_l^z, \tag{87}$$

where $\sigma^z = \begin{bmatrix} 1 & 0 \\ 0 & -1 \end{bmatrix}$ and $\sigma^+ \equiv \frac{1}{2}(\sigma^x + i\sigma^y) = \begin{bmatrix} 0 & 1 \\ 0 & 0 \end{bmatrix}$. Here we follow the setup in Sec. II A, i.e., we consider d internal states in each site of the original fermion system, so that the length of the corresponding spin chain is Ld . The fermion-parity operator reads

$$P_f = (-)^{\sum_{j,a} c_{ja}^\dagger c_{ja}} = \prod_{j,a} \sigma_{jd+a}^z, \tag{88}$$

which sets the superselection rule and is thus a \mathbb{Z}_2 symmetry of the Hamiltonian. Rigorously speaking, to keep the locality of the obtained spin Hamiltonian, we have to assume the open boundary condition. However, as long as the chain is sufficiently long, its subsystem property should not depend on the boundary condition. While a fermionic system never breaks the \mathbb{Z}_2 symmetry, the corresponding spin system may spontaneously break the \mathbb{Z}_2 symmetry, whenever the fermionic system exhibits a Majorana mode at the open boundaries [46, 71]. If the \mathbb{Z}_2 symmetry is not broken, the proof for 1D bosonic SPT systems applies directly to the fermionic SPT systems, which have even parities. Remarkably, after a few modifications, essentially the same proof applies even to fermionic SPT systems with odd parities.

While it is possible to directly describe fermionic SPT phases using fermionic MPSs [147, 148], where the anti-commutativity of fermionic operators is encoded in an additional \mathbb{Z}_2 -graded algebraic structure of the tensors, we would rather like to follow the approach in Refs. [46, 71] and work in the spin picture after the Jordan-Wigner transformation. In the spin picture, denoting $|\Psi_{\text{SB}}\rangle$ as a “physical” symmetry-broken ground state, the corresponding exact (cat) ground states read [46]

$$\begin{aligned} |\Psi\rangle &= \frac{1}{\sqrt{2}}(|\Psi_{\text{SB}}\rangle + (-)^\eta P_{\text{f}}|\Psi_{\text{SB}}\rangle) \\ &= \frac{1}{\sqrt{2}} \sum_{\{j_s\}_{s=1}^L} \text{Tr}[Z^\eta A_{j_1} \dots A_{j_L}] |j_1 \dots j_L\rangle, \end{aligned} \quad (89)$$

where $\eta = 0, 1$, $|\Psi_{\text{SB}}\rangle$ is generated by a normal tensor B_j without P_{f} symmetry and

$$Z = \sigma^z \otimes \mathbb{1}_v, \quad A_j = (\sigma^z)^{|j|} \otimes B_j, \quad j = 1, 2, \dots, 2^d, \quad (90)$$

with $|j|$ being the parity of state $|j\rangle$, i.e., $P_{\text{f}}|j\rangle = (-)^{|j|}|j\rangle$. Let us consider the spectral property of the associated quantum channel: $\mathcal{E}(\rho) \equiv \sum_{j=1}^{2^d} A_j \rho A_j^\dagger = \lambda \rho$, where λ is an eigenvalue and ρ can generally be expressed as $\rho = \sum_{w=0,x,y,z} \sigma^w \otimes \rho_w$. Defining $|w| \in \mathbb{Z}_2$ from $\sigma^w \sigma^z = (-)^{|w|} \sigma^z \sigma^w$, we obtain

$$\begin{aligned} \mathcal{E}(\rho) &= \sum_{w=0,x,y,z} \sigma^w \otimes \sum_{j=1}^{2^d} (-)^{|w||j|} B_j \rho_w B_j^\dagger \\ &= \sum_{w=0,x,y,z} \sigma^w \otimes \lambda \rho_w, \end{aligned} \quad (91)$$

implying that the spectrum of \mathcal{E} is the union of those of \mathcal{E}_\pm defined by $\mathcal{E}_\pm(\cdot) = \sum_{j=1}^{2^d} (\pm)^{|j|} B_j(\cdot) B_j^\dagger$, with each eigenvalue doubled. The doubling arises from the fact that, given ρ_+ (ρ_-) as an eigenstate of \mathcal{E}_+ (\mathcal{E}_-) with eigenvalue λ_+ (λ_-), $\sigma^0 \otimes \rho_+$ and $\sigma^z \otimes \rho_+$ ($\sigma^x \otimes \rho_+$ and $\sigma^y \otimes \rho_+$) are two degenerate eigenstates of \mathcal{E} with the same eigenvalue λ_+ (λ_-). Recalling that B_j is a normal tensor, we know that, after normalization, the spectral radius of \mathcal{E}_+ is one and that it only has a single eigenvalue equal to one. Let μ_- be the spectral radius of \mathcal{E}_- . Since B_j is not P_{f} -symmetric, we have $\mu_- < 1$

[104]. By gauge transforming B_j 's such that $\mathcal{E}_+(\mathbb{1}_v) = \mathbb{1}_v$ and $\mathcal{E}_+(\Lambda_+) = \Lambda_+$, we have

$$\begin{aligned} \mathcal{E}^\infty(\cdot) &\equiv \lim_{l \rightarrow \infty} \mathcal{E}^l(\cdot) = \frac{1}{2} \sigma^0 \otimes \mathbb{1}_v \text{Tr}[\sigma^0 \otimes \Lambda_+(\cdot)] \\ &\quad + \frac{1}{2} \sigma^z \otimes \mathbb{1}_v \text{Tr}[\sigma^z \otimes \Lambda_+(\cdot)], \end{aligned} \quad (92)$$

which satisfies $Z \mathcal{E}^\infty(Z \cdot Z) Z = \mathcal{E}^\infty(\cdot)$. According to Fig. 9, the ES in the thermodynamic limit of the subsystem is given by the spectrum of $\frac{1}{4}(\sigma^0 \otimes \sigma^0 + \sigma^z \otimes \sigma^z) \otimes \Lambda_+^{\otimes 2}$, which does not depend on η in Eq. (89) and is at least two-fold degenerate. If there are additional symmetries, then following the analysis for symmetric normal MPSs we know that a nontrivial projective representation on the virtual level may enforce an r -fold degeneracy in the spectrum of Λ_+ , leading to a total of $2r^2$ -fold degeneracy in the ES.

When the parity symmetry-broken state is evolved by a parity symmetric MPU U , we find that the cat-state structure (89) stays valid since $P_{\text{f}}U = UP_{\text{f}}$ by assumption. For an individual $|\Psi_{\text{SB}}\rangle$, we know that the degeneracy in the time-evolved fixed point $\Lambda_+(t)$ determined from $U^t|\Psi_{\text{SB}}\rangle$ should stay unchanged. Since the convergence bound given in Ref. [144] applies equally to the quantum channels with multiple steady states, the Lieb-Robinson bound on the entanglement gap given in Theorem 2 is also applicable to fermionic SPT states with Majorana modes. Moreover, the coefficient C in Eq. (27) can be tightened by a factor of 2 due to the normalization prefactor $\frac{1}{\sqrt{2}}$ in Eq. (89). Also, denoting the spectral radius of $\mathcal{E}_+ - \mathcal{E}_+^\infty$ as μ_+ , we have $\mu = \min\{\mu_+, \mu_-\}$.

VI. DISCUSSIONS

While the Lieb-Robinson bound places a rigorous upper bound on the maximal splitting between degenerate ES values, it is usually a highly nontrivial problem to determine the degree of degeneracy, especially when the system undergoes partial symmetry breaking. In addition, the derivation of the rigorous Lieb-Robinson bounds on entanglement gaps makes full use of the translation invariance and the results are meaningful only up to $t^* \sim \frac{L}{v}$. It is natural to ask what happens when the translation invariance breaks down or/and in longer time scales. Here we give some heuristic arguments to address these issues.

A. Partial symmetry breaking

1. Free fermions

For free-fermion systems with Altland-Zirnbauer symmetries, we have explained the effect of dynamical symmetry breaking and the reduction of symmetry classes [33]. The only two classes whose reduced class is nontrivial are classes BDI and DIII, both of which reduce to class D. In stark contrast, the former gives a surjective group homomorphism $\mathbb{Z} \rightarrow \mathbb{Z}_2$, while the latter gives a trivial one $\mathbb{Z}_2 \rightarrow 0$ ($\subset \mathbb{Z}_2$). If

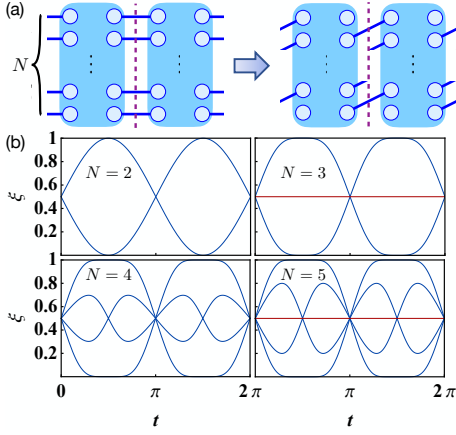


FIG. 10. (a) Quench from N decoupled dimer chains described by H_0 (93) to another flat-band Hamiltonian H (94) with inter-chain couplings. Both H_0 and H belong to class BDI. (b) Dynamics of the single-particle ES for $N = 2, 3, 4, 5$ demonstrating the nontrivial reduction $\mathbb{Z} \rightarrow \mathbb{Z}_2$. The red lines correspond to the topological entanglement modes at $\xi = \frac{1}{2}$, which persist only for odd N . Here we set $J = 1$ in all panels.

we look at the ES dynamics for a quenched class BDI system with winding number $W \in \mathbb{Z}^+$, up to the Lieb-Robinson time t^* , we expect two persistent $\xi = \frac{1}{2}$ modes if W is odd, while all the topological modes at $\xi = \frac{1}{2}$ immediately multifurcate if W is even. For a nontrivial class DIII system, however, the entanglement gap should immediately open after a quench.

We give an analytically solvable *flat-band* model to demonstrate the nontrivial $\mathbb{Z} \rightarrow \mathbb{Z}_2$ reduction. For simplicity, we focus on the ES under the open boundary condition, whose double gives the exact ES under the periodic boundary condition due to the zero correlation length imposed by the band flatness. Consider N copies of dimer chains described by the Hamiltonian

$$H_0 = -J_0 \sum_j \sum_{\alpha=1}^N (c_{2j+1,\alpha}^\dagger c_{2j,\alpha} + \text{H.c.}), \quad (93)$$

where $c_{x\alpha}$ denotes the fermion annihilation operator at the x th site of the α th chain. Starting from the ground state of H_0 , we suddenly quench the Hamiltonian into (see Fig. 10(a))

$$H = -J \sum_j \sum_{\alpha=1}^{N-1} (c_{2j+1,\alpha}^\dagger c_{2j,\alpha+1} + \text{H.c.}). \quad (94)$$

As shown in Fig. 10(b), the ES dynamics indeed demonstrates the expected surjective group homomorphism $\mathbb{Z} \rightarrow \mathbb{Z}_2$. The detailed calculations are given in Appendix I 1, where we prove the existence/absence of $\xi = \frac{1}{2}$ mode for odd/even N . We also note that the $\mathbb{Z} \rightarrow \mathbb{Z}_2$ reduction here should be distinguished from that in Ref. [32] which concerns the *spatial-temporal* topology of quench dynamics starting from a topologically *trivial* state according to a topological Hamiltonian.

TABLE II. Two possible quench protocols that partially break the symmetry into $\tilde{G} = \mathbb{Z}_2 \times \mathbb{Z}_2$ and $\tilde{G} = \mathbb{Z}_3 \times \mathbb{Z}_3$ starting from a SPT state protected by $G = \mathbb{Z}_6 \times \mathbb{Z}_6$. Here ν and $\tilde{\nu}$ label the SPT phases protected by G and \tilde{G} , whose (minimal) degeneracies in the open-boundary ES are denoted by r and \tilde{r} , respectively. In addition, $s \equiv \frac{r}{\tilde{r}}$ is the number of splitting ($s = 1$ means no splitting), as numerically verified in Figs. 16(b) and (c).

$G = \mathbb{Z}_6 \times \mathbb{Z}_6$		$\tilde{G} = \mathbb{Z}_2 \times \mathbb{Z}_2$			$\tilde{G} = \mathbb{Z}_3 \times \mathbb{Z}_3$		
$\nu \in \mathbb{Z}_6$	r	$\tilde{\nu} \in \mathbb{Z}_2$	\tilde{r}	s	$\tilde{\nu} \in \mathbb{Z}_3$	\tilde{r}	s
0	1	0	1	1	0	1	1
1	6	1	2	3	2	3	2
2	3	0	1	3	1	3	1
3	2	1	2	1	0	1	2
4	3	0	1	3	2	3	1
5	6	1	2	3	1	3	2

2. Interacting systems

The Haldane phase [149], which is a prototypical SPT phase corresponding to the nontrivial element in $H^2(\mathbb{Z}_2 \times \mathbb{Z}_2, \text{U}(1)) = \mathbb{Z}_2$, always becomes trivial upon any symmetry breaking quench since $H^2(\mathbb{Z}_2, \text{U}(1)) = H^2(0, \text{U}(1)) = 0$. See Ref. [33] for a numerical demonstration for an immediate opening of the entanglement gap. Here, we consider a more general situation where the initial SPT is protected by some unitary symmetries that form a group G , and the postquench Hamiltonian H only respects the symmetries in a subgroup $\tilde{G} < G$.

It is, in general, very difficult to determine the reduced \tilde{G} -symmetric SPT phase and the corresponding ES degeneracy from a given G -symmetric SPT phase. See Appendix I 2 for an exact mathematical formulation of this problem in terms of category-theoretic languages. Here, let us consider a class of minimal but yet nontrivial examples — $G = \mathbb{Z}_N \times \mathbb{Z}_N \rightarrow \tilde{G} = \mathbb{Z}_n \times \mathbb{Z}_n$, where $N = np$ with $p \in \mathbb{Z}^+$. Suppose that the initial state correspond to $\nu \in \mathbb{Z}_N = H^2(\mathbb{Z}_N \times \mathbb{Z}_N, \text{U}(1))$. By choosing the coboundary gauge properly, the projective representation V on the virtual level satisfies

$$V_{(a,b)} V_{(a',b')} = \omega_N^{\nu a'b} V_{(a+a', b+b')}, \quad (95)$$

where $(a,b), (a',b') \in \mathbb{Z}_N \times \mathbb{Z}_N$. Regarding the elements in the subgroup $\mathbb{Z}_n \times \mathbb{Z}_n$, we find

$$\begin{aligned} \tilde{V}_{a,b} \tilde{V}_{a',b'} &= V_{ap,bp} V_{a'p,b'p} \\ &= \omega_N^{\nu a'b p^2} V_{(a+a')p, (b+b')p} \\ &= \omega_n^{p\nu a'b} \tilde{V}_{a+a', b+b'}, \end{aligned} \quad (96)$$

where we have used the fact that $(a,b) \in \mathbb{Z}_n \times \mathbb{Z}_n$ corresponds to $(ap,bp) \in \mathbb{Z}_N \times \mathbb{Z}_N$. This implies that the group homomorphism from $\mathbb{Z}_N = H^2(\mathbb{Z}_N \times \mathbb{Z}_N, \text{U}(1))$ to $\mathbb{Z}_n = H^2(\mathbb{Z}_n \times \mathbb{Z}_n, \text{U}(1))$ is given by

$$\nu \rightarrow \tilde{\nu} = p\nu \mod n. \quad (97)$$

Note that such a group homomorphism can be trivial, as is the case for $N = 4$ and $n = 2$ due to $\tilde{\nu} = 2\nu \bmod 2 = 0$. The minimal realizations of nontrivial group homomorphisms turn out to be $N = 6$ and $n = 3$, which gives rise to $\mathbb{Z}_6 \rightarrow \mathbb{Z}_3 : \nu \rightarrow \tilde{\nu} = -\nu \bmod 3$, and $N = 6$ and $n = 2$, which gives rise to $\mathbb{Z}_6 \rightarrow \mathbb{Z}_2 : \nu \rightarrow \tilde{\nu} = \nu \bmod 2$. Using the fact that the ES of a $\mathbb{Z}_N \times \mathbb{Z}_N$ -symmetric SPT state characterized by ν is (at least) $\frac{N}{\text{GCD}(\nu, N)}$ -fold degenerate under the open boundary condition [111], where GCD is the greatest common divisor, we can figure out how many branches the original ES should split into. The results are summarized in Table II and are numerically verified by some minimal models (see Appendix I3).

B. Effects of disorder

As schematically illustrated in the right top panel in Fig. 2, disorder can dramatically alter the universal dynamical behavior of the entanglement growth. In this subsection, we qualitatively address the impact of disorder on the ES dynamics in 1D SPT systems.

Since the entanglement-gap opening is ultimately related to operator spreading and propagation of correlation, we expect disorder in the postquench Hamiltonian H to *stabilize* the SPT order during quench dynamics, provided that the disorder does respect the symmetry. For free fermions in 1D, the Anderson localization occurs at an arbitrarily small disorder strength and introduces a new length scale ξ [150], which is a typical localization length of the eigenfunctions of H and measures how far a wave packet can diffuse. As illustrated in Fig. 11(a), for $l \gg \xi$, we expect that Δ_E^{sp} is saturated at $e^{-O(l)}$ and the SPT order survives even in the limit of $t \rightarrow \infty$ (see numerical signatures in Appendix J1). On the other hand, for very weak disorder, l may be comparable to or even smaller than ξ , and we can still observe the opening of the entanglement gap. This occurs even for a half-chain bipartition, unless the disorder configuration happens to respect the half-chain translation symmetry.

In the presence of interactions, we may expect qualitatively different behavior because the entanglement-entropy growth is *unbounded* in the many-body localized phase [151], although it is logarithmical and hence extremely slow [152–156]. In this case, we conjecture that, after a possible transient similar to the noninteracting case, Δ_E^{mb} grows no faster than a *power law*, which is similar to the behavior of out-of-time-order correlators [157–159]. This is supported by the numerics on a phenomenological model (see Appendix J2).

C. Longer time scales

While our rigorous results ensure the persistence of (approximate) ES degeneracy until a time scale that grows linearly long with the subsystem size, these results are not useful for describing the dynamical behavior at longer time scales. In fact, previous numerical studies on some two-band free-fermion models have revealed the possibility for a single-

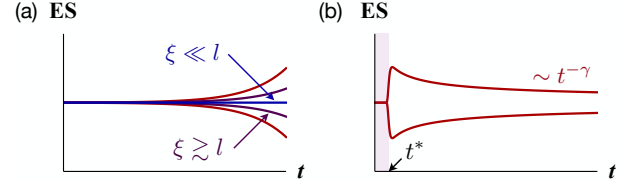


FIG. 11. (a) Expected influence of disorder on the single-particle-ES dynamics starting from a topological state. When the localization length ξ is larger or comparable with the subsystem length l , we can still observe the splitting (purple curve) just like the clean case (red curve). On the other hand, if l is much larger than ξ , the ES splitting will become invisible. (b) Power-law relaxation of the single-particle ES for $t \gg t^*$, where t^* is the time scale set by the Lieb-Robinson bound. This phenomenon is discovered in Refs. [81–83], where it is also conjectured that the $\xi = \frac{1}{2}$ modes will revive in the limit of $t \rightarrow \infty$ if \bar{H}_∞ given in Eq. (98) is topologically nontrivial.

particle topological entanglement mode to return to $\xi = \frac{1}{2}$ in the long-time limit [81–83]. In these studies, a conjecture is made to the effect that such behavior is determined by the topology of the time-averaged Hamiltonian

$$\bar{H}_\infty \equiv \lim_{T \rightarrow \infty} \frac{1}{T} \int_0^T dt e^{-iHt} H_0 e^{iHt}, \quad (98)$$

at least for two-band systems in class D and class BDI. It would be interesting to examine whether this is indeed true and, if yes, to what extent (e.g., multiple bands and other symmetry classes). Moreover, it is found in Ref. [83] that the long-time relaxation dynamics obey some universal *power law*, i.e., $\Delta_E^{\text{sp}}(t) - \Delta_E^{\text{sp}}(\infty) \sim t^{-\gamma}$ ($\gamma > 0$) for sufficiently large t (see Fig. 11(b)). This behavior can quantitatively be understood from steepest descent calculations, which require the lattice system to be infinite. Remarkably, the power-law relaxation of local observables has been rigorously proved for general finite single-band systems in arbitrary dimensions starting from any state with local correlations (not necessarily Gaussian) and within the revival time [160–162]. These rigorous results raise another interesting question concerning whether the signature of free-fermion topology could emerge in quench dynamics starting from an interacting quantum many-body state.

As for the long-time behavior of interacting systems, we generally do not have an extensive number of conserved quantities and the steady state should resemble an excited state of the postquench Hamiltonian H with energy $\langle \Psi_0 | H | \Psi_0 \rangle$, provided that the eigenstate thermalization hypothesis holds true [151, 163, 164]. Even if the ground state of H is in an SPT phase, the topological features generally disappear in the excited states. Hence, the retrieval of ES degeneracy in the steady state seems unlikely. The scenario should be very simple if H is many-body localized — the topological information in the initial state, i.e., the degeneracy in the many-body ES, is expected to persist in the long-time limit without a transient loss or revival.

VII. SUMMARY AND OUTLOOK

The Lieb-Schultz-Mattis-Oshikawa-Hastings theorem [165–167], the Lieb-Robinson bound [53] and the entanglement area law [68] are of critical importance in quantum many-body systems. These rigorous results are of great current interest in light of theoretical insights from topological material science [168–170] and quantum information [54, 73–75], and of rapidly growing experimental relevance [55–57, 76–78]. In addition to these fundamental achievements, we have established a general principle for the dynamics of entanglement gaps in SPT systems that are driven out of equilibrium by a local Hamiltonian or MPU. For free fermions, we have extensively used both the band and the Wannier-function pictures to derive a Lieb-Robinson bound on the single-particle entanglement gap (Theorem 1). As a byproduct, we have clarified the relation between the Lieb-Robinson velocity and the group velocity of band dispersions. For interacting SPT systems, we have employed the tensor-network approaches and the techniques of function algebra to derive the Lieb-Robinson bound on the many-body entanglement gap (Theorem 2). This result illustrates that the shortcoming of tensor-network approaches as numerical tools does not hinder its powerfulness as analytical tools for dealing with long-time quantum dynamics. We have also considered the impact of partial symmetry breaking, in which case the ES degeneracy may immediately be lifted partially or completely. Possible effects of disorder and relaxation behaviors at longer time scales have also been discussed.

As future studies, it would be of fundamental importance to go beyond the tensor-network formalism and prove a Lieb-Robinson bound on the many-body entanglement gap for continuous quench dynamics starting from exact ground states of local Hamiltonians. As discussed in Appendix F, while improving MPUs to continuously generated unitaries alone seems plausible, it is far from clear how we can improve the assumption of MPS initial states to exact ground states. It is also natural to consider the generalization to higher dimensions [47], where we may have to use other indicators to measure the sharpness of SPT order. Moreover, some techniques used here may break down. For example, we cannot construct an exponentially localized Wannier function for a two-dimensional Chern insulator [132]. Finally, we note that considerable efforts have recently been made for generalizing the notions of Lieb-Robinson bounds and topological phases to lattice systems with long-range hoppings and interactions [171–174]. It would also be interesting to relax the locality assumption and consider long-range systems, which can naturally be implemented with trapped ions [6, 7, 56, 57], Rydberg atoms [5], polar molecules [175] and nitrogen-vacancy centers [4].

ACKNOWLEDGMENTS

We acknowledge Y. Ashida, M. A. Cazalilla, M.-C. Chung, I. Danshita, K. Fujimoto, R. Hamazaki, K. Kawabata, N. Matsumoto, and M. McGinley for valuable discussions. In partic-

ular, Z. G. appreciates Z. Wang for providing a simple picture about the monotonicity of Eq. (21). This work was supported by KAKENHI Grant No. JP18H01145, No. JP17H02922 and a Grant-in-Aid for Scientific Research on Innovative Areas “Topological Materials Science (KAKENHI Grant No. JP15H05855) from the Japan Society for the Promotion of Science. Z. G. was supported by MEXT. N. K. was supported by the Leading Graduate Schools “ALPS. The authors thank the Yukawa Institute for Theoretical Physics at Kyoto University, where this work was initiated during the International Molecule Program YITP-T-18-01 on “Floquet Theory: Fundamentals and Applications”.

Appendix A: Band theory with a complex wave number

In this appendix, we discuss how to define 1D Bloch Hamiltonians with complex wave numbers through analytic continuation. This is always possible for quasi-local hoppings, which decay exponentially with respect to the hopping range. We argue that the analytically continued Hamiltonian should generally be diagonalizable, even if the original one respects certain anti-unitary symmetries. In addition, we prove and explain why the Lieb-Robinson velocity in Eq. (21) is monotonic with respect to the imaginary wave number and thus upper bounds the maximal relative group velocity. Finally, we provide an example of the SSH model.

1. Analytic continuation

A Bloch Hamiltonian $H(k)$ can generally be expanded as

$$H(k) = \sum_{n \in \mathbb{Z}} e^{ikn} H_n, \quad (\text{A1})$$

where each Fourier component can be obtained as

$$H_n = \int_{-\pi}^{\pi} \frac{dk}{2\pi} H(k) e^{-ikn} = H_{-n}^{\dagger}. \quad (\text{A2})$$

A sufficient condition for the rhs of Eq. (A1) to converge is

$$\sum_{n \in \mathbb{Z}} \|H_n\| < \infty, \quad (\text{A3})$$

which is valid even if $H(k)$ is non-Hermitian and is obviously satisfied by any model with a finite hopping range R , i.e.,

$$H_n = H_{-n} = \mathbb{O}, \quad \forall n > R. \quad (\text{A4})$$

For such a class of models, the analytic continuation to the complex wave number

$$H(k + i\kappa) \equiv \sum_{n \in \mathbb{Z}} e^{ikn - \kappa n} H_n \quad (\text{A5})$$

is well-defined for $\forall \kappa \in \mathbb{R}$ and satisfies $H(k + i\kappa + 2\pi) = H(k + i\kappa)$ and $H(k + i\kappa)^{\dagger} = H(k - i\kappa)$ for $\forall k \in [-\pi, \pi]$.

The analytic continuation can be applied to a wider class of Bloch Hamiltonians whose Fourier components satisfy

$$\|H_n\| \leq C_0 e^{-\kappa_0|n|}, \quad \forall n \in \mathbb{Z}, \quad (\text{A6})$$

where $C_0, \kappa_0 \in \mathbb{R}^+$ do not depend on n . One can easily check the validity of Eq. (A3). In this case, for $\forall \kappa \in (-\kappa_0, \kappa_0)$, we have

$$\|e^{-\kappa n} H_n\| \leq C_0 e^{-(\kappa_0 - |\kappa|)|n|}, \quad \forall n \in \mathbb{Z}, \quad (\text{A7})$$

so that $H(k + i\kappa)$ in Eq. (A5) converges. Now let us show that if $H(k)$ is gapped and satisfies Eq. (A6), then the flattened Hamiltonian or the Bloch projector (17) also satisfies Eq. (A6) but with C_0 and κ_0 modified. To see this, we note that the n th Fourier component of the Bloch projector can be written as

$$P_n = \int_{-\pi}^{\pi} \frac{dk}{2\pi} \oint_{\gamma_{<}} \frac{dz}{2\pi i} \frac{e^{-ikn - \kappa n}}{z - H(k - i\kappa)} \quad (\text{A8})$$

by deforming the integral contour. With length of $\gamma_{<}$ denoted as $l_{\gamma_{<}} \equiv \oint_{\gamma_{<}} |dz|$, such an integral (A8) can be bounded from above by

$$\begin{aligned} \|P_n\| &\leq \int_{-\pi}^{\pi} \frac{dk}{2\pi} \oint_{\gamma_{<}} \frac{|dz|}{2\pi} \left\| \frac{1}{z - H(k - i\kappa)} \right\| e^{-\kappa n} \\ &\leq \frac{l_{\gamma_{<}}}{2\pi} \max_{k \in [-\pi, \pi], z \in \gamma_{<}} \left\| \frac{1}{z - H(k - i\kappa)} \right\| e^{-\kappa n}, \end{aligned} \quad (\text{A9})$$

provided that $\det[z - H(k - i\kappa)] \neq 0$ for $\forall z \in \gamma_{<}$, which can always be satisfied by sufficiently small κ due to a finite gap. This result ensures the existence of $\kappa > 0$ such that $P_{<}(k)$ can be analytically continued to $\{k : |\text{Re } k| \leq \pi, |\text{Im } k| \leq \kappa\}$, implying that condition (i) in Theorem 1 can always be satisfied.

On the other hand, the analytic continuation cannot be applied to long-range hopping, i.e., $\|H_n\| \sim O(n^{-\gamma})$ with $\gamma \geq 0$ — while $H(k)$ stays well-defined for $\gamma > 1$, Eq. (A5) diverges whenever $\kappa \neq 0$. Therefore, Theorem 1 cannot be applied to long-range systems.

2. Diagonalizability

We argue that condition (ii) in Theorem 1 is also satisfied in general — that is, there always exists a nonzero κ_0 such that $H(k + i\kappa)$ is diagonalizable for $\forall |\kappa| < \kappa_0$. To show this, it is sufficient to show that $H(k + i\kappa)$ becomes non-diagonalizable only at a discrete set of complex wave numbers. This is expected to be true if $H(k + i\kappa)$ does not respect any symmetries, since an obvious mechanism for being nondiagonalizable is the emergence of a second-order exceptional point [176], which requires the fine-tuning of two parameters. Here, these two parameters are k and κ . However, if $H(k + i\kappa)$ respects an anti-unitary symmetry or anti-symmetry \mathcal{S} for given k and κ , i.e.,

$$\mathcal{S}H(k + i\kappa)\mathcal{S}^{-1} = \pm H(k + i\kappa), \quad (\text{A10})$$

we only need to fine tune a single parameter to create an exceptional point. This type of Hamiltonians have been actively studied in the context of non-Hermitian topological systems [177–180], where \mathcal{S} is typically the parity-time symmetry and $H(k + i\kappa)$ may not be analytic and thus κ is no more than a control parameter. In the following, we will show that $H(k + i\kappa)$, which is an analytic continuation of $H(k)$ with an anti-unitary symmetry \mathcal{S} , satisfies

$$\mathcal{S}H(k + i\kappa)\mathcal{S}^{-1} = \pm H(k - i\kappa) \quad (\text{A11})$$

instead of Eq. (A10), so we still need to fine-tune both k and κ to make $H(k + i\kappa)$ non-diagonalizable.

By imposing Eq. (A10) for $\kappa = 0$, we can use Eq. (A2) to obtain

$$\begin{aligned} \mathcal{S}H_n\mathcal{S}^{-1} &= \int_{-\pi}^{\pi} \frac{dk}{2\pi} \mathcal{S}H(k)\mathcal{S}^{-1} e^{ikn} \\ &= \pm \int_{-\pi}^{\pi} \frac{dk}{2\pi} H(k) e^{ikn} = \pm H_{-n}. \end{aligned} \quad (\text{A12})$$

Therefore, the action of \mathcal{S} on $H(k + i\kappa)$ gives

$$\begin{aligned} \mathcal{S}H(k + i\kappa)\mathcal{S}^{-1} &= \sum_{n \in \mathbb{Z}} e^{-ikn - \kappa n} \mathcal{S}H_n\mathcal{S}^{-1} \\ &= \pm \sum_{n \in \mathbb{Z}} e^{i(k - i\kappa)(-n)} H_{-n} \\ &= \pm H(k - i\kappa). \end{aligned} \quad (\text{A13})$$

Similarly, we can show that $\mathcal{S}H(k)\mathcal{S}^{-1} = \pm H(-k)$, which is the case of the particle-hole symmetry, gives $\mathcal{S}H(k + i\kappa)\mathcal{S}^{-1} = \pm H(-k + i\kappa)$ by analytic continuation and thus $H(k + i\kappa)$ is expected to stay diagonalizable for sufficiently small κ .

Finally, we note that even if $H(k + i\kappa)$ happens to be non-diagonalizable, Eq. (19) should still be valid with C replaced by a polynomial of t . This is because $H(k + i\kappa)$ can always be transformed into the Jordan normal form and a nontrivial Jordan block with size $s \geq 2$ contributes a polynomial prefactor with degree $s - 1$ in $e^{-iH(k + i\kappa)t}$.

3. Monotonicity of Eq. (21)

We prove that Eq. (21) is monotonic in terms of κ and thus reaches its minimum at $\kappa = 0$. To simplify the notation, we first introduce

$$\Delta_{\alpha\beta}(k) \equiv \epsilon_{k\alpha} - \epsilon_{k\beta}, \quad (\text{A14})$$

which satisfies $\overline{\Delta_{\alpha\beta}(k + i\kappa)} = \Delta_{\alpha\beta}(k - i\kappa)$ for $k, \kappa \in \mathbb{R}$. For further simplification, we omit the subscript “ $\alpha\beta$ ” and define

$$v(k, \kappa) \equiv \text{Re} \Delta'(k + i\kappa). \quad (\text{A15})$$

We then have $v(k, \kappa) = v(k, -\kappa)$ and

$$V(k, \kappa) \equiv \frac{1}{2\kappa} \int_{-\kappa}^{\kappa} d\kappa' v(k, \kappa') = \frac{\text{Im} \Delta(k + i\kappa)}{\kappa}. \quad (\text{A16})$$

To show the monotonicity of $\max_{k \in [-\pi, \pi]} |V(k, \kappa)|$, it is sufficient to show that $V(k, \kappa)$ as a function of k is *majorized* by $V(k, \kappa')$ for $\forall \kappa' > \kappa$. By the statement that an integrable real function $f_1 : I \equiv [a, b] \rightarrow \mathbb{R}$ majorizes $f_2 : I \rightarrow \mathbb{R}$, we mean that there exists a kernel $K(x; x') : I \times I \rightarrow \mathbb{R}^+ \cup \{0\}$ satisfying

$$\int_I dx K(x; x') = \int_I dx' K(x; x') = 1 \quad (\text{A17})$$

and

$$f_2(x) = \int_I dx' K(x; x') f_1(x'). \quad (\text{A18})$$

Such a definition is a straightforward generalization of the majorization for real vectors, which can also be regarded as functions with I being a discrete set. That is, a real vector \mathbf{a} is majorized by \mathbf{b} if there exists a *doubly stochastic matrix* M_{ds} , whose entries are all non-negative and the sum of each row/column equals to one, such that $\mathbf{a} = M_{\text{ds}} \mathbf{b}$ [135]. Note that $K(x; x')$ is a continuous version of M_{ds} . If f_1 majorizes f_2 , for $\forall x \in I$, we have

$$f_2(x) \leq \int_I dx' K(x; x') \max_{x \in I} f_1(x) = \max_{x \in I} f_1(x) \quad (\text{A19})$$

due to $K(x; x') \geq 0$, $f_1(x') \leq \max_{x \in I} f_1(x)$ for $\forall x' \in I$ and Eq. (A17). Since Eq. (A19) is true for $\forall x \in I$, we have $\max_{x \in I} f_2(x) \leq \max_{x \in I} f_1(x)$. Similarly, we have $\min_{x \in I} f_2(x) \leq \min_{x \in I} f_1(x)$ and thus $\max_{x \in I} |f_1(x)| \geq \max_{x \in I} |f_2(x)|$.

Now let us consider the kernel that transforms $V(k, \kappa_1)$ into $V(k, \kappa_2)$ with $\kappa_1 \geq \kappa_2$. Since $v(k, \kappa)$ is a *harmonic function* which is periodic in k and even in κ , it can generally be expanded as

$$v(k, \kappa) = \sum_{n=1}^{\infty} [a_n \cos(nk) + b_n \sin(nk)] \cosh(n\kappa), \quad (\text{A20})$$

where $a_n, b_n \in \mathbb{R}$. Accordingly, we can obtain a general form of $V(k, \kappa)$ in Eq. (A16):

$$V(k, \kappa) = \sum_{n=1}^{\infty} [A_n \cos(nk) + B_n \sin(nk)] \frac{\sinh(n\kappa)}{\kappa}, \quad (\text{A21})$$

where we have redefined the coefficients as $A_n = \frac{a_n}{n}$ and $B_n = \frac{b_n}{n}$. This general form (A21) implies the following kernel that transforms $V(k, \kappa_1)$ into $V(k, \kappa_2)$:

$$K(k, \kappa_2; k', \kappa_1) = \frac{1}{2\pi} + \frac{1}{\pi} \sum_{n=1}^{\infty} \frac{\kappa_1 \sinh(n\kappa_2)}{\kappa_2 \sinh(n\kappa_1)} \cos[n(k - k')], \quad (\text{A22})$$

where the constant term is determined by Eq. (A17). To see why the kernel takes this form, we have only to note that $\cos[n(k - k')] = \cos(nk) \cos(nk') + \sin(nk) \sin(nk')$ and $\int_{-\pi}^{\pi} \frac{dk'}{\pi} \cos(nk') V(k', \kappa) = (\int_{-\pi}^{\pi} \frac{dk'}{\pi} \cos(nk') V(k', \kappa))$ gives the Fourier coefficient before $\cos(nk)$ ($\sin(nk)$), which should be modified in an n -dependent manner following the

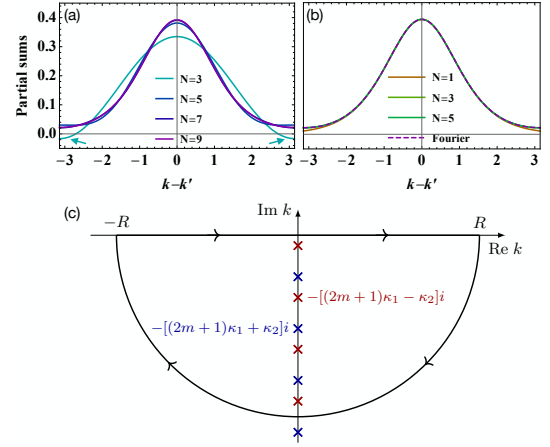


FIG. 12. Partial sums $\sum_{n=-N/2}^{(N-1)/2}$ of the kernel function $K(k, \kappa_2; k', \kappa_1)$ with $\kappa_1 = 2$ and $\kappa_2 = 0$ expanded as in (a) Eq. (A23) and (b) Eq. (A26). The curve labeled by “Fourier” in (b) is nothing but the curve in (a) for $N = 9$. Note that the partial sum of the Fourier series may be not positive for certain $k - k'$ (see arrows in (a)), but $K(k, \kappa_2; k', \kappa_1)$ is clearly positive from Eq. (A26). (c) Contour integral and poles of $Y(k; \kappa_2, \kappa_1)$. In the limit of $R \rightarrow \infty$, as in the case in Eq. (A29), we should sum up all the residues with respect to the poles on the lower-half imaginary axis.

change of κ . We can rewrite Eq. (A22) into a more compact form

$$K(k, \kappa_2; k', \kappa_1) = \frac{1}{2\pi} \sum_{n \in \mathbb{Z}} \frac{\kappa_1 \sinh(n\kappa_2)}{\kappa_2 \sinh(n\kappa_1)} e^{in(k-k')}. \quad (\text{A23})$$

We can use Eq. (A23) to check that

$$K(k, \kappa; k', \kappa) = \frac{1}{2\pi} \sum_{n \in \mathbb{Z}} e^{in(k-k')} = \delta(k - k'). \quad (\text{A24})$$

Another special case that transforms $V(k, \kappa)$ into $V(k, 0) = v(k, 0)$ reads

$$K(k, 0; k', \kappa) = \frac{1}{2\pi} \sum_{n \in \mathbb{Z}} \frac{n\kappa}{\sinh(n\kappa)} e^{in(k-k')}. \quad (\text{A25})$$

In general, whenever $\kappa_1 > \kappa_2$, the Fourier coefficients in Eq. (A23) decays as $e^{-(\kappa_1 - \kappa_2)|n|}$ for large $|n|$, implying the convergence.

The remaining problem is to confirm whether Eq. (A23) is non-negative for $\forall \kappa_1 > \kappa_2 = 0$. This is not clear at first glance since the partial sum in Eq. (A23) generally contains negative parts (see Fig. 12(a)), especially when κ_2 is close to κ_1 . Nevertheless, the positivity becomes clear in a different expansion:

$$K(k, \kappa_2; k', \kappa_1) = \sum_{n \in \mathbb{Z}} Y(k - k' + 2n\pi; \kappa_2, \kappa_1), \quad (\text{A26})$$

where

$$Y(k; \kappa_2, \kappa_1) = \frac{\sin(\frac{\kappa_2}{\kappa_1} \pi)}{2\kappa_2 [\cosh(\frac{\pi}{\kappa_1} k) + \cos(\frac{\kappa_2}{\kappa_1} \pi)]} \quad (\text{A27})$$

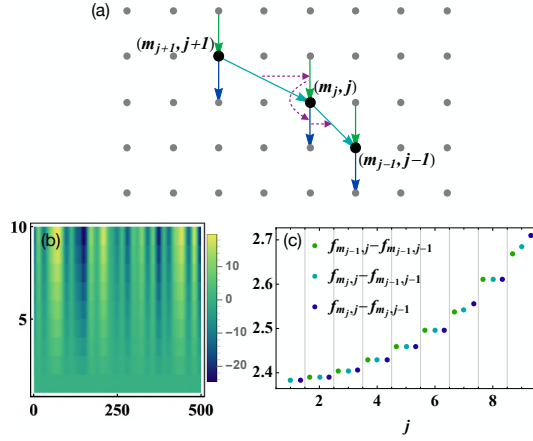


FIG. 13. (a) 2D array with the maximum of each row marked as (m_j, j) . The solid arrows denote the differences between the starting point to the end point, which are all positive. The dashed arrows highlight the order relations (descent along the arrow) between these differences. (b) A randomly generated array with $L = 500$ and (c) the differences in (a) for the j th rows with $j = 1, 2, \dots, 9$.

is positive over \mathbb{R} . In particular, when $\kappa_2 = 0$, Eq. (A27) becomes

$$Y(k; 0, \kappa) = \frac{\pi}{2\kappa[\cosh(\frac{\pi}{\kappa}k) + 1]}. \quad (\text{A28})$$

To prove Eq. (A26), we have only to calculate the n th Fourier coefficient of the rhs:

$$\begin{aligned} & \int_{-\pi}^{\pi} \frac{dk}{2\pi} \sum_{m \in \mathbb{Z}} Y(k + 2m\pi; \kappa_2, \kappa_1) e^{-ink} \\ &= \int_{-\infty}^{\infty} \frac{dk}{2\pi} Y(k; \kappa_2, \kappa_1) e^{-ink} \\ &= \int_{-\infty}^{\infty} \frac{dk}{4\pi i \kappa_2} \left[\frac{e^{-ink}}{e^{-\frac{\pi(k+i\kappa_2)}{\kappa_1}} + 1} - \frac{e^{-ink}}{e^{-\frac{\pi(k-i\kappa_2)}{\kappa_1}} + 1} \right] \\ &= \frac{\kappa_1}{2\pi \kappa_2} \sum_{m=0}^{\infty} (e^{-n[(2m+1)\kappa_1 - \kappa_2]} - e^{-n[(2m+1)\kappa_1 + \kappa_2]}) \\ &= \frac{\kappa_1}{2\pi \kappa_2} \frac{\sinh(n\kappa_2)}{\sinh(n\kappa_1)}, \end{aligned} \quad (\text{A29})$$

where we have used the residue theorem in deriving the fourth equality (see Fig. 12(c)). The final result in Eq. (A29) indeed coincides with that in Eq. (A23).

In fact, a simple picture is available from a discrete version of the problem. We consider a 2D array $f : \mathbb{Z} \times \mathbb{Z} \rightarrow \mathbb{R}$, which satisfies that for $\forall j, j' \in \mathbb{Z}$, $f_{j,j'} = -f_{j,-j'}$ (so that $f_{j,0} = 0$), $f_{j+L,j'} = f_{j,j'}$ ($L \in \mathbb{Z}^+$) and the discrete Laplace equation

$$4f_{j,j'} = f_{j+1,j'} + f_{j-1,j'} + f_{j,j'+1} + f_{j,j'-1}. \quad (\text{A30})$$

By imposing the boundary condition

$$f_{j,1} = -f_{j,-1} = h\Delta' \left(\frac{2\pi j}{L} \right), \quad (\text{A31})$$

we have $f(k, \kappa) \equiv \text{Im}\Delta(k + i\kappa) = \lim_{L \rightarrow \infty, h \rightarrow 0} f(\frac{kL}{2\pi}, \frac{\kappa}{h})$ since $f(k, \kappa)$ is a harmonic function satisfying

$$\begin{aligned} f(k, \kappa) &= f(k + 2\pi, \kappa) = -f(k, -\kappa), \\ \partial_{\kappa} f(k, \kappa)|_{\kappa=0} &= \Delta'(k). \end{aligned} \quad (\text{A32})$$

The discrete counterpart of the monotonicity of $\kappa^{-1} \max_{k \in [-\pi, \pi]} f(k, \kappa)$ reads

$$\frac{1}{j'+1} \max_{j \in \mathbb{Z}_L} f_{j,j'+1} \geq \frac{1}{j'} \max_{j \in \mathbb{Z}_L} f_{j,j'} \quad (\text{A33})$$

for $\forall j' \geq 1$. In fact, we can prove a stronger result

$$\max_{j \in \mathbb{Z}_L} f_{j,j'+1} - \max_{j \in \mathbb{Z}_L} f_{j,j'} \geq \max_{j \in \mathbb{Z}_L} f_{j,j'} - \max_{j \in \mathbb{Z}_L} f_{j,j'-1}, \quad (\text{A34})$$

which implies Eq. (A33). Denoting $m_{j'}$ as the horizontal label where $f_{m_{j'},j'}$ reaches the maximum for a given j' , we have

$$\begin{aligned} & \max_{j \in \mathbb{Z}_L} f_{j,j'+1} - \max_{j \in \mathbb{Z}_L} f_{j,j'} \\ & \geq f_{m_{j'},j'+1} - f_{m_{j'},j'} \\ & = 3f_{m_{j'},j'} - f_{m_{j'}-1,j'} - f_{m_{j'}+1,j'} - f_{m_{j'},j'-1} \\ & \geq f_{m_{j'},j'} - f_{m_{j'},j'-1} \\ & \geq \max_{j \in \mathbb{Z}_L} f_{j,j'} - \max_{j \in \mathbb{Z}_L} f_{j,j'-1}, \end{aligned} \quad (\text{A35})$$

which completes the proof. We provide a schematic illustration and a numerical verification in Fig. 13. Similarly, we can prove the monotonicity of $\frac{1}{j'} \min_{j \in \mathbb{Z}_L} f_{j,j'}$ and thus the monotonicity of $\frac{1}{j'} \max_{j \in \mathbb{Z}_L} |f_{j,j'}|$.

The above idea can also be implemented directly in a continuous manner, provided that k^* , which makes $f(k^*, \kappa)$ maximal or minimal for a given κ , forms a smooth curve of κ . Let us focus on the case of maximum since the minimum counterpart is quite similar. By definition, along this curve we have

$$\partial_k^2 f dk + \partial_k \partial_{\kappa} f d\kappa = 0, \quad \partial_k^2 f = -\partial_{\kappa}^2 f \leq 0, \quad (\text{A36})$$

so the second-order differential along this curve satisfies

$$\begin{aligned} d^2 f &= \partial_k^2 f dk^2 + \partial_{\kappa}^2 f d\kappa^2 + 2\partial_k \partial_{\kappa} f dk d\kappa \\ &= \partial_{\kappa}^2 f d\kappa^2 - \partial_k^2 f dk^2 + 2(\partial_k^2 f dk + \partial_k \partial_{\kappa} f d\kappa) dk \\ &= \partial_{\kappa}^2 f \left[1 + \left(\frac{dk}{d\kappa} \right)^2 \right] \Big|_{k=k^*} d\kappa^2. \end{aligned} \quad (\text{A37})$$

Introducing $F(\kappa) \equiv f(k^*(\kappa), \kappa)$, we find from Eqs. (A36) and (A37) that

$$F''(\kappa) \geq 0. \quad (\text{A38})$$

This result is sufficient to show

$$\kappa_1^{-1} F(\kappa_1) \geq \kappa_2^{-1} F(\kappa_2), \quad \forall \kappa_1 > \kappa_2 \geq 0. \quad (\text{A39})$$

To see this, we consider the equivalent inequality

$$\frac{F(\kappa_1) - F(\kappa_2)}{\kappa_1 - \kappa_2} \geq \frac{F(\kappa_2) - F(0)}{\kappa_2}. \quad (\text{A40})$$

According to the mean-value theorem, there exists $\xi_1 \in [\kappa_2, \kappa_1]$ and $\xi_2 \in [0, \kappa_2]$ such that $F'(\xi_1) = \frac{F(\kappa_1) - F(\kappa_2)}{\kappa_1 - \kappa_2}$ and $F'(\xi_2) = \frac{F(\kappa_2) - F(0)}{\kappa_2}$, so the above inequality becomes $F'(\xi_2) \geq F'(\xi_1)$, which is ensured by Eq. (A38).

4. Example: SSH model

We consider a general quench in the SSH model:

$$\begin{aligned} H_0(k) &= -(J_1 + J_2 \cos k)\sigma^x - J_2 \sin k \sigma^y \\ \rightarrow H(k) &= -(J'_1 + J'_2 \cos k)\sigma^x - J'_2 \sin k \sigma^y, \end{aligned} \quad (\text{A41})$$

$$|\text{Im } \epsilon_{k+i\kappa, \pm}| = \sqrt{\frac{1}{2} \left[\sqrt{(J_1'^2 + J_2'^2 + 2J_1'J_2' \cos k \cosh \kappa)^2 + (2J_1'J_2' \sin k \sinh \kappa)^2} - (J_1'^2 + J_2'^2 + 2J_1'J_2' \cos k \cosh \kappa) \right]} \quad (\text{A42})$$

over $k \in [-\pi, \pi]$. Note that κ can be chosen freely, as long as $|\kappa| < |\ln \frac{J_1}{J_2}|$ (otherwise $P_<(k + i\kappa)$ may become non-analytic). We plot $v_{\text{LR}} = \kappa^{-1} \max_{k \in [-\pi, \pi]} |\text{Im } \epsilon_{k+i\kappa, \pm}|$ in Fig. 7(b) for the quench protocol used in the main text: $J_1 = J'_2 = 0.5$ and $J_2 = J'_1 = 1$. The κ dependence of v_{LR} turns out to be rather weak, at least for $\kappa \in [0, \ln 2]$.

To evaluate C , we first write down the initial Bloch projec-

where σ^x and σ^y are Pauli matrices. To evaluate v_{LR} , we have only to numerically maximize

tor

$$P_<(k) = \frac{1}{2} \begin{bmatrix} 1 & \frac{J_1 + J_2 e^{-ik}}{\sqrt{J_1'^2 + J_2'^2 + 2J_1'J_2' \cos k}} \\ \frac{J_1 + J_2 e^{ik}}{\sqrt{J_1'^2 + J_2'^2 + 2J_1'J_2' \cos k}} & 1 \end{bmatrix}. \quad (\text{A43})$$

By introducing

$$F(k, \kappa, J_1, J_2) = \frac{J_1^2 + J_2^2 e^{2\kappa} + 2J_1 J_2 e^\kappa \cos k}{\sqrt{(J_1^2 + J_2^2)^2 + 4J_1 J_2 (J_1^2 + J_2^2) \cosh \kappa \cos k + 2J_1^2 J_2^2 (\cos 2k + \cosh 2\kappa)}}, \quad (\text{A44})$$

we can express the norm of Eq. (A43) with respect to a complex wave number as

$$\|P_<(k + i\kappa)\| = \frac{1}{2} [F(k, \kappa, J_1, J_2) + F(k, -\kappa, J_1, J_2)]. \quad (\text{A45})$$

Moreover, the left and right eigenvectors are found to be

$$\begin{aligned} \langle k = 0, \mathbf{a} | u_{k+i\kappa, \pm}^{\text{R}} \rangle &= \frac{1}{\sqrt{2}} \left[\mp \sqrt{\frac{J_1' + J_2' e^{ik - \kappa}}{J_1' + J_2' e^{-ik + \kappa}}} \right], \\ \langle k = 0, \mathbf{a} | u_{k+i\kappa, \pm}^{\text{L}} \rangle &= \frac{1}{\sqrt{2}} \left[\mp \sqrt{\frac{J_1' + J_2' e^{ik + \kappa}}{J_1' + J_2' e^{-ik - \kappa}}} \right], \end{aligned} \quad (\text{A46})$$

where \mathbf{a} labels the sublattice degrees of freedom, leading to

$$\begin{aligned} \|u_{k+i\kappa, \pm}^{\text{R}}\| &= \sqrt{\frac{1}{2} [1 + F(k, -\kappa, J_1', J_2)]}, \\ \|u_{k+i\kappa, \pm}^{\text{L}}\| &= \sqrt{\frac{1}{2} [1 + F(k, \kappa, J_1', J_2)]}. \end{aligned} \quad (\text{A47})$$

Substituting Eqs. (A45) and (A47) into Eq. (20) yields

$$\begin{aligned} C &= \int_{-\pi}^{\pi} \frac{dk}{4\pi} [1 + F(k, -\kappa, J_1', J_2)][1 + F(k, \kappa, J_1', J_2)] \\ &\quad \times [F(k, \kappa, J_1, J_2) + F(k, -\kappa, J_1, J_2)]. \end{aligned} \quad (\text{A48})$$

In Fig. 6(c), we choose $\kappa = 0.6$, leading to $C \simeq 12.225$.

Appendix B: Exact zero modes

In Sec. IV A, we have argued that the emergent Kramers degeneracy and the nontrivial \mathbb{Z}_2 topology necessarily support zero modes in R_{d} in Eq. (28). Here, we prove this statement by showing that the invertibility of R_{d} implies a trivial \mathbb{Z}_2 topological index.

Theorem 4 *Given two skew-symmetric real matrices R_{d} and R_{o} such that $R \equiv \sigma^0 \otimes R_{\text{d}} + \sigma^x \otimes R_{\text{o}}$ is unitary and $\text{Pf } R = -1$, we must have $\det R_{\text{d}} = 0$.*

Proof.— If $\det R_{\text{d}} \neq 0$, we can apply the formula

$$\text{Pf } R = \text{Pf } R_{\text{d}} \text{Pf } (R_{\text{d}} - R_{\text{o}} R_{\text{d}}^{-1} R_{\text{o}}). \quad (\text{B1})$$

This formula can be derived from the identity

$$\text{Pf}(BAB^T) = \det B \text{Pf} A, \quad (\text{B2})$$

which is valid for arbitrary $A^T = -A$ and B , and

$$\begin{aligned} & \begin{pmatrix} R_d & 0 \\ 0 & R_d - R_o R_d^{-1} R_o \end{pmatrix} \\ &= \begin{pmatrix} \mathbb{1} & 0 \\ -R_o R_d^{-1} & \mathbb{1} \end{pmatrix} \begin{pmatrix} R_d & R_o \\ R_o & R_d \end{pmatrix} \begin{pmatrix} \mathbb{1} & -R_d^{-1} R_o \\ 0 & \mathbb{1} \end{pmatrix}. \end{aligned} \quad (\text{B3})$$

Since R is unitary, we have $\{R_d, R_o\} = \mathbb{0}$ and $R_d^2 + R_o^2 = -\mathbb{1}$, leading to

$$\begin{aligned} R_d - R_o R_d^{-1} R_o &= R_d + R_d^{-1} R_o^2 \\ &= R_d + R_d^{-1} (-\mathbb{1} - R_d^2) = -R_d^{-1}. \end{aligned} \quad (\text{B4})$$

Combining Eq. (B4) with Eq. (B1), we have

$$\text{Pf} R = \text{Pf} R_d \text{Pf}(-R_d^{-1}) = \frac{(\text{Pf} R_d)^2}{\det R_d} = 1, \quad (\text{B5})$$

where we have used Eq. (B2) with $A = B = R_d^{-1}$ and $\det A = (\text{Pf} A)^2$ for $\forall A^T = -A$. This result (B5) contradicts the assumption $\text{Pf} R = -1$, implying $\det R_d = 0$. \square

Appendix C: Proof of Weyl's perturbation theorem

In this appendix, we follow Ref. [84] to prove Weyl's perturbation theorem. To this end, we first introduce the *min-max principle*.

Lemma 8 (Min-max principle) *For any Hermitian operator O on an n -dimensional Hilbert space, its j th largest eigenvalue λ_j ($j = 1, 2, \dots, n$) is given by*

$$\begin{aligned} \lambda_j &= \max_{\dim V=j} \min_{|\psi\rangle \in V} \langle \psi | O | \psi \rangle \\ &= \min_{\dim W=n+1-j} \max_{|\psi\rangle \in W} \langle \psi | O | \psi \rangle, \end{aligned} \quad (\text{C1})$$

where V and W are Hilbert subspaces and $|\psi\rangle$ is a normalized state vector.

Proof.— We denote the eigenstate with eigenvalue λ_j as $|\psi_j\rangle$ ($j = 1, 2, \dots, n$) and define the following two special classes of Hilbert spaces with dimensions j and $n+1-j$, respectively:

$$\begin{aligned} V_j &\equiv \text{span}\{|\psi_1\rangle, |\psi_2\rangle, \dots, |\psi_j\rangle\}, \\ W_j &\equiv \text{span}\{|\psi_j\rangle, |\psi_{j+1}\rangle, \dots, |\psi_n\rangle\}. \end{aligned} \quad (\text{C2})$$

With V chosen to be V_j , the rhs of the first line in Eq. (C1) gives λ_j , implying

$$\lambda_j \leq \max_{\dim V=j} \min_{|\psi\rangle \in V} \langle \psi | O | \psi \rangle. \quad (\text{C3})$$

Similarly, with a choice of $W = W_j$, the second line in Eq. (C1) gives λ_j , implying

$$\lambda_j \geq \min_{\dim W=n+1-j} \max_{|\psi\rangle \in W} \langle \psi | O | \psi \rangle. \quad (\text{C4})$$

On the other hand, for an arbitrary Hilbert subspace V with dimension j , we must have $\dim(V \cap W_j) \geq 1$. Otherwise, if $V \cap W_j = \emptyset$, the full Hilbert space containing $V \cup W_j$ will be at least $n+1$ dimensional, contradicting the assumption. This implies that for $\forall V$ with $\dim V = j$, we have

$$\begin{aligned} \min_{|\psi\rangle \in V} \langle \psi | O | \psi \rangle &\leq \min_{|\psi\rangle \in V \cap W_j} \langle \psi | O | \psi \rangle \\ &\leq \max_{|\psi\rangle \in W_j} \langle \psi | O | \psi \rangle = \lambda_j, \end{aligned} \quad (\text{C5})$$

leading to

$$\lambda_j \geq \max_{\dim V=j} \min_{|\psi\rangle \in V} \langle \psi | O | \psi \rangle. \quad (\text{C6})$$

Combining Eqs. (C3) and (C6), we obtain the first line in Eq. (C1). By analogy, from $\dim(V_j \cap W) \geq 1$ for $\forall W$ with $\dim W = n-j+1$, we can derive

$$\lambda_j \leq \min_{\dim W=n+1-j} \max_{|\psi\rangle \in W} \langle \psi | O | \psi \rangle. \quad (\text{C7})$$

Combining Eqs. (C4) and (C7), we obtain the second line in Eq. (C1). \square

Now let us turn to the proof of Theorem 3. For $\forall V$ with $\dim V = j$, we can decompose O as $O' + (O - O')$ to obtain

$$\begin{aligned} & \min_{|\psi\rangle \in V} \langle \psi | O | \psi \rangle \\ &= \min_{|\psi\rangle \in V} (\langle \psi | O' | \psi \rangle + \langle \psi | O - O' | \psi \rangle) \\ &\geq \min_{|\psi\rangle \in V} \langle \psi | O' | \psi \rangle + \min_{|\psi\rangle \in V} \langle \psi | O - O' | \psi \rangle \\ &\geq \min_{|\psi\rangle \in V} \langle \psi | O' | \psi \rangle - \|O - O'\|. \end{aligned} \quad (\text{C8})$$

After maximizing the rhs of Eq. (C8) with respect to V and using the first line in Eq. (C1), we obtain

$$\lambda_j \geq \lambda'_j - \|O - O'\|. \quad (\text{C9})$$

Following a similar procedure, we can derive

$$\max_{|\psi\rangle \in W} \langle \psi | O | \psi \rangle \leq \max_{|\psi\rangle \in W} \langle \psi | O' | \psi \rangle + \|O - O'\|, \quad (\text{C10})$$

which gives rise to (due to the second line in Eq. (C1))

$$\lambda_j \leq \lambda'_j + \|O - O'\|. \quad (\text{C11})$$

Theorem 3 follows from the combination of Eqs. (C9) and (C11).

Appendix D: Proof of Lemma 2

We first show the following lemma which provides the relation between $|W_{j\alpha}^{(L)}\rangle$ and $|W_{j\alpha}^{(\infty)}\rangle$.

Lemma 9 *Given $|W_{j\alpha}^{(\infty)}\rangle$ as a Wannier function of an infinite 1D lattice system, the Wannier function $|W_{j\alpha}^{(L)}\rangle$ of the corresponding finite system with length L reads*

$$|W_{j\alpha}^{(L)}\rangle = \sum_{n \in \mathbb{Z}} P_{\mathbb{Z}_L} |W_{j+nL, \alpha}^{(\infty)}\rangle, \quad (\text{D1})$$

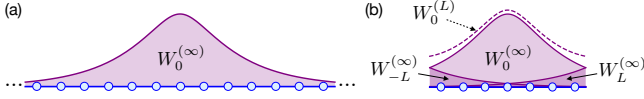


FIG. 14. (a) Wannier function $W_0^{(\infty)}$ centered at the origin of an infinite lattice. (b) Infinite-system Wannier functions $W_0^{(\infty)}$ and $W_{\pm L}^{(\infty)}$ projected onto a finite lattice \mathbb{Z}_L under the periodic boundary condition. The finite-system Wannier function $W_0^{(L)}$ (dashed curve) is related to the infinite-system ones by Eq. (D1).

where $P_{\mathbb{Z}_L} \equiv \sum_{j \in \mathbb{Z}_L} \sum_{a=1}^d |ja\rangle\langle ja|$ is the projector onto the finite lattice, with d and $|j, a\rangle$ being the number of internal states per site and the state localized at the j th site in an internal state a .

Proof.— Let us first write down the Wannier function defined on an infinite lattice:

$$|W_{j\alpha}^{(\infty)}\rangle = \int_{\text{B.Z.}} \frac{dk}{2\pi} e^{ik(x-j)} |u_{k\alpha}\rangle, \quad (\text{D2})$$

where $|u_{k\alpha}\rangle = \sum_{a=1}^d u_{\alpha a}(k) |k=0, a\rangle$ is the Bloch wave function with $|k=0, a\rangle \equiv \sum_{j \in \mathbb{Z}} |ja\rangle$, and $x \equiv \sum_{j \in \mathbb{Z}} j |j\rangle\langle j| \otimes \mathbb{1}_I$ is the position operator with $\mathbb{1}_I$ being the identity acting on the internal-state Hilbert space. When the lattice is finite, say with length L , the Wannier function is defined in the form of a discrete Fourier transformation:

$$|W_{j\alpha}^{(L)}\rangle = \frac{1}{L} \sum_{k \in \frac{2\pi}{L}\mathbb{Z}_L} e^{ik(x_L-j)} |u_{k\alpha}\rangle, \quad (\text{D3})$$

where $|u_{k\alpha}\rangle$ follows the previous definition for an infinite lattice except for $|k=0, a\rangle \equiv \sum_{j \in \mathbb{Z}_L} |ja\rangle$ and $e^{ikx_L} \equiv \sum_{j \in \mathbb{Z}_L} e^{ikj} |j\rangle\langle j| \otimes \mathbb{1}_I$.

For $\forall j' \in \mathbb{Z}_L$ and $a = 1, 2, \dots, d$, the coefficient of $|j'a\rangle$ on the rhs in Eq. (D1) is given by

$$\sum_{n \in \mathbb{Z}} \langle j'a | W_{j+nL, \alpha}^{(\infty)} \rangle = \sum_{n \in \mathbb{Z}} \int_0^{2\pi} \frac{dk}{2\pi} e^{ik(j'-j-nL)} u_{\alpha a}(k). \quad (\text{D4})$$

Using the identity

$$\sum_{n \in \mathbb{Z}} \delta(x - 2n\pi) = \frac{1}{2\pi} \sum_{n \in \mathbb{Z}} e^{inx}, \quad (\text{D5})$$

we can further simplify the rhs of Eq. (D4) as

$$\sum_{n \in \mathbb{Z}} \int_0^{2\pi} \frac{dk}{2\pi} e^{ik(j'-j)} \delta(kL - 2n\pi) u_{\alpha a}(k) = \langle j'a | W_{j\alpha}^{(L)} \rangle, \quad (\text{D6})$$

which completes the proof of Lemma 9. \square

A schematic illustration of Lemma 9 is shown in Fig. 14. Just like $|W_{j\alpha}^{(\infty)}\rangle$'s, we note that a finite-size Wannier function

in Eq. (D1) satisfies the orthonormal relation:

$$\begin{aligned} & \langle W_{j'\alpha'}^{(L)} | W_{j\alpha}^{(L)} \rangle \\ &= \sum_{n, n' \in \mathbb{Z}} \sum_{j'' \in \mathbb{Z}_L, a} \langle W_{j'+n'L, \alpha'}^{(\infty)} | j''a \rangle \langle j''a | W_{j+nL, \alpha}^{(\infty)} \rangle \\ &= \sum_{n, n' \in \mathbb{Z}} \sum_{j'' \in \mathbb{Z}_L, a} \langle W_{j'\alpha'}^{(\infty)} | j'' - n'L, a \rangle \\ & \quad \times \langle j'' - n'L, a | W_{j+(n-n')L, \alpha}^{(\infty)} \rangle \\ &= \sum_{m \in \mathbb{Z}} \langle W_{j'\alpha'}^{(\infty)} | W_{j+mL, \alpha}^{(\infty)} \rangle = \delta_{j'j} \delta_{\alpha'\alpha}, \end{aligned} \quad (\text{D7})$$

where we have used $\langle j' | W_{j\alpha}^{(\infty)} \rangle = \langle j' + p | W_{j+p, \alpha}^{(\infty)} \rangle$ for $\forall p \in \mathbb{Z}$, which is a property also inherited by $|W_{j\alpha}^{(L)}\rangle$ with $j', j \in \mathbb{Z}_L$.

Now we turn to prove Lemma 2. We first express $\langle j | P_{\leq}^{(L)} | j' \rangle$, which is an operator acting on the internal-state Hilbert space, in terms of Wannier function projectors:

$$\langle j | P_{\leq}^{(L)} | j' \rangle = \sum_{j'' \in \mathbb{Z}_L, \alpha \in \mathcal{O}} \langle j | W_{j''\alpha}^{(L)} \rangle \langle W_{j''\alpha}^{(L)} | j' \rangle. \quad (\text{D8})$$

According to Eq. (D1), the above expression can be rewritten as

$$\langle j | P_{\leq}^{(L)} | j' \rangle = \sum_{j'' \in \mathbb{Z}_L, \alpha \in \mathcal{O}} \sum_{n, n' \in \mathbb{Z}} \langle j | W_{j''+nL, \alpha}^{(\infty)} \rangle \langle W_{j''+n'L, \alpha}^{(\infty)} | j' \rangle. \quad (\text{D9})$$

On the other hand, we have

$$\langle j | P_{\leq}^{(\infty)} | j' \rangle = \sum_{j'' \in \mathbb{Z}_L, n \in \mathbb{Z}} \sum_{\alpha \in \mathcal{O}} \langle j | W_{j''+nL, \alpha}^{(\infty)} \rangle \langle W_{j''+nL, \alpha}^{(\infty)} | j' \rangle. \quad (\text{D10})$$

Combining Eqs. (D9) and (D10), we obtain

$$\begin{aligned} & \langle j | P_{\leq}^{(L)} | j' \rangle - \langle j | P_{\leq}^{(\infty)} | j' \rangle \\ &= \sum_{j'' \in \mathbb{Z}_L, \alpha \in \mathcal{O}} \sum_{n \neq n' \in \mathbb{Z}} \langle j | W_{j''+nL, \alpha}^{(\infty)} \rangle \langle W_{j''+n'L, \alpha}^{(\infty)} | j' \rangle \\ &= \sum_{j'' \in \mathbb{Z}_L, \alpha \in \mathcal{O}} \sum_{n \in \mathbb{Z}} \sum_{m \in \mathbb{Z} \setminus \{0\}} \langle j | W_{j''+nL, \alpha}^{(\infty)} \rangle \langle W_{j''+nL, \alpha}^{(\infty)} | j' + mL \rangle \\ &= \sum_{m \in \mathbb{Z} \setminus \{0\}} \langle j | P_{\leq}^{(\infty)} | j' + mL \rangle, \end{aligned} \quad (\text{D11})$$

where we again use $\langle j' | W_{j\alpha}^{(\infty)} \rangle = \langle j' + p | W_{j+p, \alpha}^{(\infty)} \rangle$ for $\forall p \in \mathbb{Z}$.

Appendix E: Basic properties of matrix-product unitaries

We briefly review Ref. [110] and introduce the several basic properties of MPUs, which are crucial for proving the main result. By definition, for $\forall L \in \mathbb{Z}^+$, U in Eq. (22) in the main text obeys

$$U^\dagger U = \mathbb{1} \equiv \mathbb{1}^{\otimes L} \Rightarrow d^{-L} \text{Tr}[U^\dagger U] = 1, \quad (\text{E1})$$

A direct corollary of Lemma 10 is that the spectrum of \mathcal{E} , i.e., the transfer matrix of an MPS, stays invariant during the stroboscopic time evolution governed by an MPU. In particular, μ as the spectral radius of $\mathcal{E} - \mathcal{E}^\infty$ is conserved.

Appendix F: Interacting systems undergoing continuous evolution

We argue that the Lieb-Robinson bound on the many-body entanglement gap for MPUs implies qualitatively the same result for continuous time evolutions generated by local Hamiltonians. To this end, we first prove that the difference in time-evolution operators, which can be highly nonlocal, rigorously bounds the difference in any reduced density operator after the time evolution.

Lemma 11 *Given an arbitrary wave function $|\Psi_0\rangle$ defined on a bipartite system $S \cup \bar{S}$ and two unitaries U and U' satisfying $\|U - U'\| \leq \epsilon$, denoting $\rho_S \equiv \text{Tr}_{\bar{S}} |\Psi\rangle\langle\Psi|$ and $\rho'_S \equiv \text{Tr}_{\bar{S}} |\Psi'\rangle\langle\Psi'|$ as the density operators of the evolved wave functions $|\Psi\rangle \equiv U|\Psi_0\rangle$ and $|\Psi'\rangle \equiv U'|\Psi_0\rangle$, we have $\|\rho_S - \rho'_S\| \leq \epsilon$.*

Proof.— We first point out a useful norm inequality for the commutator of a positive-semidefinite Hermitian operator A ($A^\dagger = A$ and $A \geq 0$) and an arbitrary operator B [182]:

$$\|[A, B]\| \leq \|A\| \|B\|. \quad (\text{F1})$$

Note that there is an improvement of factor $\frac{1}{2}$ compared with $\|[A, B]\| \leq 2\|A\| \|B\|$, which holds for arbitrary A and B .

Let us move on to prove Lemma 11. Noting that $\rho_S - \rho'_S$ is Hermitian, according to the definition of the operator norm, we have

$$\begin{aligned} \|\rho_S - \rho'_S\| &= \max_{\|\psi\rangle\|=1} \langle\psi|\rho_S - \rho'_S|\psi\rangle \\ &= \max_{P_\psi} \text{Tr}[P_\psi \otimes \mathbb{1}_{\bar{S}} (|\Psi\rangle\langle\Psi| - |\Psi'\rangle\langle\Psi'|)] \\ &= \max_{P_\psi} \langle\Psi_0|U(P_\psi \otimes \mathbb{1}_{\bar{S}})U^\dagger - U'(P_\psi \otimes \mathbb{1}_{\bar{S}})U'^\dagger|\Psi_0\rangle \quad (\text{F2}) \\ &\leq \max_{P_\psi} \|U(P_\psi \otimes \mathbb{1}_{\bar{S}})U^\dagger - U'(P_\psi \otimes \mathbb{1}_{\bar{S}})U'^\dagger\| \\ &\leq \max_{P_\psi} \|[P_\psi \otimes \mathbb{1}_{\bar{S}}, U^\dagger U']\|, \end{aligned}$$

where $P_\psi \equiv |\psi\rangle\langle\psi|$ is a rank-one projector, i.e., $P_\psi^2 = P_\psi$ and $\text{Tr} P_\psi = 1$. Since $P_\psi \otimes \mathbb{1}_{\bar{S}} \geq 0$ and $\|P_\psi \otimes \mathbb{1}_{\bar{S}}\| = 1$, we find from Eq. (F1) that for $\forall P_\psi$

$$\begin{aligned} &\|[P_\psi \otimes \mathbb{1}_{\bar{S}}, U^\dagger U']\| \\ &= \|[P_\psi \otimes \mathbb{1}_{\bar{S}}, U^\dagger U' - \mathbb{1}]\| \quad (\text{F3}) \\ &\leq \|U^\dagger U' - \mathbb{1}\| = \|U - U'\|. \end{aligned}$$

Combining Eq. (F3) with Eq. (F2), we obtain

$$\|\rho_S - \rho'_S\| \leq \|U - U'\| \leq \epsilon. \quad (\text{F4})$$

Now let us discuss how to combine Lemma 11 with Theorem 2 and the main result of Ref. [115] to bound the many-body entanglement gap in a continuous quench dynamics

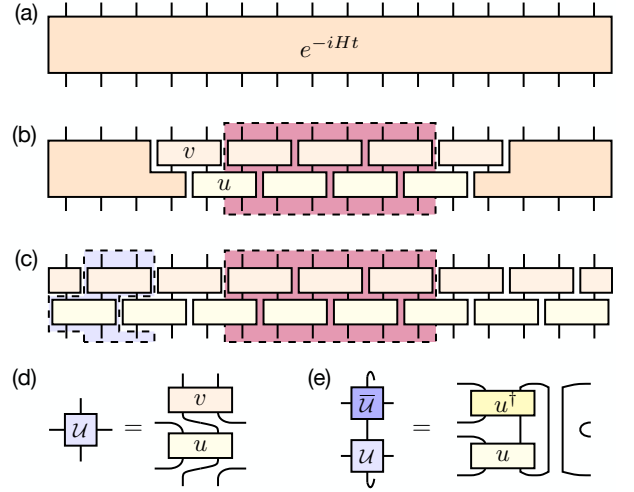


FIG. 15. (a) Continuous time evolution e^{-iHt} generated by a local Hamiltonian H and its (b) partial and (c) complete approximations by local unitaries, which are denoted as U'_c and U_c . If we focus on a subsystem marked in the red rectangle, (b) and (c) make no difference — starting from the same initial state, the reduced density operators of the states evolved by (b) and (c) coincide with each other. (d) Building block of (c), which can be regarded as an MPU. (e) Quantum channel associated with (d) takes the form $\rho \text{Tr}[\dots]$.

starting from an SPT MPS. According to Ref. [115], given a local Hamiltonian $H = \sum_j h_j$, we can approximate it with a bilayer unitary circuit or quantum cellular automaton U_c such that

$$\|e^{-iHt} - U_c\| \leq O\left(\frac{L}{|\Omega|}\right) e^{-\kappa_c(|\Omega| - v_c t)}, \quad (\text{F5})$$

where L is the total system size, $|\Omega|$ is the number of sites that a single unitary acts on, and κ_c and v_c are constants independent of L . While the bound diverges in the thermodynamic limit, we can make a cut off of the circuit approximation at the length scale of the subsystem without changing the reduced density operator. For such a truncated circuit U'_c , we have

$$\|e^{-iHt} - U'_c\| \leq O\left(\frac{l}{|\Omega|}\right) e^{-\kappa_c(|\Omega| - v_c t)}, \quad (\text{F6})$$

where the rhs is finite in the thermodynamic limit. See Figs. (15)(a), (b) and (c) for the relations and distinctions in e^{-iHt} , U'_c and U_c .

On the other hand, to apply Theorem 2, we should still regard the approximated reduced density operator as resulting from the time evolution by U_c . After putting $|\Omega|$ sites into one, we can regard U_c as an MPU generated by the block given in Fig. 15(d), which is simple (see Fig. 15(e)). Under such a rescaling, the parameters in Theorem 2 reads $k_0 = t = 1$, $D_U = d^{|\Omega|}$ and

$$\mu \rightarrow \mu^{|\Omega|}, \quad l \rightarrow \frac{l}{|\Omega|}, \quad (\text{F7})$$

while D stays invariant. Therefore, the many-body entanglement gap of the approximated density operator $\rho'_{[1,l]}$ is bounded by

$$\Delta_E^{\text{mb}} \leq \text{poly} \left(\frac{l}{|\Omega|} \right) e^{-\kappa l + \kappa' |\Omega|}, \quad (\text{F8})$$

where $\kappa = -\ln \mu$ and

$$\kappa' = \ln d + (D^2 + 1)\kappa, \quad (\text{F9})$$

provided that

$$\frac{l}{|\Omega|} - 2 \geq \coth \left(\frac{\kappa}{2} |\Omega| \right). \quad (\text{F10})$$

As for the many-body entanglement gap of the exact density operator $\rho_{[1,l]}$, we have

$$\begin{aligned} \Delta_E^{\text{mb}} &\equiv |\zeta_{r^2} - \zeta_1| \\ &\leq |\zeta_{r^2} - \zeta'_{r^2}| + |\zeta'_{r^2} - \zeta'_1| + |\zeta'_{r^2} - \zeta'_1| \\ &\leq 2\|\rho_{[1,l]} - \rho'_{[1,l]}\| + \Delta_E^{\text{mb}} \\ &\leq 2\|e^{-iHt} - U'_c\| + \Delta_E^{\text{mb}}, \end{aligned} \quad (\text{F11})$$

where we have used Lemma 11 in deriving the last inequality. Combining Eqs. (F6) and (F8) with Eq. (F11) and taking (we use \simeq since $|\Omega|$ should be an even integer dividing l)

$$|\Omega| \simeq \frac{\kappa_c v_c t + \kappa' l}{\kappa_c + \kappa'}, \quad (\text{F12})$$

we obtain

$$\Delta_E^{\text{mb}} \leq O(1) e^{-\frac{\kappa_c \kappa}{\kappa_c + \kappa'} (l - \frac{\kappa'}{\kappa} v_c t)}, \quad (\text{F13})$$

which indeed takes the form of Lieb-Robinson bound. We note that, at large length scales such that $\coth(\frac{\kappa}{2} |\Omega|) = 1 + o(1)$, Eq. (F10) can be satisfied by

$$t < \frac{\kappa_c + \kappa'}{\kappa_c} \left(\frac{1}{3} - \frac{\kappa}{\kappa_c + \kappa'} - o(1) \right) \frac{l}{v_c}, \quad (\text{F14})$$

where the rhs is positive due to $\kappa' > 5\kappa$, which arises from Eq. (F9) and $D \geq 2$ for an arbitrary SPT MPS.

On the other hand, it seems that we cannot derive a Lieb-Robinson bound by simply combining Theorem 2 with the errors in approximating ground states with MPSs [141]. Even if we only require the MPS approximation to be locally good [183, 184], the needed bond dimension scales like a polynomial of the inverse of error, implying an exponentially large bond dimension and a doubly exponentially large (due to the prefactor) bound predicted by Theorem 2 for an exponentially small error. We leave this problem for future work, which probably requires new ideas to directly estimate the entanglement gap in the exact ground state.

Appendix G: Convergence bounds for unital channels

We briefly review Ref. [144] and discuss how to bound $\|\mathcal{E}^l - \mathcal{E}^\infty\|$ by using function algebra. Applying Lemma 6 to $\mathcal{M} = \mathcal{E} - \mathcal{E}^\infty$ leads to the following theorem.

Theorem 6 (Main result of Ref. [144] for unital channels) *Let \mathcal{E} be a unital channel acting on a $D \times D$ -dimensional operator space such that $\|\mathcal{E}^n\| \leq C$ for $\forall n \in \mathbb{N}$. Let $\mu \equiv \lim_{n \rightarrow \infty} \|\mathcal{E}^n - \mathcal{E}^\infty\|^{\frac{1}{n}}$ be the spectral radius of $\mathcal{E} - \mathcal{E}^\infty$. We denote the minimal polynomial of $\mathcal{E} - \mathcal{E}^\infty$ as $m(z) = m_{\mathcal{E} - \mathcal{E}^\infty}(z) = \sum_{j=1}^J (z - \mu_j)^{s_j}$, where μ_j 's are different eigenvalues of $\mathcal{E} - \mathcal{E}^\infty$ and s_j is the size of the largest Jordan block with eigenvalue μ_j , and define the corresponding Blaschke product as*

$$B(z) \equiv \prod_{j=1}^J \left(\frac{z - \mu_j}{1 - \bar{\mu}_j z} \right)^{s_j}. \quad (\text{G1})$$

Then, for $l > \frac{\mu}{1-\mu}$, we have

$$\begin{aligned} \|\mathcal{E}^l - \mathcal{E}^\infty\| &\leq 2C \|z^l\|_{W/mW} \\ &\leq \mu^{l+1} \frac{4e^2 C \sqrt{|m|} (|m| + 1)}{l[1 - (1 + l^{-1})\mu]^{\frac{3}{2}}} \\ &\quad \times \sup_{|z|=(1+l^{-1})\mu} \left| \frac{1}{B(z)} \right|, \end{aligned} \quad (\text{G2})$$

where $|m| = \sum_{j=1}^J s_j$ is the degree of m and C is upper bounded by $\sqrt{\frac{D}{2}}$ [145].

Since the detailed proof in Ref. [144] is rather technical, it is worthwhile to sketch the outline here. First, we note that ‘‘sup’’ in Eq. (G2) arises from the following Cauchy-Schwarz inequality:

$$\begin{aligned} \|f_r\|_W &= \sum_{p \in \mathbb{N}} r^p |f_p| \\ &\leq \sqrt{\left(\sum_{p \in \mathbb{N}} r^{2p} \right) \left(\sum_{p \in \mathbb{N}} |f_p|^2 \right)} \\ &= \sqrt{\frac{1}{1-r^2} \sup_{0 \leq \rho < 1} \int_0^{2\pi} \frac{d\phi}{2\pi} |f(\rho e^{i\phi})|^2} \\ &\leq \frac{\|f\|_{H^\infty}}{\sqrt{1-r^2}}, \quad \forall f \in W, \end{aligned} \quad (\text{G3})$$

where $r \in (0, 1)$ can arbitrarily be chosen, $f_r(z) \equiv f(rz)$ and $\|f\|_{H^\infty} \equiv \sup_{z \in \mathbb{D}} |f(z)|$. In the typical case with $s_j = 1$, i.e., if $\mathcal{M} = \mathcal{E} - \mathcal{E}^\infty$ is diagonalizable [185], $\|z^l\|_{W/mW}$ is, by definition, upper bounded by $\|g_r\|_W$ as long as $g_r(\mu_j) = g(r\mu_j) = \mu_j^l$ for $\forall j = 1, 2, \dots, J$. An example is

$$g(z) = \sum_{j=1}^J \mu_j^l \frac{\tilde{B}_j(z)}{\tilde{B}_j(r\mu_j)}, \quad (\text{G4})$$

where $\tilde{B}_j(z) \equiv \frac{\tilde{B}(z)}{z - r\mu_j}$ and $\tilde{B}(z) \equiv \prod_{j=1}^J \frac{z - r\mu_j}{1 - r\bar{\mu}_j z}$ is the modified Blaschke product. Combining Eqs. (G3) and (G4), we

obtain

$$\begin{aligned} \|z^l\|_{W/mW} &\leq \|g_r\|_W \leq \frac{\|g\|_{H^\infty}}{\sqrt{1-r^2}} = \frac{1}{\sqrt{1-r^2}} \sup_{|z|=1} |g(z)| \\ &= \frac{1}{\sqrt{1-r^2}} \sup_{|z|=1} \left| \sum_{j=1}^J \frac{\mu_j^l}{(z - r\mu_j) \tilde{B}_j(r\mu_j)} \right|, \end{aligned} \quad (\text{G5})$$

where $|\tilde{B}(z)| = 1$ for $\forall |z| = 1$ is used. We will eventually arrive at Eq. (G2) by further bounding the rightmost expression in Eq. (G5), which can be rewritten in terms of a contour integral as

$$\oint_{|w|=(1+l^{-1})\mu} \frac{dw}{2\pi i} \frac{w^l}{\tilde{B}_r(w)(z - rw)} \quad (\text{G6})$$

for $l > \frac{\mu}{1-\mu}$, and set

$$r = \sqrt{1 - \frac{1 - (1+l^{-1})\mu}{|m|}}. \quad (\text{G7})$$

Appendix H: Generalization to finite interacting systems

We generalize Theorem 2 to the case of finite L . While we still have the decomposition given in Eq. (55), $|\Phi_{\alpha\beta}\rangle$'s are no longer orthogonal to each other. To compute the ES, we use the following generalization of Lemma 4:

Lemma 12 *For a bipartite state $|\Psi\rangle = \sum_{j=1}^J |\phi_j\rangle |\psi_j\rangle$, where $|\phi_j\rangle$'s and $|\psi_j\rangle$'s are generally neither normalized nor orthogonal to each other, the entanglement spectrum under such a bipartition coincides with the spectrum of $\bar{M}_\psi^{\frac{1}{2}} M_\phi \bar{M}_\psi^{\frac{1}{2}}$ (\bar{M}_ψ : complex conjugation of M_ψ) or $\bar{M}_\phi^{\frac{1}{2}} M_\psi \bar{M}_\phi^{\frac{1}{2}}$ (except for zeros), where $[M_\phi]_{jj'} = \langle \phi_j | \phi_{j'} \rangle$ and $[M_\psi]_{jj'} = \langle \psi_j | \psi_{j'} \rangle$.*

Proof.— It is equivalent to consider the spectrum of $\rho_\phi = \text{Tr}_\psi |\Psi\rangle \langle \Psi|$ and that of $\rho_\psi = \text{Tr}_\phi |\Psi\rangle \langle \Psi|$. To be specific, we focus on the former, which can be explicitly written as

$$\begin{aligned} \rho_\phi &= \sum_{j,j'} |\phi_j\rangle \langle \phi_{j'}| \text{Tr}[|\psi_j\rangle \langle \psi_{j'}|] \\ &= \sum_{j,j'} [M_\psi]_{jj'} |\phi_j\rangle \langle \phi_{j'}|. \end{aligned} \quad (\text{H1})$$

Since M_ψ is Hermitian, it can be expressed as $U^\dagger \Lambda U$ with $\Lambda = \text{diag}\{\Lambda_k\}_{k=1}^J$ and U being unitary. To be concrete, we have $[M_\psi]_{jj'} = \sum_{j''} \bar{U}_{j''j} \Lambda_{j''} U_{j''j}$. Introducing $|\tilde{\phi}_j\rangle = \sum_{j'} \sqrt{\Lambda_j} U_{jj'} |\phi_{j'}\rangle$, we can rewrite ρ_ϕ as

$$\rho_\phi = \sum_j |\tilde{\phi}_j\rangle \langle \tilde{\phi}_j| \quad (\text{H2})$$

to which we can apply Lemma 4 – the spectrum of ρ_ϕ coincides with that of

$$\begin{aligned} \langle \tilde{\phi}_j | \tilde{\phi}_{j'} \rangle &= \sum_{j'',j'''} \sqrt{\Lambda_j \Lambda_{j'}} \bar{U}_{j''j} \bar{U}_{j''j'} \langle \phi_{j''} | \phi_{j'''} \rangle \\ &= \sum_{j'',j'''} \sqrt{\Lambda_j \Lambda_{j'}} \bar{U}_{jj''} [M_\phi]_{j''j'''} U_{j''j'}^T \sqrt{\Lambda_{j'}} \\ &= [\sqrt{\Lambda} \bar{U} M_\phi U^T \sqrt{\Lambda}]_{jj'}. \end{aligned} \quad (\text{H3})$$

From the fact that unitary conjugation preserves the spectrum, we know that the spectrum of ρ_ϕ should be given by that of

$$U^T \sqrt{\Lambda} \bar{U} A U^T \sqrt{\Lambda} \bar{U} = \bar{M}_\psi^{\frac{1}{2}} M_\phi \bar{M}_\psi^{\frac{1}{2}}. \quad (\text{H4})$$

Note that the spectrum of $\bar{M}_\psi^{\frac{1}{2}} M_\phi \bar{M}_\psi^{\frac{1}{2}}$ is nothing but the squared absolute values of the singular values of $M_\phi^{\frac{1}{2}} \bar{M}_\psi^{\frac{1}{2}}$, which are the same as those of $(M_\phi^{\frac{1}{2}} \bar{M}_\psi^{\frac{1}{2}})^T = M_\psi^{\frac{1}{2}} \bar{M}_\phi^{\frac{1}{2}}$ and thus give the same spectrum as that of $\bar{M}_\phi^{\frac{1}{2}} M_\psi \bar{M}_\phi^{\frac{1}{2}}$ (this can directly be obtained by considering ρ_ψ following a similar analysis as above). \square

In fact, this result has already been obtained in Ref. [47], where it is used to calculate the ES of a projected entangled-pair state.

To bound the many-body entanglement gap, we need the following lemma.

Lemma 13 *Let M, M', M_0, M'_0 be non-negative definite Hermitian matrices and let the j th largest eigenvalue of $\bar{M}'^{\frac{1}{2}} M \bar{M}'^{\frac{1}{2}}$ and that of $\bar{M}'_0^{\frac{1}{2}} M_0 \bar{M}'_0^{\frac{1}{2}}$ be denoted as λ_j and λ_{0j} , respectively. Then for $\forall j$, we have*

$$\begin{aligned} |\lambda_j - \lambda_{0j}| &\leq \min\{\|\bar{M}'_0 \delta\| + \|\bar{M}'_0^{\frac{1}{2}} \delta' \bar{M}'_0^{\frac{1}{2}}\|, \\ &\quad \|\bar{M}_0 \delta'\| + \|\bar{M}_0^{\frac{1}{2}} \delta \bar{M}_0^{\frac{1}{2}}\|\} + \|\delta' \delta\|, \end{aligned} \quad (\text{H5})$$

where $\delta \equiv M - M_0$ and $\delta' \equiv M' - M'_0$.

Proof.— We first note the following useful norm inequality: for any two Hermitian matrices A and B with $B \geq 0$ (so that $B^{\frac{1}{2}}$ is well-defined), we have

$$\|B^{\frac{1}{2}} A B^{\frac{1}{2}}\| \leq \|AB\|. \quad (\text{H6})$$

This is because the spectrum of $B^{\frac{1}{2}} A B^{\frac{1}{2}}$ coincides with that of AB due to $\text{Tr}[(B^{\frac{1}{2}} A B^{\frac{1}{2}})^n] = \text{Tr}[(AB)^n]$ for $\forall n \in \mathbb{N}$ [181]. Moreover, $B^{\frac{1}{2}} A B^{\frac{1}{2}}$ is Hermitian so its norm is nothing but the spectral radius, which is no more than the norm of AB . This result is a special case of Proposition IX.1.1 in Ref. [84].

Let us turn to the proof of the lemma. Denoting the j th largest eigenvalue of $\bar{M}'^{\frac{1}{2}} M_0 \bar{M}'^{\frac{1}{2}}$ as λ'_j , which is also the j th largest eigenvalue of $\bar{M}_0^{\frac{1}{2}} M' \bar{M}_0^{\frac{1}{2}}$, we use Weyl's perturbation

theorem to obtain

$$\begin{aligned}
|\lambda_j - \lambda_{0j}| &\leq |\lambda_j - \lambda'_j| + |\lambda'_j - \lambda_{0j}| \\
&\leq \|\bar{M}'^{\frac{1}{2}} M \bar{M}'^{\frac{1}{2}} - \bar{M}'^{\frac{1}{2}} M_0 \bar{M}'^{\frac{1}{2}}\| \\
&\quad + \|\bar{M}_0^{\frac{1}{2}} M' \bar{M}_0^{\frac{1}{2}} - \bar{M}_0^{\frac{1}{2}} M'_0 \bar{M}_0^{\frac{1}{2}}\| \\
&= \|\bar{M}'^{\frac{1}{2}} \delta \bar{M}'^{\frac{1}{2}}\| + \|\bar{M}_0^{\frac{1}{2}} \delta' \bar{M}_0^{\frac{1}{2}}\| \\
&\leq \|\bar{M}' \delta\| + \|\bar{M}_0^{\frac{1}{2}} \delta' \bar{M}_0^{\frac{1}{2}}\| \\
&\leq \|\bar{M}' \delta\| + \|\bar{M}_0^{\frac{1}{2}} \delta' \bar{M}_0^{\frac{1}{2}}\| + \|\bar{\delta}' \delta\|,
\end{aligned} \tag{H7}$$

where we have used $\|A + B\| \leq \|A\| + \|B\|$ in the last step. Replacing M and M_0 with M' and M'_0 , respectively, and following a similar procedure, we obtain

$$|\lambda_j - \lambda_{0j}| \leq \|\bar{M}_0 \delta'\| + \|\bar{M}_0^{\frac{1}{2}} \delta \bar{M}_0^{\frac{1}{2}}\| + \|\bar{\delta}' \delta\|. \tag{H8}$$

Combining Eqs. (H7) and (H8), we obtain Eq. (H5). \square

To apply Lemma 13 to the many-body entanglement gap, we have only to choose

$$\begin{aligned}
M_{\alpha\beta, \alpha'\beta'} &= a_L \langle \alpha' | \mathcal{E}^l (|\beta'\rangle \langle \beta|) | \alpha \rangle, \\
M'_{\alpha\beta, \alpha'\beta'} &= a_L \langle \beta' | \mathcal{E}^{L-l} (|\alpha'\rangle \langle \alpha|) | \beta \rangle, \\
M_0 &= a_L \mathbb{1}_v \otimes \Lambda, \quad M'_0 = a_L \Lambda \otimes \mathbb{1}_v,
\end{aligned} \tag{H9}$$

where $a_L = (\text{Tr } \mathcal{E}^L)^{-\frac{1}{2}}$ is a finite-size normalization factor. Following the derivation of Eq. (73) in the main text, we can upper bound each term on the rhs of Eq. (H5) as

$$\begin{aligned}
\|\bar{M}'_0 \delta\| &\leq a_L^2 \left(\frac{D}{2}\right)^{\frac{3}{4}} \|\mathcal{E}^l - \mathcal{E}^\infty\|, \\
\|\bar{M}_0 \delta'\| &\leq a_L^2 \left(\frac{D}{2}\right)^{\frac{3}{4}} \|\mathcal{E}^{L-l} - \mathcal{E}^\infty\|, \\
\|\bar{M}_0^{\frac{1}{2}} \delta \bar{M}_0^{\frac{1}{2}}\| &\leq a_L^2 \sqrt{\frac{D}{2}} \|\mathcal{E}^l - \mathcal{E}^\infty\|, \\
\|\bar{M}_0^{\frac{1}{2}} \delta' \bar{M}_0^{\frac{1}{2}}\| &\leq a_L^2 \sqrt{\frac{D}{2}} \|\mathcal{E}^{L-l} - \mathcal{E}^\infty\|, \\
\|\bar{\delta}' \delta\| &\leq a_L^2 D^2 \|\mathcal{E}^l - \mathcal{E}^\infty\| \|\mathcal{E}^{L-l} - \mathcal{E}^\infty\|.
\end{aligned} \tag{H10}$$

Using the techniques in Sec. VD to bound $\|\mathcal{E}^l - \mathcal{E}^\infty\|$ associated with a time evolved MPS, we obtain the following theorem.

Theorem 7 (Finite interacting systems) *Starting from an SPT MPS with length L and bond dimension D subject to the periodic boundary condition, the many-body entanglement gap of a length- l subsystem after t time-evolution steps by a*

trivial symmetric MPU with bond dimension D_U is bounded from above by

$$\begin{aligned}
\Delta_E^{\text{mb}} &\leq (\text{Tr } \mathcal{E}^L)^{-1} [\min\{b_{1/2}(l, t) + b_{3/4}(L-l, t), \\
&\quad b_{1/2}(L-l, t) + b_{3/4}(l, t)\} + 4b_1(l, t)b_1(L-l, t)]
\end{aligned} \tag{H11}$$

for any $\min\{l, L-l\} - 2k_0 t \geq \frac{1+\mu}{1-\mu}$, where

$$b_\alpha(l, t) = C_\alpha (l - 2k_0 t)^{D^2-1} e^{-\frac{l-v_\alpha t}{\xi}}, \tag{H12}$$

with k_0 , μ and ξ being the same as those in Theorem 2, $v_\alpha = 2k_0 - (\alpha + \frac{1}{2}) \frac{\ln D_U}{\ln \mu}$, and the coefficient

$$C_\alpha = e^2 2^{\frac{5}{2}-\alpha} D^{\frac{3}{2}+\alpha} (D^2+1) \mu^{1-D^2} (1+\mu)^{D^2+\frac{1}{2}} (1-\mu)^{D^2-\frac{5}{2}} \tag{H13}$$

depends only on the initial state.

Two remarks are in order here. First, we note that in the thermodynamic limit of the entire system, we have $\text{Tr } \mathcal{E}^L = 1$ and $b_\alpha(\infty, t) = 0$ so that Theorem 2 is reproduced. Even if L is finite, we still find that Δ_E^{mb} is exponentially small up to

$$t \sim \min \left\{ \frac{\min\{l, L-l\}}{v_{1/2}}, \frac{\max\{l, L-l\}}{v_{3/4}}, \frac{L}{v_1} \right\}, \tag{H14}$$

provided that $\min\{l, L-l\} > \frac{v_{1/2}(1+\mu)}{(v_{1/2}-2k_0)(1-\mu)}$. Second, in the special case of the zero correlation length, i.e., $\mu = 0$, which corresponds to fixed points of entanglement renormalization [186], we can infer from Theorem 7 that the degeneracy is exact up to $t \sim \frac{l}{2k_0}$. This is intuitively rather clear since the entanglement edge modes are absolutely localized (without an exponential tail) for fixed-point states and it takes a finite time for a nonzero overlap to develop between the edge modes by a locality-preserving MPU.

Appendix I: Details on ES dynamics upon partial symmetry breaking

1. Flat-band model for class BDI \rightarrow class D

Thanks to the flat-band nature of the Hamiltonians given in Eqs. (93) and (94), it suffices to consider the $2N$ sites closest to the entanglement cut (purple dashed line in Fig. 10(a)). Restricted to the single-particle Hilbert subspace of these sites, the projector onto the Fermi sea of H_0 reads $P_0 = \frac{1}{2} \bigoplus_{j=1}^N (\sigma^0 + \sigma^x)$. The ES dynamics is then determined by the spectrum of $E_S(t) = P_S P(t) P_S$, where $P_S = \frac{1}{2} \bigoplus_{j=1}^N (\sigma^0 + \sigma_z)$ is the projector onto the left half N sites and

$$P(t) = e^{-iH^{\text{sp}} t} P_0 e^{iH^{\text{sp}} t}, \quad H^{\text{sp}} = 1 \oplus \bigoplus_{j=1}^{N-1} e^{it\sigma_x} \oplus 1, \tag{I1}$$

where we have already set $J = 1$. After straightforward calculations, we obtain the following matrix form of $E_S(t)$:

$$E_S(t) = \frac{1}{2} \begin{bmatrix} 1 & -i \sin t & 0 & 0 & \cdots & 0 & 0 \\ i \sin t & 1 & -i \sin t \cos t & 0 & \cdots & 0 & 0 \\ 0 & i \sin t \cos t & 1 & -i \sin t \cos t & \cdots & 0 & 0 \\ 0 & 0 & i \sin t \cos t & 1 & \cdots & 0 & 0 \\ \vdots & \vdots & \vdots & \vdots & \ddots & \vdots & \vdots \\ 0 & 0 & 0 & 0 & \cdots & 1 & -i \sin t \cos t \\ 0 & 0 & 0 & 0 & \cdots & i \sin t \cos t & 1 \end{bmatrix}_{N \times N}, \quad (12)$$

whose characteristic polynomial reads

$$\begin{aligned} f_N(\xi; t) &\equiv \det[\xi \mathbb{I}_{N \times N} - E_S(t)] \\ &= \left(\xi - \frac{1}{2}\right) F_{N-1}\left(\xi - \frac{1}{2}; \frac{\sin 2t}{4}\right) \\ &\quad - \frac{\sin^2 t}{4} F_{N-2}\left(\xi - \frac{1}{2}; \frac{\sin 2t}{4}\right). \end{aligned} \quad (13)$$

Here, $F_N(x; a)$ is defined recursively as

$$F_N(x; a) = x F_{N-1}(x; a) - a^2 F_{N-2}(x; a), \quad (14)$$

with initial conditions $F_1(x; a) = x$ and $F_2(x; a) = x^2 - a^2$ (or $F_{-1}(x; a) = 0$ and $F_0(x; a) = 1$). In fact, we have an analytic expression $F_N(x; a) \equiv \prod_{j=1}^N (x - 2a \cos \frac{j\pi}{N+1})$, which enjoys the properties $F_N(bx; ab) = b^N F_N(x; a)$, $F_N(x; a) = F_N(x; -a)$ and, in particular, $F_N(-x; a) = (-1)^N F_N(x; a)$. Using the recursive relation (14), we can rewrite $f_N(\xi; t)$ into

$$\begin{aligned} f_N(\xi; t) &= F_N\left(\xi - \frac{1}{2}; \frac{\sin 2t}{4}\right) \\ &\quad - \frac{\sin^4 t}{4} F_{N-2}\left(\xi - \frac{1}{2}; \frac{\sin 2t}{4}\right). \end{aligned} \quad (15)$$

The roots of $f_N(\xi; t)$ give the ES dynamics. Since $F_N(x; a)$ is an odd function of x for odd N , we have $F_{2n+1}(0; a) = 0$ so that $\xi = \frac{1}{2}$ is always a root of $f_N(\xi; t)$ if N is odd. Moreover, defining $g_{2n+1}(\xi; t) \equiv f_{2n+1}(\xi; t)/(\xi - \frac{1}{2})$, we find

$$\begin{aligned} g_{2n+1}\left(\frac{1}{2}; t\right) &= \left(-\frac{\sin^2 2t}{16}\right)^n \left(1 + \frac{n}{\cos^2 t}\right), \\ f_{2n}\left(\frac{1}{2}; t\right) &= \left(-\frac{\sin^2 2t}{16}\right)^n \frac{1}{\cos^2 t}, \end{aligned} \quad (16)$$

which are generally nonzero except for some special time points. Therefore, for an even N , all the initial topological entanglement modes at $\xi = \frac{1}{2}$ split, while one and only one $\xi = \frac{1}{2}$ mode survives for an odd N .

Let us calculate the full ES dynamics for $N = 1, 2, 3, 4, 5$. When $N = 1$, we have $f_1(\xi; t) = \xi - \frac{1}{2}$, implying the persistence of the topological entanglement mode at $\xi = \frac{1}{2}$. This is a trivial result since $H = 0$ and there is no dynamics. When $N = 2$, we find $f_2(\xi; t) = (\xi - \frac{1}{2})^2 - \frac{1}{4} \sin^2 t$, so the two entanglement modes oscillate as

$$\xi = \frac{1}{2} (1 \pm \sin t). \quad (17)$$

When $N = 3$, we find $f_3(\xi; t) = (\xi - \frac{1}{2})[(\xi - \frac{1}{2})^2 - \frac{1}{4} \sin^2 t (1 + \cos^2 t)]$, implying a persistent topological mode at $\xi = \frac{1}{2}$ and two oscillating modes

$$\xi = \frac{1}{2} (1 \pm \sin t \sqrt{1 + \cos^2 t}). \quad (18)$$

When $N = 4$, we find $f_4(\xi; t) = (\xi - \frac{1}{2})^4 - \frac{1}{4} \sin^2 t (1 + 2 \cos^2 t) (\xi - \frac{1}{2})^2 + \frac{1}{16} \sin^4 t \cos^2 t$, so all of the four modes oscillate in time as

$$\xi = \frac{1}{2} \pm \frac{\sin t}{4} \sqrt{2 + 4 \cos^2 t \pm 2 \sqrt{1 + 4 \cos^4 t}}. \quad (19)$$

Finally, we find the characteristic polynomial for $N = 5$ to be $f_5(\xi; t) = (\xi - \frac{1}{2})[(\xi - \frac{1}{2})^4 - \frac{1}{4} \sin^2 t (1 + 3 \cos^2 t) (\xi - \frac{1}{2})^2 + \frac{1}{16} \sin^4 t \cos^2 t (2 + \cos^2 t)]$. Except for a constant solution $\xi = \frac{1}{2}$, the other four modes oscillate as

$$\xi = \frac{1}{2} \pm \frac{\sin t}{4} \sqrt{2 + 6 \cos^2 t \pm 2 \sqrt{5 \cos^4 t - 2 \cos^2 t + 1}}. \quad (110)$$

These exact ES dynamics are plotted in Fig. 10(b).

2. Mathematical formulation

Having the above simple example in mind, we are ready to introduce a general mathematical formalism for dealing with partial symmetry breaking. We first recall that the classification of gapped free-fermion systems at equilibrium is given by the homotopy group $\pi_{d_s}(\mathcal{S})$, where d_s is the spatial dimension and \mathcal{S} is the classifying space satisfying symmetry constraints. If we are interested in the stable topology, we can take the limit of infinite bands and obtain the well-known K -theory classification [107]. For example, $\mathcal{S} = \mathcal{R}_1 \equiv \lim_{n \rightarrow \infty} \text{O}(n)$ for class BDI and $\mathcal{S} = \mathcal{R}_2 \equiv \lim_{n \rightarrow \infty} \text{O}(2n)/\text{U}(n)$ for class D. However, we emphasize that the general formalism applies equally to the finite-band case, although the practical calculations could be intractable. Denoting \mathcal{S} and $\tilde{\mathcal{S}}$ as the classifying spaces subject to symmetries G and \tilde{G} with $\tilde{G} < G$, we have $\mathcal{S} \subset \tilde{\mathcal{S}}$ since a G -symmetric system is always \tilde{G} -symmetric but the converse is generally not true. Therefore, we have a natural inclusion $\iota : \mathcal{S} \rightarrow \tilde{\mathcal{S}}$, which is a morphism (continuous map) in \mathbf{Top}_* (category of pointed topological spaces). Such an inclusion induces a group homomorphism $\iota_* : \pi_{d_s}(\mathcal{S}) \rightarrow \pi_{d_s}(\tilde{\mathcal{S}})$ through $[f] \mapsto [\iota \circ f]$, where $f : S^{d_s} \rightarrow \mathcal{S}$ is a continuous map from d_s D sphere

to \mathcal{S} and $[f]$ is its homotopy equivalence class. In fact, π_{d_s} can be regarded as a *functor* from \mathbf{Top}_* to \mathbf{Grp} (category of groups) or \mathbf{Ab} (category of Abelian groups) if $d_s \geq 2$, which maps not only pointed topological spaces into homotopy groups but also continuous maps between topological spaces into group homomorphisms between the corresponding homotopy groups [187]. In particular, ι_* is the image of ι that makes the following diagram commute:

$$\begin{array}{ccc} \mathcal{S} & \xrightarrow{\iota} & \tilde{\mathcal{S}} \\ \pi_{d_s} \downarrow & & \downarrow \pi_{d_s} \\ \pi_{d_s}(\mathcal{S}) & \xrightarrow{\iota_*} & \pi_{d_s}(\tilde{\mathcal{S}}) \end{array} \quad (\text{I11})$$

For class BDI \rightarrow class D in 1D, we have $d_s = 1$, $\pi_1(\mathcal{R}_1) = \mathbb{Z}$, $\pi_1(\mathcal{R}_2) = \mathbb{Z}_2$ and $\iota_*(N) = N \bmod 2$ for $\forall N \in \mathbb{Z}$, as illustrated in the previous subsection.

Let us move on to discuss interacting SPT systems classified by group cohomology [188]. We note that the group-cohomology classification is actually *complete* in 1D [70–72], although not in higher dimensions [189]. Instead of the classifying spaces, we focus directly on the symmetry groups. The inclusion ι of \tilde{G} into G , which is a natural group homomorphism, induces another group homomorphism from $H^{d_{\text{st}}}(G, \text{U}(1))$ to $H^{d_{\text{st}}}(\tilde{G}, \text{U}(1))$, where $d_{\text{st}} \equiv d_s + 1 \in \mathbb{Z}^+$ is the *spacetime* dimension. To see this, we only have to note that an d_{st} -cocycle $\omega : G^{\times d_{\text{st}}} \rightarrow \text{U}(1)$ can naturally be restricted to $\tilde{\omega} : \tilde{G}^{\times d_{\text{st}}} \rightarrow \text{U}(1)$ through $\tilde{\omega}(\tilde{g}_1, \tilde{g}_2, \dots, \tilde{g}_{d_{\text{st}}}) = \omega(\tilde{g}_1, \tilde{g}_2, \dots, \tilde{g}_{d_{\text{st}}})$, which obviously satisfies the cocycle property $d\tilde{\omega} = 1$. In fact, any group cohomology $h : G \rightarrow H^{d_{\text{st}}}(G, \text{U}(1))$ ($\text{U}(1)$ can actually be replaced by other Abelian groups) is a *contravariant* functor from \mathbf{Grp} to \mathbf{Ab} , which map not only groups into Abelian cohomology groups but also group homomorphisms into those between cohomology groups [190]. By contravariant, we mean that the directions of morphisms are reversed by the functor. In particular, the reduction of SPT phases is determined by the induced map ι^* that makes the following diagram commute:

$$\begin{array}{ccc} \tilde{G} & \xrightarrow{\iota} & G \\ h \downarrow & & \downarrow h \\ H^{d_{\text{st}}}(\tilde{G}, \text{U}(1)) & \xleftarrow{\iota^*} & H^{d_{\text{st}}}(G, \text{U}(1)) \end{array} \quad (\text{I12})$$

In the main text, we have given the simplest nontrivial example with $d_{\text{st}} = 2$, $H^2(G, \text{U}(1)) = \mathbb{Z}_N$, $H^2(\tilde{G}, \text{U}(1)) = \mathbb{Z}_n$ and $\iota^*(\nu) = \frac{N}{n}\nu \bmod n$.

Finally, let us comment on the impact of SPT-order reduction on the ES dynamics. For free-fermion systems, the bulk-edge correspondence usually has a very simple form — the number of edge states, or the degeneracy in ES, is simply given by the bulk topological number [52, 191, 192]. As a prototypical example (e.g., class BDI \rightarrow class D in 1D), a single (no) $\xi = \frac{1}{2}$ mode survives a surjective $\mathbb{Z} \rightarrow \mathbb{Z}_2$ reduction if the original topological number is odd (even). For interacting

SPT systems in 1D, the open boundary ES degeneracy r is determined by the minimal dimension of the *irreducible projective representations* of the symmetry group. Such a minimal dimension is 1 if the projective representation can be lifted to a linear representation, but is otherwise no less than 2 according to Lemma 5. In fact, there is a character theory for projective representations [193], which shares many similarities with the conventional character theory for linear representations. For example, denoting the dimension of the α th irreducible projective representation with respect to a 2-cocycle ω as d_α , we have $d_\alpha ||G|$ and $\sum_{\alpha=1}^{R_\omega} d_\alpha^2 = |G|$, where R_ω is the number of ω -regular conjugacy classes, i.e., those conjugacy classes with a representative element g satisfying $\omega(g, h) = \omega(h, g)$ for $\forall h \in N_g \equiv \{h \in G : gh = hg\} < G$. An immediate corollary is that, for $G = \mathbb{Z}_N \times \mathbb{Z}_N$ with N being a prime, we have $r = N$ for any G -symmetric SPT state. By simple analysis, we can also infer that possible $r > 1$ for $G = \mathbb{Z}_6 \times \mathbb{Z}_6$ is 2, 3 and 6. These conclusions are consistent with the results in Table II.

3. Minimal models for quenched interacting SPT systems

Let us introduce the interacting counterparts of flat-band free-fermion models, in the sense that these minimal models have *zero* correlation lengths. In $(1+1)$ D spacetime, a G -symmetric SPT state with zero correlation length can be built from a 2-cocycle (which satisfies $\omega(gh, k)\omega(g, h) = \omega(g, hk)\omega(h, k)$ for $\forall g, h, k \in G$) as [188]

$$|\Psi\rangle = \frac{1}{|G|^{\frac{L}{2}}} \sum_{\{g_j\}_{j=1}^L} \prod_{j=1}^L \omega(g_j^{-1} g_{j+1}, g_{j+1}^{-1})^{-1} |g_1 g_2 \dots g_L\rangle. \quad (\text{I13})$$

Here the local Hilbert space $\mathbb{C}^{|G|}$ is spanned by $\{|g\rangle : g \in G\}$ and the on-site symmetry representation is regular: $\rho_g = \sum_{h \in G} |gh\rangle\langle h|$ for $\forall g \in G$. Note that such a construction (I13) applies equally to continuous symmetries if we replace \sum_g by $\int dg$ [188]. To demonstrate the impact of partial symmetry breaking on the ES dynamics, we consider the simplest case in which the Hamiltonian is a sum of commutative two-site operators:

$$H = \sum_{j=1}^L h_j, \quad h_j = \sum_{g_j, g_{j+1}} h(g_j, g_{j+1}) |g_j g_{j+1}\rangle \langle g_j g_{j+1}|, \quad (\text{I14})$$

whose eigenstates are simply Fock states. To partially break the symmetry from G to \tilde{G} , we require

$$h(g, g') = h(\tilde{g}g, \tilde{g}g') \in \mathbb{R}, \quad \forall g, g' \in G \text{ and } \tilde{g} \in \tilde{G}, \quad (\text{I15})$$

and otherwise

$$h(g, g') \neq h(g''g, g''g'), \quad \forall g'' \in G \setminus \tilde{G}. \quad (\text{I16})$$

As illustrated in Fig. 16(a), due to the fact that h_j 's commute with each other, the open boundary ES at time t are simply the squared singular values of

$$[M(t)]_{gg'} = e^{-ih(g, g')t} \omega(g^{-1}g', g'^{-1})^{-1}. \quad (\text{I17})$$

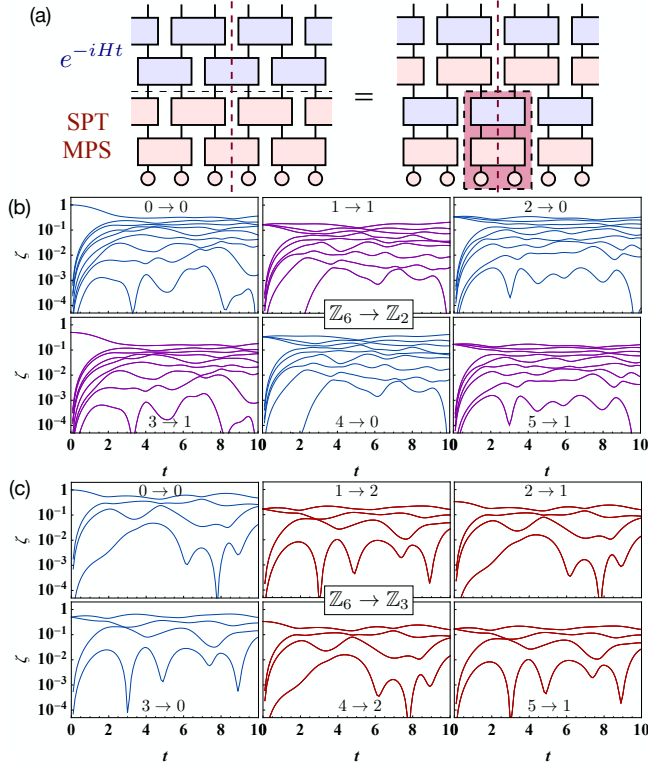


FIG. 16. (a) Reduction of the many-body ES into a two-site ES from the commutativity of all the two-site unitaries. The array of circles is the product state $|G\rangle^{\otimes L}$ with $|G\rangle \equiv |G|^{-\frac{1}{2}} \sum_g |g\rangle$. The red and blue two-site unitaries are given by $\sum_{g,g'} \omega(g^{-1}g', g'^{-1})^{-1} |gg'\rangle \langle gg'|$ and $\sum_{g,g'} e^{-ih(g,g')t} |gg'\rangle \langle gg'|$, respectively. The two-site state marked in the red rectangle reads $\sum_{g,g'} [M(t)]_{gg'} |gg'\rangle$, where $[M(t)]_{gg'}$ is given in Eq. (II7). (b) Many-body ES dynamics for a topological number reduction $\mathbb{Z}_6 \rightarrow \mathbb{Z}_2$ from a partial symmetry breaking quench $G = \mathbb{Z}_6 \times \mathbb{Z}_6 \rightarrow \tilde{G} = \mathbb{Z}_2 \times \mathbb{Z}_2$. (c) Same as (b) but for $\mathbb{Z}_6 \rightarrow \mathbb{Z}_3$ from $G = \mathbb{Z}_6 \times \mathbb{Z}_6 \rightarrow \tilde{G} = \mathbb{Z}_3 \times \mathbb{Z}_3$. In (b) and (c), blue, purple and red curves are of degeneracy 1, 2 and 3, respectively. The expressions $j \rightarrow j'$ ($j \in \mathbb{Z}_6$ and $j' \in \mathbb{Z}_{2,3}$) specify the group homomorphism from $H^2(G, \text{U}(1))$ to $H^2(\tilde{G}, \text{U}(1))$. See also Table II.

We can then numerically determine the degeneracies r and \tilde{r} in the initial ES and that after the quench.

In Figs. 16(b) and (c), we plot the ES dynamics for two different partial symmetry breaking quenches $G = \mathbb{Z}_6 \times \mathbb{Z}_6 \rightarrow \tilde{G} = \mathbb{Z}_2 \times \mathbb{Z}_2$ and $G = \mathbb{Z}_6 \times \mathbb{Z}_6 \rightarrow \tilde{G} = \mathbb{Z}_3 \times \mathbb{Z}_3$. We randomly sample $h(g, g')$ among $[-1, 1]$ while keeping the \tilde{G} -symmetry requirement (II5). The behaviors of ES splitting agree perfectly with the results in Table II. While not shown here, we have also checked that the ES always becomes non-degenerate upon the partial symmetry breaking quench $G = \mathbb{Z}_4 \times \mathbb{Z}_4 \rightarrow \tilde{G} = \mathbb{Z}_2 \times \mathbb{Z}_2$. This is fully consistent with the fact that the induced group homomorphism from \mathbb{Z}_4 to \mathbb{Z}_2 is trivial, as mentioned in Sec. VIA 2.

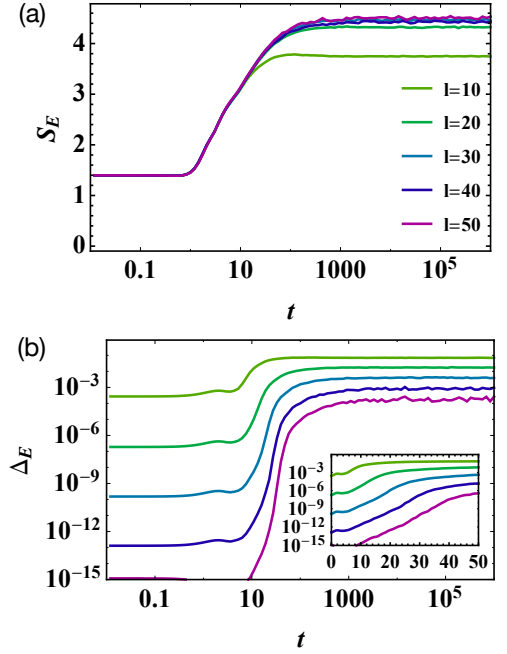


FIG. 17. Dynamics of (a) the entanglement entropy and (b) the single-particle entanglement gap after a quench to the disordered SSH model (J1) from a clean state. Inset in (b): the same as the main panel but in the log-linear scale. We choose $L = 2l + 1$ so that the entanglement bipartition is asymmetric and the initial entanglement gap is finite. The numbers of disorder realizations for $l = 10, 20, 30, 40$ and 50 are $10^4, 5 \times 10^3, 2 \times 10^3, 10^3$ and 5×10^2 , respectively. The parameters are quenched as $(\bar{J}, \bar{J}', f) = (0.5, 1, 0) \rightarrow (1, 0.5, 0.6)$. Note that the early-time data of Δ_E^{sp} for $l = 50$ (only a part of which is visible) are not reliable due to a finite numerical resolution.

Appendix J: Numerical simulations for disordered systems

In this appendix, we provide some numerical pieces of evidence to support the qualitative discussions in Sec. VIB.

1. Disordered SSH model

We consider the entanglement dynamics in a disordered SSH model described by the Hamiltonian

$$H = - \sum_j (J_j b_j^\dagger a_j + J'_j a_{j+1}^\dagger b_j + \text{H.c.}), \quad (\text{J1})$$

where a_j and b_j denote the sublattice fermionic modes in the j th unit cell, and the hopping amplitudes

$$J_j \in [(1-f)\bar{J}, (1+f)\bar{J}], \quad J'_j \in [(1-f)\bar{J}', (1+f)\bar{J}'] \quad (\text{J2})$$

are uniformly and independently sampled. We start from a topological state with $(\bar{J}, \bar{J}', f) = (0.5, 1, 0)$ (no disorder) and quench the parameters to $(\bar{J}, \bar{J}', f) = (1, 0.5, 0.6)$. The length of the subsystem is chosen to be $l = \frac{1}{2}(L - 1)$ so that the entanglement gap in the initial state becomes nonzero due to the asymmetric entanglement bipartition.

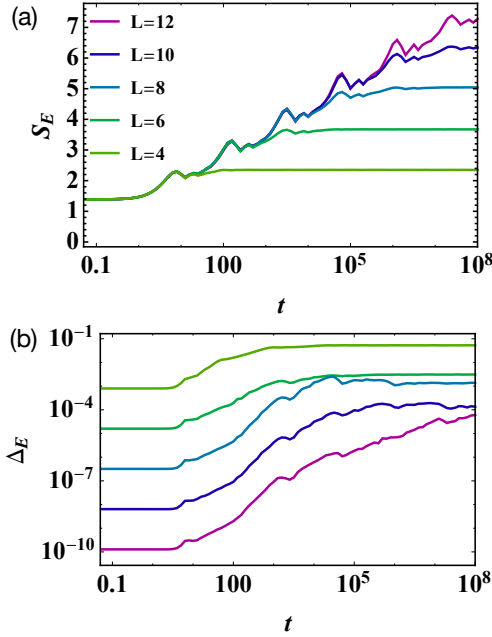


FIG. 18. Dynamics of (a) the half-chain entanglement entropy and (b) the many-body entanglement gap starting from the $\mathbb{Z}_2 \times \mathbb{Z}_2$ SPT MPS (J3) and evolving in time according to the disordered Hamiltonian given in Eq. (J7). The numbers of disorder realizations for $L = 4, 6, 8, 10$ and 12 are 5×10^4 , 10^4 , 5×10^3 , 5×10^2 and 3×10^2 , respectively. The parameters in Eqs. (J4) and (J7) are set to be $p = q = 0.49$, $J_0 = 3$ and $\kappa = 3$.

As shown in Fig. 17(a), we find that the entanglement entropy grows logarithmically — a feature usually associated with many-body localized systems. Since there is no interaction in our model, one may naïvely expect that the entanglement grows extremely slowly like $\ln \ln t$ [194], as might be inferred from a dynamical version of the strong-disorder renormalization group [154]. However, there is a crucial difference in our setup — the initial state $|\Psi_0\rangle$ is not a product state (in real space) and has a nonzero correlation length. We denote U_0 as a local unitary such that $U_0|\Psi_0\rangle$ becomes a product state; then the quench dynamics in this new frame is governed by $U_0 H U_0^\dagger$ (H is given by Eq. (J1) with the postquench parameters), which now involves small but finite long-range hoppings. We expect this effect to dramatically change the common paradigm of entanglement growth in Anderson insulators. On the other hand, the entanglement entropy eventually becomes saturated at a constant independent of (sufficiently large) l , as a manifestation of a finite localization length.

In stark contrast to the slow growth of entanglement entropy, the numerical results (see Fig. 17(b)) suggests an exponentially fast growth of the single-particle entanglement gap before saturation, which is similar to the clean case. Nevertheless, due again to the finiteness of the localization length, the saturation value decreases exponentially with respect to l , implying that the topological entanglement edge modes are stable even in the long-time limit.

2. Phenomenological model for many-body localization

The minimal group that supports an interacting SPT phase protected by unitary symmetries is $G = \mathbb{Z}_2 \times \mathbb{Z}_2 = \{(m, n) : m, n \in \mathbb{Z}_2\}$, whose second cohomology group reads $H^2(\mathbb{Z}_2 \times \mathbb{Z}_2, \text{U}(1)) = \mathbb{Z}_2$. By specifying the on-site symmetry as the regular representation $\rho_{(m,n)} = Z^m \otimes Z^n$ with $Z = |0\rangle\langle 0| - |1\rangle\langle 1|$ acting on a local qubit, we can construct a nontrivial MPS as

$$|\Psi_0\rangle = \sum_{\{j_s=00,01,10,11\}} \text{Tr}[A_{j_1} A_{j_2} \dots A_{j_L}] |j_1 j_2 \dots j_L\rangle, \quad (\text{J3})$$

where a local state $|j\rangle$ consists of two qubits and the injective tensor A_j is given by

$$\begin{aligned} A_{00} &= \sqrt{(1-p)(1-q)}\sigma^0, & A_{01} &= \sqrt{q(1-p)}\sigma^x, \\ A_{10} &= i\sqrt{p(1-q)}\sigma^y, & A_{11} &= \sqrt{pq}\sigma^z, \end{aligned} \quad (\text{J4})$$

with $p, q \in (0, 1)$. We can check that the projective representation on the virtual level is nontrivial:

$$\begin{aligned} V_{(0,0)} &= \sigma^0, & V_{(1,0)} &= \sigma^x, \\ V_{(0,1)} &= \sigma^y, & V_{(1,1)} &= \sigma^z. \end{aligned} \quad (\text{J5})$$

To slightly lift the exact four-fold degeneracy in the ES of a finite segment, we choose $p = q = 0.49$ in Eq. (J4).

To simulate the effect of many-body localization, we recall that a fully many-body localized Hamiltonian can generally be written as

$$H_{\text{MBL}} = \sum_j h_j \tau_j^z + \sum_{j,j'} J_{jj'} \tau_j^z \tau_{j'}^z + \dots, \quad (\text{J6})$$

where $\tau_j^z = U_{\text{loc}} Z_j U_{\text{loc}}^\dagger$ is the spin operator of the logic qubit which is related to the physical one by a local unitary transformation [151]. Inspired by this phenomenology, we expect that an Ising Hamiltonian with random and exponentially decay long-range interactions,

$$H' = \sum_{j < j'} J_{jj'} Z_j Z_{j'}, \quad J_{jj'} \in [-J_0 e^{-\kappa(j'-j)}, J_0 e^{-\kappa(j'-j)}], \quad (\text{J7})$$

where $J_{jj'}$'s are sampled uniformly and independently, would be sufficient to capture the essential physics of the dynamical interplay between many-body localization and SPT order. Note that this Ising Hamiltonian (J7) respects the $\mathbb{Z}_2 \times \mathbb{Z}_2$ symmetry.

Figure 18(a) shows that the half-chain entanglement entropy of the state $|\Psi_t\rangle = e^{-iH't}|\Psi_0\rangle$ essentially follows a logarithmic growth. The separation between two successive local peaks is very close to e^κ (as a multiple, since we take the logarithmic scale), consistent with the argument that the logarithmic growth of entanglement entropy results basically from the decoherence of remote spins [155]. In stark contrast with the previous noninteracting case, the entanglement entropy eventually becomes saturated at an *extensive* quantity (i.e., proportional to L). Regarding the growth of the many-body entanglement gap, the numerical results in Fig. 18(b)

seem to suggest a power law. This result is to some extent expected once we accept that the entanglement gap in an SPT

state is bounded essentially by the correlation at the subsystem length scale, which we have proved for clean systems.

-
- [1] Immanuel Bloch, Jean Dalibard, and Sylvain Nascimbène, “Quantum simulations with ultracold quantum gases,” *Nat. Phys.* **8**, 267 (2012).
 - [2] R. Blatt and C. F. Roos, “Quantum simulations with trapped ions,” *Nat. Phys.* **8**, 277 (2012).
 - [3] Andrew A. Houck, Hakan E. Türeci, and Jens Koch, “On-chip quantum simulation with superconducting circuits,” *Nat. Phys.* **8**, 292 (2012).
 - [4] Soonwon Choi, Joonhee Choi, Renate Landig, Georg Kucsko, Hengyun Zhou, Junichi Isoya, Fedor Jelezko, Shinobu Onoda, Hitoshi Sumiya, Vedika Khemani, Curt von Keyserlingk, Norman Y. Yao, Eugene Demler, and Mikhail D. Lukin, “Observation of discrete time-crystalline order in a disordered dipolar many-body system,” *Nature* **543**, 221 (2017).
 - [5] Hannes Bernien, Sylvain Schwartz, Alexander Keesling, Harry Levine, Ahmed Omran, Hannes Pichler, Soonwon Choi, Alexander S. Zibrov, Manuel Endres, Markus Greiner, Vladan Vuletić, and Mikhail D. Lukin, “Probing many-body dynamics on a 51-atom quantum simulator,” *Nature* **551**, 579 (2017).
 - [6] J. Zhang, P. W. Hess, A. Kyprianidis, P. Becker, A. Lee, J. Smith, G. Pagano, I.-D. Potirniche, A. C. Potter, A. Vishwanath, N. Y. Yao, and C. Monroe, “Observation of a discrete time crystal,” *Nature* **543**, 217 (2017).
 - [7] J. Zhang, G. Pagano, P. W. Hess, A. Kyprianidis, P. Becker, H. Kaplan, A. V. Gorshkov, Z.-X. Gong, and C. Monroe, “Observation of a many-body dynamical phase transition with a 53-qubit quantum simulator,” *Nature* **551**, 601 (2017).
 - [8] Pasquale Calabrese and John Cardy, “Quantum quenches in extended systems,” *J. Stat. Mech.*, P06008 (2007).
 - [9] Fabian H L Essler and Maurizio Fagotti, “Quench dynamics and relaxation in isolated integrable quantum spin chains,” *J. Stat. Mech.*, 064002 (2016).
 - [10] Aditi Mitra, “Quantum quench dynamics,” *Annu. Rev. Condens. Matter Phys.* **9**, 245 (2018).
 - [11] M. Z. Hasan and C. L. Kane, “Colloquium: Topological insulators,” *Rev. Mod. Phys.* **82**, 3045–3067 (2010).
 - [12] Xiao-Liang Qi and Shou-Cheng Zhang, “Topological insulators and superconductors,” *Rev. Mod. Phys.* **83**, 1057–1110 (2011).
 - [13] B. A. Bernevig and T. L. Hughes, *Topological Insulators and Topological Superconductors* (Princeton University Press, Princeton, NJ, 2013).
 - [14] Ching-Kai Chiu, Jeffrey C. Y. Teo, Andreas P. Schnyder, and Shinsei Ryu, “Classification of topological quantum matter with symmetries,” *Rev. Mod. Phys.* **88**, 035005 (2016).
 - [15] Matthew S. Foster, Maxim Dzero, Victor Gurarie, and Emil A. Yuzbashyan, “Quantum quench in a $p+ip$ superfluid: Winding numbers and topological states far from equilibrium,” *Phys. Rev. B* **88**, 104511 (2013).
 - [16] Luca D’Alessio and Marcos Rigol, “Dynamical preparation of floquet chern insulators,” *Nat. Commun.* **6**, 8336 (2015).
 - [17] M. D. Caio, N. R. Cooper, and M. J. Bhaseen, “Quantum quenches in chern insulators,” *Phys. Rev. Lett.* **115**, 236403 (2015).
 - [18] Szabolcs Vajna and Balázs Dóra, “Topological classification of dynamical phase transitions,” *Phys. Rev. B* **91**, 155127 (2015).
 - [19] Jan Carl Budich and Markus Heyl, “Dynamical topological order parameters far from equilibrium,” *Phys. Rev. B* **93**, 085416 (2016).
 - [20] Ying Hu, Peter Zoller, and Jan Carl Budich, “Dynamical buildup of a quantized hall response from nontopological states,” *Phys. Rev. Lett.* **117**, 126803 (2016).
 - [21] M. D. Caio, N. R. Cooper, and M. J. Bhaseen, “Hall response and edge current dynamics in chern insulators out of equilibrium,” *Phys. Rev. B* **94**, 155104 (2016).
 - [22] Justin H. Wilson, Justin C. W. Song, and Gil Refael, “Remnant geometric hall response in a quantum quench,” *Phys. Rev. Lett.* **117**, 235302 (2016).
 - [23] Zhoushen Huang and Alexander V. Balatsky, “Dynamical quantum phase transitions: Role of topological nodes in wave function overlaps,” *Phys. Rev. Lett.* **117**, 086802 (2016).
 - [24] Ce Wang, Pengfei Zhang, Xin Chen, Jinlong Yu, and Hui Zhai, “Scheme to measure the topological number of a chern insulator from quench dynamics,” *Phys. Rev. Lett.* **118**, 185701 (2017).
 - [25] Matthias Tarnowski, F. Nur Ünal, Nick Fläschner, Benno S. Rem, André Eckardt, Klaus Sengstock, and Christof Weitenberg, “Measuring topology from dynamics by obtaining the chern number from a linking number,” *Nat. Commun.* **10**, 1728 (2019).
 - [26] N. Fläschner, D. Vogel, M. Tarnowski, B. S. Rem, D.-S. Lühmann, M. Heyl, J. C. Budich, L. Mathey, K. Sengstock, and C. Weitenberg, “Observation of dynamical vortices after quenches in a system with topology,” *Nat. Phys.* **14**, 265 (2018).
 - [27] Chao Yang, Linhu Li, and Shu Chen, “Dynamical topological invariant after a quantum quench,” *Phys. Rev. B* **97**, 060304(R) (2018).
 - [28] Po-Yao Chang, “Topology and entanglement in quench dynamics,” *Phys. Rev. B* **97**, 224304 (2018).
 - [29] Motohiko Ezawa, “Topological quantum quench dynamics carrying arbitrary hopf and second chern numbers,” *Phys. Rev. B* **98**, 205406 (2018).
 - [30] Lin Zhang, Long Zhang, Sen Niu, and Xiong-Jun Liu, “Dynamical classification of topological quantum phases,” *Sci. Bull.* **63**, 1385 (2018).
 - [31] Wei Sun, Chang-Rui Yi, Bao-Zong Wang, Wei-Wei Zhang, Barry C. Sanders, Xiao-Tian Xu, Zong-Yao Wang, Joerg Schmiedmayer, Youjin Deng, Xiong-Jun Liu, Shuai Chen, and Jian-Wei Pan, “Uncover topology by quantum quench dynamics,” *Phys. Rev. Lett.* **121**, 250403 (2018).
 - [32] Zongping Gong and Masahito Ueda, “Topological entanglement-spectrum crossing in quench dynamics,” *Phys. Rev. Lett.* **121**, 250601 (2018).
 - [33] Max McGinley and Nigel R. Cooper, “Topology of one-dimensional quantum systems out of equilibrium,” *Phys. Rev. Lett.* **121**, 090401 (2018).
 - [34] Max McGinley and Nigel R. Cooper, “Classification of topological insulators and superconductors out of equilibrium,” *Phys. Rev. B* **99**, 075148 (2019).
 - [35] M. D. Caio, G. Möller, N. R. Cooper, and M. J. Bhaseen, “Topological marker currents in chern insulators,” *Nat. Phys.* **15**, 257 (2019).

- [36] Shuangyuan Lu and Jinlong Yu, “Stability of entanglement-spectrum crossing in quench dynamics of one-dimensional gapped free-fermion systems,” *Phys. Rev. A* **99**, 033621 (2019).
- [37] A unitary or anti-unitary operator is a symmetry (anti-symmetry) if it commutes (anti-commutes) with the Hamiltonian.
- [38] Ari M. Turner, Yi Zhang, and Ashvin Vishwanath, “Entanglement and inversion symmetry in topological insulators,” *Phys. Rev. B* **82**, 241102(R) (2010).
- [39] Lukasz Fidkowski, “Entanglement spectrum of topological insulators and superconductors,” *Phys. Rev. Lett.* **104**, 130502 (2010).
- [40] Taylor L. Hughes, Emil Prodan, and B. Andrei Bernevig, “Inversion-symmetric topological insulators,” *Phys. Rev. B* **83**, 245132 (2011).
- [41] Po-Yao Chang, Christopher Mudry, and Shinsei Ryu, “Symmetry-protected entangling boundary zero modes in crystalline topological insulators,” *J. Stat. Mech.* , P09014 (2014).
- [42] Hui Li and F. D. M. Haldane, “Entanglement spectrum as a generalization of entanglement entropy: Identification of topological order in non-abelian fractional quantum hall effect states,” *Phys. Rev. Lett.* **101**, 010504 (2008).
- [43] Frank Pollmann, Ari M. Turner, Erez Berg, and Masaki Oshikawa, “Entanglement spectrum of a topological phase in one dimension,” *Phys. Rev. B* **81**, 064439 (2010).
- [44] R. Thomale, A. Sterdyniak, N. Regnault, and B. Andrei Bernevig, “Entanglement gap and a new principle of adiabatic continuity,” *Phys. Rev. Lett.* **104**, 180502 (2010).
- [45] Ari M. Turner, Frank Pollmann, and Erez Berg, “Topological phases of one-dimensional fermions: An entanglement point of view,” *Phys. Rev. B* **83**, 075102 (2011).
- [46] Lukasz Fidkowski and Alexei Kitaev, “Topological phases of fermions in one dimension,” *Phys. Rev. B* **83**, 075103 (2011).
- [47] J. Ignacio Cirac, Didier Poilblanc, Norbert Schuch, and Frank Verstraete, “Entanglement spectrum and boundary theories with projected entangled-pair states,” *Phys. Rev. B* **83**, 245134 (2011).
- [48] Hannes Pichler, Guanyu Zhu, Alireza Seif, Peter Zoller, and Mohammad Hafezi, “Measurement protocol for the entanglement spectrum of cold atoms,” *Phys. Rev. X* **6**, 041033 (2016).
- [49] B. P. Lanyon, C. Maier, M. Holzäpfel, T. Baumgratz, C. Hempel, P. Jurcevic, I. Dhand, A. S. Buyskikh, A. J. Daley, M. Cramer, M. B. Plenio, R. Blatt, and C. F. Roos, “Efficient tomography of a quantum many-body system,” *Nat. Phys.* **13**, 1158 (2017).
- [50] M. Dalmonte, B. Vermersch, and P. Zoller, “Quantum simulation and spectroscopy of entanglement hamiltonians,” *Nat. Phys.* **14**, 827 (2018).
- [51] Xiao-Gang Wen, “Colloquium: Zoo of quantum-topological phases of matter,” *Rev. Mod. Phys.* **89**, 041004 (2017).
- [52] Yasuhiro Hatsugai, “Chern number and edge states in the integer quantum hall effect,” *Phys. Rev. Lett.* **71**, 3697–3700 (1993).
- [53] Elliott H. Lieb and Derek W. Robinson, “The finite group velocity of quantum spin systems,” *Commun. Math. Phys.* **28**, 251 (1972).
- [54] S. Bravyi, M. B. Hastings, and F. Verstraete, “Lieb-robinson bounds and the generation of correlations and topological quantum order,” *Phys. Rev. Lett.* **97**, 050401 (2006).
- [55] Marc Cheneau, Peter Barmettler, Dario Poletti, Manuel Endres, Peter Schaub, Takeshi Fukuhara, Christian Gross, Immanuel Bloch, Corinna Kollath, and Stefan Kuhr, “Light-cone-like spreading of correlations in a quantum many-body system,” *Nature* **481**, 484 (2012).
- [56] Philip Richerme, Zhe-Xuan Gong, Aaron Lee, Crystal Senko, Jacob Smith, Michael Foss-Feig, Spyridon Michalakis, Alexey V. Gorshkov, and Christopher Monroe, “Non-local propagation of correlations in quantum systems with long-range interactions,” *Nature* **511**, 198 (2014).
- [57] P. Jurcevic, B. P. Lanyon, P. Hauke, C. Hempel, P. Zoller, R. Blatt, and C. F. Roos, “Quasiparticle engineering and entanglement propagation in a quantum many-body system,” *Nature* **511**, 202 (2014).
- [58] G. Vidal, J. I. Latorre, E. Rico, and A. Kitaev, “Entanglement in quantum critical phenomena,” *Phys. Rev. Lett.* **90**, 227902 (2003).
- [59] Pasquale Calabrese and John Cardy, “Entanglement entropy and quantum field theory,” *J. Stat. Mech.* , P06002 (2004).
- [60] Shinsei Ryu and Tadashi Takayanagi, “Holographic derivation of entanglement entropy from the anti-de sitter space/conformal field theory correspondence,” *Phys. Rev. Lett.* **96**, 181602 (2006).
- [61] Pasquale Calabrese and John Cardy, “Evolution of entanglement entropy in one-dimensional systems,” *J. Stat. Mech.* , P04010 (2005).
- [62] Pasquale Calabrese and John Cardy, “Entanglement entropy dynamics of heisenberg chains,” *J. Stat. Mech.* , P03001 (2006).
- [63] Maurizio Fagotti and Pasquale Calabrese, “Evolution of entanglement entropy following a quantum quench: Analytic results for the xy chain in a transverse magnetic field,” *Phys. Rev. A* **78**, 010306 (2008).
- [64] J. Schachenmayer, B. P. Lanyon, C. F. Roos, and A. J. Daley, “Entanglement growth in quench dynamics with variable range interactions,” *Phys. Rev. X* **3**, 031015 (2013).
- [65] P. Hauke and L. Tagliacozzo, “Spread of correlations in long-range interacting quantum systems,” *Phys. Rev. Lett.* **111**, 207202 (2013).
- [66] Ehud Altman and Ronen Vosk, “Universal dynamics and renormalization in many-body-localized systems,” *Annu. Rev. Cond. Matt. Phys.* **6**, 383 (2015).
- [67] M. B. Hastings and Xiao-Gang Wen, “Quasiadiabatic continuation of quantum states: The stability of topological ground-state degeneracy and emergent gauge invariance,” *Phys. Rev. B* **72**, 045141 (2005).
- [68] M. B. Hastings, “An area law for one-dimensional quantum systems,” *J. Stat. Mech.* , P08024 (2007).
- [69] Karel Van Acoleyen, Michaël Mariën, and Frank Verstraete, “Entanglement rates and area laws,” *Phys. Rev. Lett.* **111**, 170501 (2013).
- [70] Xie Chen, Zheng-Cheng Gu, and Xiao-Gang Wen, “Classification of gapped symmetric phases in one-dimensional spin systems,” *Phys. Rev. B* **83**, 035107 (2011).
- [71] Xie Chen, Zheng-Cheng Gu, and Xiao-Gang Wen, “Complete classification of one-dimensional gapped quantum phases in interacting spin systems,” *Phys. Rev. B* **84**, 235128 (2011).
- [72] Norbert Schuch, David Pérez-García, and Ignacio Cirac, “Classifying quantum phases using matrix product states and projected entangled pair states,” *Phys. Rev. B* **84**, 165139 (2011).
- [73] Fernando G. S. L. Brandão and Michał Horodecki, “An area law for entanglement from exponential decay of correlations,” *Nat. Phys.* **9**, 721 (2013).
- [74] Fernando G. S. L. Brandão and Michał Horodecki, “Exponential decay of correlations implies area law,” *Commun. Math. Phys.* **333**, 761 (2015).

- [75] Jaeyoon Cho, “Realistic area-law bound on entanglement from exponentially decaying correlations,” *Phys. Rev. X* **8**, 031009 (2018).
- [76] Rajibul Islam, Ruichao Ma, Philipp M. Preiss, M. Eric Tai, Alexander Lukin, Matthew Rispoli, and Markus Greiner, “Measuring entanglement entropy in a quantum many-body system,” *Nature* **528**, 77 (2015).
- [77] Adam M. Kaufman, M. Eric Tai, Alexander Lukin, Matthew Rispoli, Robert Schittko, Philipp M. Preiss, and Markus Greiner, “Quantum thermalization through entanglement in an isolated many-body system,” *Science* **353**, 794 (2016).
- [78] Alexander Lukin, Matthew Rispoli, Robert Schittko, M. Eric Tai, Adam M. Kaufman, Soonwon Choi, Vedika Khemani, Julian Léonard, and Markus Greiner, “Probing entanglement in a many-body-localized system,” *Science* **364**, 256 (2019).
- [79] Tiff Brydges, Andreas Elben, Petar Jurcevic, Benoît Vermersch, Christine Maier, Ben P. Lanyon, Peter Zoller, Rainer Blatt, and Christian F. Roos, “Probing rényi entanglement entropy via randomized measurements,” *Science* **364**, 260 (2019).
- [80] This phenomenon should be distinguished from the ES crossings emerging in quantum quenches from trivial to topological Hamiltonians [28, 32, 36], which correspond to higher dimensional topology and are also observed in Floquet topological systems [195, 196].
- [81] Ming-Chiang Chung, Yi-Hao Jhu, Pochung Chen, and Chung-Yu Mou, “Quench dynamics of topological maximally entangled states,” *J. Phys.: Condens. Matter* **25**, 285601 (2013).
- [82] Ming-Chiang Chung, Yi-Hao Jhu, Pochung Chen, Chung-Yu Mou, and Xin Wan, “A memory of majorana modes through quantum quench,” *Sci. Rep.* **6**, 29172 (2016).
- [83] Yi-Hao Jhu, Pochung Chen, and Ming-Chiang Chung, “Relaxation of the entanglement spectrum in quench dynamics of topological systems,” *J. Stat. Mech.*, 073105 (2017).
- [84] Rajendra Bhatia, *Matrix Analysis* (Springer, New York, 1997).
- [85] M. B. Plenio, J. Eisert, J. Dreißig, and M. Cramer, “Entropy, entanglement, and area: Analytical results for harmonic lattice systems,” *Phys. Rev. Lett.* **94**, 060503 (2005).
- [86] Michael M. Wolf, “Violation of the entropic area law for fermions,” *Phys. Rev. Lett.* **96**, 010404 (2006).
- [87] Michael M. Wolf, Frank Verstraete, Matthew B. Hastings, and J. Ignacio Cirac, “Area laws in quantum systems: Mutual information and correlations,” *Phys. Rev. Lett.* **100**, 070502 (2008).
- [88] J. Eisert, M. Cramer, and M. B. Plenio, “Colloquium: Area laws for the entanglement entropy,” *Rev. Mod. Phys.* **82**, 277 (2010).
- [89] Bela Bauer and Chetan Nayak, “Area laws in a many-body localized state and its implications for topological order,” *J. Stat. Mech.*, P09005 (2013).
- [90] Christian K. Burrell and Tobias J. Osborne, “Bounds on the speed of information propagation in disordered quantum spin chains,” *Phys. Rev. Lett.* **99**, 167201 (2007).
- [91] Michael Levin and Xiao-Gang Wen, “Detecting topological order in a ground state wave function,” *Phys. Rev. Lett.* **96**, 110405 (2006).
- [92] Alexei Kitaev and John Preskill, “Topological entanglement entropy,” *Phys. Rev. Lett.* **96**, 110404 (2006).
- [93] Luigi Amico, Rosario Fazio, Andreas Osterloh, and Vlatko Vedral, “Entanglement in many-body systems,” *Rev. Mod. Phys.* **80**, 517 (2008).
- [94] J I Latorre and A Riera, “A short review on entanglement in quantum spin systems,” *J. Phys. A* **42**, 504002 (2009).
- [95] Nicolas Laflorencie, “Quantum entanglement in condensed matter systems,” *Phys. Rep.* **646**, 1 (2016).
- [96] Sergey Bravyi, “Lagrangian representation for fermionic linear optics,” *Quantum. Inf. Comput.* **5**, 216 (2005).
- [97] Here we have tacitly assumed the particle-number conservation, as is the usually case for various quantum simulators. The generalization to the case with pairing terms is straightforward.
- [98] Ingo Peschel, “Calculation of reduced density matrices from correlation functions,” *J. Phys. A* **36**, L205 (2003).
- [99] M. Fannes, B. Nachtergaele, and R. F. Werner, “Finitely correlated states on quantum spin chains,” *Commun. Math. Phys.* **144**, 443 (1992).
- [100] D. Pérez-García, F. Verstraete, M. M. Wolf, and J. I. Cirac, “Matrix product state representations,” *Quantum Inf. Comput.* **7**, 401 (2007).
- [101] F. Verstraete, V. Murg, and J. I. Cirac, “Matrix product states, projected entangled pair states, and variational renormalization group methods for quantum spin systems,” *Adv. Phys.* **57**, 143 (2008).
- [102] Romn Orús, “A practical introduction to tensor networks: Matrix product states and projected entangled pair states,” *Ann. Phys.* **349**, 117 (2014).
- [103] J.I. Cirac, D. Prez-Garcia, N. Schuch, and F. Verstraete, “Matrix product density operators: Renormalization fixed points and boundary theories,” *Ann. Phys.* **378**, 100 (2017).
- [104] D. Pérez-García, M. M. Wolf, M. Sanz, F. Verstraete, and J. I. Cirac, “String order and symmetries in quantum spin lattices,” *Phys. Rev. Lett.* **100**, 167202 (2008).
- [105] Alexander Altland and Martin R. Zirnbauer, “Nonstandard symmetry classes in mesoscopic normal-superconducting hybrid structures,” *Phys. Rev. B* **55**, 1142–1161 (1997).
- [106] Andreas P. Schnyder, Shinsei Ryu, Akira Furusaki, and Andreas W. W. Ludwig, “Classification of topological insulators and superconductors in three spatial dimensions,” *Phys. Rev. B* **78**, 195125 (2008).
- [107] A. Kitaev, “Periodic table for topological insulators and superconductors,” *AIP Conf. Proc.* **1134**, 22 (2009).
- [108] A. Y. Kitaev, “Unpaired majorana fermions in quantum wires,” *Phys. Usp.* **44**, 131 (2001).
- [109] Hoi Chun Po, Lukasz Fidkowski, Takahiro Morimoto, Andrew C. Potter, and Ashvin Vishwanath, “Chiral floquet phases of many-body localized bosons,” *Phys. Rev. X* **6**, 041070 (2016).
- [110] J Ignacio Cirac, David Pérez-García, Norbert Schuch, and Frank Verstraete, “Matrix product unitaries: structure, symmetries, and topological invariants,” *J. Stat. Mech.*, 083105 (2017).
- [111] Zongping Gong, Christoph Sünderhauf, Norbert Schuch, and J. Ignacio Cirac, “Classification of matrix-product unitaries with symmetries,” (2018), arXiv:1812.09183.
- [112] M. Burak Şahinoğlu, Sujeet K. Shukla, Feng Bi, and Xie Chen, “Matrix product representation of locality preserving unitaries,” *Phys. Rev. B* **98**, 245122 (2018).
- [113] B. Pirvu, V. Murg, J. I. Cirac, and F. Verstraete, “Matrix product operator representations,” *New J. Phys.* **12**, 025012 (2010).
- [114] Here we do not consider those anomalous MPUs with non-trivial chiral indices, since we use the MPUs to approximate genuine 1D dynamics generated by local Hamiltonians instead of the edge dynamics of 2D systems [109].
- [115] Tobias J. Osborne, “Efficient approximation of the dynamics of one-dimensional quantum spin systems,” *Phys. Rev. Lett.* **97**, 157202 (2006).
- [116] C. W. von Keyserlingk and S. L. Sondhi, “Phase structure

- of one-dimensional interacting floquet systems. i. abelian symmetry-protected topological phases,” *Phys. Rev. B* **93**, 245145 (2016).
- [117] C. W. von Keyserlingk and S. L. Sondhi, “Phase structure of one-dimensional interacting floquet systems. ii. symmetry-broken phases,” *Phys. Rev. B* **93**, 245146 (2016).
- [118] Vedika Khemani, Achilleas Lazarides, Roderich Moessner, and S. L. Sondhi, “Phase structure of driven quantum systems,” *Phys. Rev. Lett.* **116**, 250401 (2016).
- [119] Adam Nahum, Jonathan Ruhman, Sagar Vijay, and Jeongwan Haah, “Quantum entanglement growth under random unitary dynamics,” *Phys. Rev. X* **7**, 031016 (2017).
- [120] Adam Nahum, Sagar Vijay, and Jeongwan Haah, “Operator spreading in random unitary circuits,” *Phys. Rev. X* **8**, 021014 (2018).
- [121] C. W. von Keyserlingk, Tibor Rakovszky, Frank Pollmann, and S. L. Sondhi, “Operator hydrodynamics, otocs, and entanglement growth in systems without conservation laws,” *Phys. Rev. X* **8**, 021013 (2018).
- [122] Tibor Rakovszky, Frank Pollmann, and C. W. von Keyserlingk, “Diffusive hydrodynamics of out-of-time-ordered correlators with charge conservation,” *Phys. Rev. X* **8**, 031058 (2018).
- [123] Vedika Khemani, Ashvin Vishwanath, and David A. Huse, “Operator spreading and the emergence of dissipative hydrodynamics under unitary evolution with conservation laws,” *Phys. Rev. X* **8**, 031057 (2018).
- [124] Amos Chan, Andrea De Luca, and J. T. Chalker, “Solution of a minimal model for many-body quantum chaos,” *Phys. Rev. X* **8**, 041019 (2018).
- [125] Christoph S nderhauf, David P rez-Garc a, David A. Huse, Norbert Schuch, and J. Ignacio Cirac, “Localization with random time-periodic quantum circuits,” *Phys. Rev. B* **98**, 134204 (2018).
- [126] Shriya Pai, Michael Pretko, and Rahul M. Nandkishore, “Localization in fractonic random circuits,” *Phys. Rev. X* **9**, 021003 (2019).
- [127] T. Rakovszky, S. Gopalakrishnan, S. A. Parameswaran, and F. Pollmann, “Signatures of information scrambling in the dynamics of the entanglement spectrum,” (2019), arXiv:1901.04444.
- [128] Eugene P. Wigner, “Normal form of antiunitary operators,” *J. Math. Phys.* **1**, 409 (1960).
- [129] Nicola Marzari, Arash A. Mostofi, Jonathan R. Yates, Ivo Souza, and David Vanderbilt, “Maximally localized wannier functions: Theory and applications,” *Rev. Mod. Phys.* **84**, 1419 (2012).
- [130] W. Kohn, “Analytic properties of bloch waves and wannier functions,” *Phys. Rev.* **115**, 809 (1959).
- [131] Jacques Des Cloizeaux, “Energy bands and projection operators in a crystal: Analytic and asymptotic properties,” *Phys. Rev.* **135**, A685 (1964).
- [132] Christian Brouder, Gianluca Panati, Matteo Calandra, Christophe Mourougane, and Nicola Marzari, “Exponential localization of wannier functions in insulators,” *Phys. Rev. Lett.* **98**, 046402 (2007).
- [133] S. Kivelson, “Wannier functions in one-dimensional disordered systems: Application to fractionally charged solitons,” *Phys. Rev. B* **26**, 4269 (1982).
- [134] Neil W. Ashcroft and N. David Mermin, *Solid State Physics* (Saunders, Philadelphia, 1976).
- [135] A. W. Marshall, I. Olkin, and B. C. Arnold, *Inequalities: Theory of Majorization and Its Applications* (Springer, New York, 2010).
- [136] Pasquale Calabrese and John Cardy, “Time dependence of correlation functions following a quantum quench,” *Phys. Rev. Lett.* **96**, 136801 (2006).
- [137] M. A. Cazalilla, “Effect of suddenly turning on interactions in the luttinger model,” *Phys. Rev. Lett.* **97**, 156403 (2006).
- [138] Pasquale Calabrese, Fabian H. L. Essler, and Maurizio Fagotti, “Quantum quench in the transverse-field ising chain,” *Phys. Rev. Lett.* **106**, 227203 (2011).
- [139] Rajendra Bhatia and Fuad Kittaneh, “Norm inequalities for partitioned operators and an application,” *Math. Ann.* **287**, 719 (1990).
- [140] F. Verstraete and J. I. Cirac, “Mapping local hamiltonians of fermions to local hamiltonians of spins,” *J. Stat. Mech.* , P09012 (2005).
- [141] F. Verstraete and J. I. Cirac, “Matrix product states represent ground states faithfully,” *Phys. Rev. B* **73**, 094423 (2006).
- [142] In the thermodynamic limit, an MPS being normal is equivalent to that its associated channel has a unique fixed point.
- [143] Michael M. Wolf, *Quantum Channels and Operations: Guided Tour* (Lecture Notes, 2012).
- [144] Oleg Szehr, David Reeb, and Michael M. Wolf, “Spectral convergence bounds for classical and quantum markov processes,” *Commun. Math. Phys.* **333**, 565 (2015).
- [145] David P rez-Garc a, Michael M. Wolf, Denes Petz, and Mary Beth Ruskai, “Contractivity of positive and trace-preserving maps under l_p norms,” *J. Math. Phys.* **47**, 083506 (2006).
- [146] Andrew C. Potter and Takahiro Morimoto, “Dynamically enriched topological orders in driven two-dimensional systems,” *Phys. Rev. B* **95**, 155126 (2017).
- [147] Nick Bultinck, Dominic J. Williamson, Jutho Haegeman, and Frank Verstraete, “Fermionic matrix product states and one-dimensional topological phases,” *Phys. Rev. B* **95**, 075108 (2017).
- [148] Anton Kapustin, Alex Turzillo, and Minyoung You, “Spin topological field theory and fermionic matrix product states,” *Phys. Rev. B* **98**, 125101 (2018).
- [149] F. D. M. Haldane, “Nonlinear field theory of large-spin heisenberg antiferromagnets: Semiclassically quantized solitons of the one-dimensional easy-axis n el state,” *Phys. Rev. Lett.* **50**, 1153–1156 (1983).
- [150] Ferdinand Evers and Alexander D. Mirlin, “Anderson transitions,” *Rev. Mod. Phys.* **80**, 1355 (2008).
- [151] Rahul Nandkishore and David A. Huse, “Many-body localization and thermalization in quantum statistical mechanics,” *Annu. Rev. Cond. Matt. Phys.* **6**, 201 (2015).
- [152] Marko  nidari , Toma  Prosen, and Peter Prelov ek, “Many-body localization in the heisenberg xxz magnet in a random field,” *Phys. Rev. B* **77**, 064426 (2008).
- [153] Jens H. Bardarson, Frank Pollmann, and Joel E. Moore, “Unbounded growth of entanglement in models of many-body localization,” *Phys. Rev. Lett.* **109**, 017202 (2012).
- [154] Ronen Vosk and Ehud Altman, “Many-body localization in one dimension as a dynamical renormalization group fixed point,” *Phys. Rev. Lett.* **110**, 067204 (2013).
- [155] Maksym Serbyn, Z. Papi , and Dmitry A. Abanin, “Universal slow growth of entanglement in interacting strongly disordered systems,” *Phys. Rev. Lett.* **110**, 260601 (2013).
- [156] Pedro Ponte, Z. Papi , Fran ois Huveneers, and Dmitry A. Abanin, “Many-body localization in periodically driven systems,” *Phys. Rev. Lett.* **114**, 140401 (2015).
- [157] Yichen Huang, Yong-Liang Zhang, and Xie Chen, “Out-of-time-ordered correlators in many-body localized systems,” *Ann. Phys.* **529**, 1600318 (2017).

- [158] Brian Swingle and Debanjan Chowdhury, “Slow scrambling in disordered quantum systems,” *Phys. Rev. B* **95**, 060201 (2017).
- [159] Ruihua Fan, Pengfei Zhang, Huitao Shen, and Hui Zhai, “Out-of-time-order correlation for many-body localization,” *Sci. Bull.* **62**, 707 (2017).
- [160] M. Gluza, C. Krumnow, M. Friesdorf, C. Gogolin, and J. Eisert, “Equilibration via gaussification in fermionic lattice systems,” *Phys. Rev. Lett.* **117**, 190602 (2016).
- [161] M. Gluza, J. Eisert, and T. Farrelly, “Equilibration towards generalized gibbs ensembles in non-interacting theories,” (2018), arXiv:1809.08268.
- [162] Chaitanya Murthy and Mark Srednicki, “Relaxation to gaussian and generalized gibbs states in systems of particles with quadratic hamiltonians,” (2018), arXiv:1809.03681.
- [163] Marcos Rigol, Vanja Dunjko, and Maxim Olshanii, “Thermalization and its mechanism for generic isolated quantum systems,” *Nature* **452**, 854 (2008).
- [164] Anatoli Polkovnikov, Krishnendu Sengupta, Alessandro Silva, and Mukund Vengalattore, “Colloquium: Nonequilibrium dynamics of closed interacting quantum systems,” *Rev. Mod. Phys.* **83**, 863 (2011).
- [165] Elliott Lieb, Theodore Schultz, and Daniel Mattis, “Two soluble models of an antiferromagnetic chain,” *Ann. Phys.* **16**, 407 (1961).
- [166] Masaki Oshikawa, “Commensurability, excitation gap, and topology in quantum many-particle systems on a periodic lattice,” *Phys. Rev. Lett.* **84**, 1535 (2000).
- [167] M. B. Hastings, “Lieb-schultz-mattis in higher dimensions,” *Phys. Rev. B* **69**, 104431 (2004).
- [168] Siddharth A. Parameswaran, Ari M. Turner, Daniel P. Arovas, and Ashvin Vishwanath, “Topological order and absence of band insulators at integer filling in non-symmorphic crystals,” *Nat. Phys.* **9**, 299 (2013).
- [169] Haruki Watanabe, Hoi Chun Po, Ashvin Vishwanath, and Michael Zaletel, “Filling constraints for spin-orbit coupled insulators in symmorphic and nonsymmorphic crystals,” *Proc. Natl. Acad. Sci. U. S. A.* **112**, 14551 (2015).
- [170] Meng Cheng, Michael Zaletel, Maissam Barkeshli, Ashvin Vishwanath, and Parsa Bonderson, “Translational symmetry and microscopic constraints on symmetry-enriched topological phases: A view from the surface,” *Phys. Rev. X* **6**, 041068 (2016).
- [171] Davide Vodola, Luca Lepori, Elisa Ercolessi, Alexey V. Gorshkov, and Guido Pupillo, “Kitaev chains with long-range pairing,” *Phys. Rev. Lett.* **113**, 156402 (2014).
- [172] Zhe-Xuan Gong, Michael Foss-Feig, Spyridon Michalakis, and Alexey V. Gorshkov, “Persistence of locality in systems with power-law interactions,” *Phys. Rev. Lett.* **113**, 030602 (2014).
- [173] Michael Foss-Feig, Zhe-Xuan Gong, Charles W. Clark, and Alexey V. Gorshkov, “Nearly linear light cones in long-range interacting quantum systems,” *Phys. Rev. Lett.* **114**, 157201 (2015).
- [174] Davide Vodola, Luca Lepori, Elisa Ercolessi, and Guido Pupillo, “Long-range ising and kitaev models: phases, correlations and edge modes,” *New J. Phys.* **18**, 015001 (2016).
- [175] Steven A. Moses, Jacob P. Covey, Matthew T. Miecnikowski, Deborah S. Jin, and Jun Ye, “New frontiers for quantum gases of polar molecules,” *Nat. Phys.* **13**, 13 (2017).
- [176] W D Heiss, “The physics of exceptional points,” *J. Phys. A* **45**, 444016 (2012).
- [177] Zongping Gong, Yuto Ashida, Kohei Kawabata, Kazuaki Takasan, Sho Higashikawa, and Masahito Ueda, “Topological phases of non-hermitian systems,” *Phys. Rev. X* **8**, 031079 (2018).
- [178] Kohei Kawabata, Ken Shiozaki, Masahito Ueda, and Masatoshi Sato, “Symmetry and topology in non-hermitian physics,” (2018), arXiv:1812.09133.
- [179] Hengyun Zhou and Jong Yeon Lee, “Periodic table for topological bands with non-hermitian symmetries,” *Phys. Rev. B* **99**, 235112 (2019).
- [180] Kohei Kawabata, Takumi Bessho, and Masatoshi Sato, “Non-hermitian topology of exceptional points,” (2019), arXiv:1902.08479.
- [181] G. De las Cuevas, T. S. Cubitt, J. I. Cirac, M. M. Wolf, and D. Prez-Garcia, “Fundamental limitations in the purifications of tensor networks,” *J. Math. Phys.* **57**, 071902 (2016).
- [182] Fuad Kittaneh, “Norm inequalities for commutators of positive operators and applications,” *Math. Z.* **258**, 845–849 (2008).
- [183] Yichen Huang, “Approximating local properties by tensor network states with constant bond dimension,” (2019), arXiv:1903.10048.
- [184] Alexander M. Dalzell and Fernando G. S. L. Brandão, “Locally accurate mps approximations for ground states of one-dimensional gapped local hamiltonians,” (2019), arXiv:1903.10241.
- [185] If this is not true, we can add an arbitrarily small perturbation \mathcal{P} such that $\mathcal{M} + \mathcal{P}$ is diagonalizable, and the tiny spectrum shift is again bounded by Weyl’s perturbation theorem. See also Ref. [144].
- [186] F. Verstraete, J. I. Cirac, J. I. Latorre, E. Rico, and M. M. Wolf, “Renormalization-group transformations on quantum states,” *Phys. Rev. Lett.* **94**, 140601 (2005).
- [187] Allen Hatcher, *Algebraic Topology* (Cambridge University Press, Cambridge, 2002).
- [188] Xie Chen, Zheng-Cheng Gu, Zheng-Xin Liu, and Xiao-Gang Wen, “Symmetry protected topological orders and the group cohomology of their symmetry group,” *Phys. Rev. B* **87**, 155114 (2013).
- [189] Anton Kapustin, “Symmetry protected topological phases, anomalies, and cobordisms: Beyond group cohomology,” (2014), arXiv:1403.1467.
- [190] Kenneth S. Brown, *Cohomology of Groups* (Springer, New York, 1982).
- [191] Shinsei Ryu and Yasuhiro Hatsugai, “Topological origin of zero-energy edge states in particle-hole symmetric systems,” *Phys. Rev. Lett.* **89**, 077002 (2002).
- [192] Emil Prodan and Hermann Schulz-Baldes, *Bulk and Boundary Invariants for Complex Topological Insulators: From K-Theory to Physics* (Springer, Berlin, 2016).
- [193] Chuangxun Cheng, “A character theory for projective representations of finite groups,” *Linear Alg. Appl.* **469**, 230 (2015).
- [194] Ferenc Iglói, Zsolt Szatmári, and Yu-Cheng Lin, “Entanglement entropy dynamics of disordered quantum spin chains,” *Phys. Rev. B* **85**, 094417 (2012).
- [195] Andrew C. Potter, Takahiro Morimoto, and Ashvin Vishwanath, “Classification of interacting topological floquet phases in one dimension,” *Phys. Rev. X* **6**, 041001 (2016).
- [196] I.-D. Potirniche, A. C. Potter, M. Schleier-Smith, A. Vishwanath, and N. Y. Yao, “Floquet symmetry-protected topological phases in cold-atom systems,” *Phys. Rev. Lett.* **119**, 123601 (2017).